Characterization of clathrin heavy chain 22 in epithelial and skeletal muscle cells

Dipl.-Biochem. Peter-Christopher Esk

geboren am 28. Januar 1978 in Hannover

September 2008

Referent: Prof. Dr. Ernst J. Ungewickell

Korreferentin: Prof. Frances M. Brodsky, DPhil

Tag der Promotion: 26. September 2008

Eidesstattliche Erklärung

Hiermit erkläre ich an Eides statt, dass ich die vorliegende Dissertation selbstständig und nur unter der Verwendung der angegebenen Quellen und Hilfsmittel verfasst habe.

Weiterhin erkläre ich an Eides statt, dass diese Dissertation nicht schon als Diplom- oder ähnliche Prüfungsarbeit verwendet wurde.

San Francisco, den 10.06.2008

(Peter-Christopher Esk)

Zusammenfassung

Die universelle Clathrin schwere Kette (CHC17) ist seit langem als Hüllprotein in Transportvorgängen, insbesondere der Clathrin-vermittelten Endozytose bekannt. Weiterhin konnte eine Rolle für CHC17 im Aufbau der mitotischen Spindel nachgewiesen werden. Clathrin schwere Kette 22 (CHC22) ist eine Isoform von CHC17, welche in allen Geweben schwach, in Skelettmuskel hingegen stark exprimiert wird. Obwohl zu 85 % identisch mit CHC17, wurde bislang keine Funktion für CHC22 gefunden.

In dieser Arbeit wird die Funktion von CHC22 als unabhängig von CHC17 definiert, auch kann CHC22 CHC17 nicht bei dessen Verlust ersetzen. CHC22 wird dagegen eine Rolle in einem CHC17-unabhängigen endosomalen Sortierungsvorgang zugewiesen. Dieser wird von ausgewählten Frachtmolekülen, unter anderem den Mannose-6-Phosphat Rezeptoren und Shiga-Toxin beim Transport von Endosomen zum *Trans*-Golgi Netzwerk genutzt. Der CHC22-abhängige Schritt folgt CHC17- und retromer-abhängigen nach.

In humanen Muskelzellen konnte eine Funktion von CHC22 für die Bildung GLUT4-speichernder Sekretvesikel gezeigt werden. CHC17 spielt hingegen keine Rolle in deren Aufbau. GLUT4-speichernde Sekretvesikel sind abhängig von Membrantransport aus dem Endosom und dem *Trans*-Golgi Netzwerk stammend. Verlust von CHC22 führt zum Verlust GLUT4-speichernder Vesikel. Gleichzeitig verlieren die Zellen ihre Insulin-reaktivität hinsichtlich Zuckeraufnahme, was die Wichtigkeit von CHC22 unterstreicht.

Schlagwörter: Clathrin, Membrantransport, Endosom

Abstract

The ubiquitous clathrin heavy chain, CHC17, is well characterized as a coat protein in membrane traffic, particularly its role in receptor-mediated endocytosis has been studied in great detail. In addition, a role for CHC17 in formation of the mitotic spindle has been described. Clathrin heavy chain 22 (CHC22) is an isoform of CHC17 present in all tissues with increased expression in skeletal muscle. Despite exhibiting 85 % sequence identity to CHC17, CHC22 function remained elusive so far.

In this study CHC22 function is revealed to be independent of CHC17. Also, CHC22 may not compensate for loss of CHC17 in either CHC17-mediated membrane trafficking or formation of the mitotic spindle. Instead, CHC22 functions in a discrete endosomal sorting step required by select cargo molecules including mannose-6-phosphate receptors and Shiga-toxin for retrograde trafficking from endosomes to the *trans*-Golgi network. This sorting step occurs downstream of CHC17- and retromer-mediated retrograde sorting at the early endosome.

In skeletal muscle CHC22 is found to be required for function of the insulin-responsive GLUT4 storage compartment. In contrast, function of this compartment is CHC17-independent. The GLUT4 storage compartment depends on delivery of the glucose transporter 4 from endosomes and the *trans*-Golgi network. Depletion of CHC22 leads to complete loss of this compartment alongside loss of insulin responsiveness regarding glucose uptake in skeletal muscle, highlighting CHC22's importance in this pathway.

Key words: clathrin, membrane traffic, endosome

Table of Contents

Abbreviations

aa	Amino acid
Akt	Thymoma viral proto-oncogene 1
AP	Adaptor protein
BFA	Brefeldin A
BSA	Bovine serum albumine
bp	Base pair
CHC	Clathrin heavy chain
CI-MPR	Cation-independent mannose-6-phosphate receptor
CMV	Cytomegalovirus
CLC	Clathrin light chain
Cy	Cyanide dye
DAPI	4'-6'-diamidino-2-phenylindole
DMSO	Dimethyl sulfoxide
DMEM	Dulbecco's Modified Eagle's Media
DNA	Deoxyribonucleic acid
ECL	Enhanced chemiluminescence
EDTA	Ethylene diamine tetraacetic acid
EE	Early endosome
EGF	Epidermal growth factor
EGF-R	Epidermal growth factor receptor
ER	Endoplasmatic reticulum

FBS	Fetal bovine serum
GFP	Green fluorescent protein
GGA	Golgi-localized, γ-earcontaining Arf-binding proteins
GLUT4	Glucose transporter 4
GSC	GLUT4 storage compartment
HA	Hemagglutinin
HEPES	4-(2-hydroxylethyl)-1-piperazine-ethanesulphonic acid
His-tag	6 x histidin protein tag
HRP	Horseradish peroxidase
IF	Immunofluorescence
Ig	Immunoglobulin
kDa	Kilo Dalton
LE	Late endosome
LHCNM2	lox-hygo-hTERT Cdk4-neo, subclone male 2
M6PR	Mannose-6-phosphate receptor
PAGE	Polyacryamide gelelecrophoresis
PBS	Phosphate buffered saline
PCR	Polymerase chain reaction
Pen	Penicillin
PIP	Phosphatidyl inositole
RNA	Ribonucleic acid
RNAi	RNA interference

RT	Room temperature
SDS	Sodium dodecyl sulfate
siRNA	Small interfering RNA
SNARE	soluble N-ethylmaleimide-sensitive factor attachment receptor
SNX	Sorting nexin
Strep	Streptomycin
STX	syntaxin
STxB	Shiga-Toxin subunit B
TBS-T	Tris buffered saline containing Tween20
Tfr	Transferrin
Tfr-R	Transferrin receptor
TGN	*Trans*-Golgi network
TGN46	TGN-localized protein of 46 kDa
v/v	Volume per volume
w/v	Weight per volume
WT	wildtype

List of figures

Chapter 1 - Introduction

Intracellular membrane transport

Eukaryotic cells are compartmentalized allowing for the creation of different reaction conditions within a single cell. The varying compartments formed are separated by membranes consisting of lipid bilayers. Therefore, resulting organelles are individualized forming specific water-based reaction milieus. However, this compartmentalization requires dedicated transport processes for nutrients, lipids or proteins to cross organelle boundaries. The transport of lipid bilayers and its enclosed cargo is collectively termed membrane transport. Membrane transport is required both for soluble and membrane-bound molecules. Transport is mainly achieved in small vesicles of $0.05 - 0.2$ μm diameter, although some exceptions exist. The composition, generation, sorting and fission of transport vesicles is a highly regulated process, involving a multitude of proteins, the interplay of which defines the exact nature of a transport vesicle. Failure to correctly traffic cargo, due to malfunction of its regulatory machinery has been demonstrated to result in a number of diseases.

Coat proteins

A key role in vesicular transport is played by coat proteins that are found on the surface of transport vesicles. The most extensively characterized coat is the clathrin coat, that is involved in transport emanating from the Golgi apparatus, endosomes and the plasma membrane. However, other coats mediate traffic between the endoplasmatic reticulum (ER) and the Golgi apparatus. Notably, distinct coats act in ER to Golgi and Golgi to ER

trafficking, making these coats far more specific. Furthermore, membrane transport processes have been described that occur without coat proteins.

The clathrin coat

This work concentrates on the function of clathrin heavy chain 22 (CHC22). This protein is the only human homologue to the well-characterized clathrin heavy chain 17. To understand CHC22-function I will introduce CHC17-function first, since large parts of this work compare the two clathrin heavy chains and understanding CHC17 is pivotal for understanding CHC22. The two variants were named for their respective encoding human chromosomes.

The clathrin coat is the best understood coat (Brodsky et al., 2001; Kirchhausen, 2000). Clathrin cages consist of pentagonal and hexagonal structures that form cages of varying size, depending on the membrane vesicle transported. The cage structure has been compared to soccer balls, fullerenes and Buckminster spheres. Several models of clathrin cages based on electron cryomicroscopy and crystal structures of discrete domains have been described (Fotin et al., 2004; Smith et al., 1998; ter Haar et al., 1998; Ybe et al., 1999). The best model available has a resolution of 12.5 Å (Fig. 1-1A).
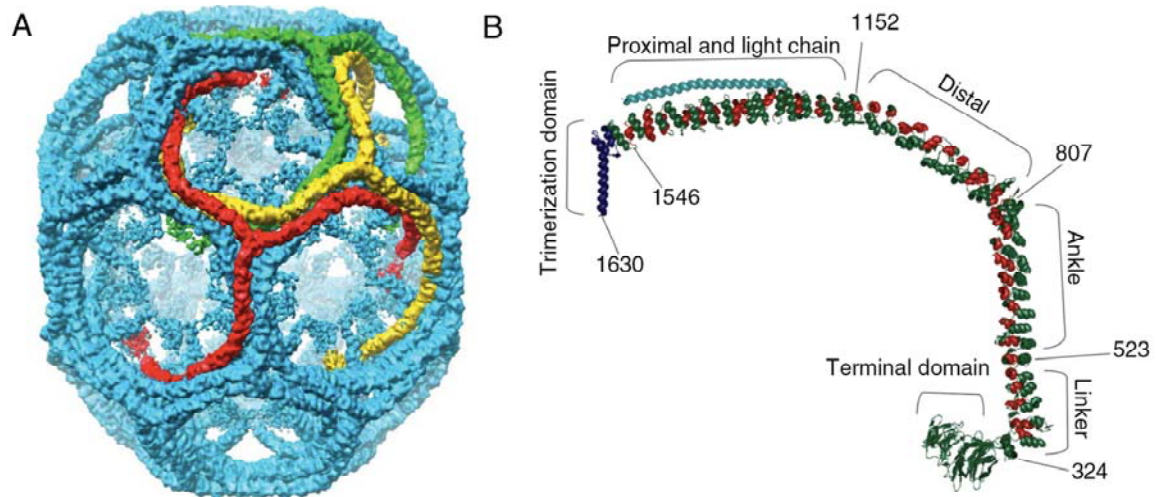
Fig. 1-1: Clathrin cages are formed of clathrin heavy chain. (A) Clathrin cage at 12.5 Å resolution (Fotin et al., 2004). Single triskelia are highlighted. (B) Domain structure of clathrin heavy chain 17 (Wilbur et al., 2005). Note that in this depiction 45 amino acids are missing from the c-terminus.

The functional unit of clathrin cages is the clathrin triskelion, named after its three-legged shape (Ungewickell and Branton, 1981). Assembly of triskelia into flat lattices on membranes and subsequent invagination of the lattice has been demonstrated to drive vesicle budding (Hinrichsen et al., 2006). Each triskelion consists of three CHC17 molecules that associate via their c-terminal trimerization domains (Fig. 1-1B). Triskelia are very stable and no monomeric CHC17 can be found in cells. In addition, each CHC17 binds one clathrin light chain molecule (CLC) via its proximal leg domain. Two variants of CLCs termed CLCa and CLCb exist in mammals. Their relative expression is tissue-dependent with splice variants present in neurons. Few functional differences have been observed. CLCb binds CHC17 with slightly higher affinity *in vitro* (Acton and Brodsky, 1990). However, both CLCs inhibit spontaneous triskelia assembly under physiological conditions and are therefore considered to be negatively regulators of cage assembly. In addition, CLCs bind to Huntingtin-interacting protein 1 (Hip1) and Hip1-

related protein (Hip1R), which in turn bind actin (Chen and Brodsky, 2005). Thus CLCs provide a bridge between budding vesicles and the actin cytoskeleton.

CHC17 does not bind membranes or membrane proteins directly. Contacts between CHC17 and the membrane are mediated by adaptor proteins. The interplay of various adaptor proteins is required for regulation and sorting specificity in clathrin-mediated transport.

Adaptor proteins for clathrin mediated vesicular trafficking

Numerous proteins have been described that modulate sorting of cargo and influence clathrin mediated vesicle budding (Benmerah and Lamaze, 2007; Owen et al., 2004; Ungewickell and Hinrichsen, 2007). Here, I will concentrate on two subsets of adaptors that play key roles in recognizing cargo, and establishing connections between cargo and clathrin, namely tetrameric adaptor proteins 1-3 (AP1-3) and monomeric Golgi-localized, γ-earcontaining Arf-binding proteins 1-3 (GGA1-3) (Fig 1-2).
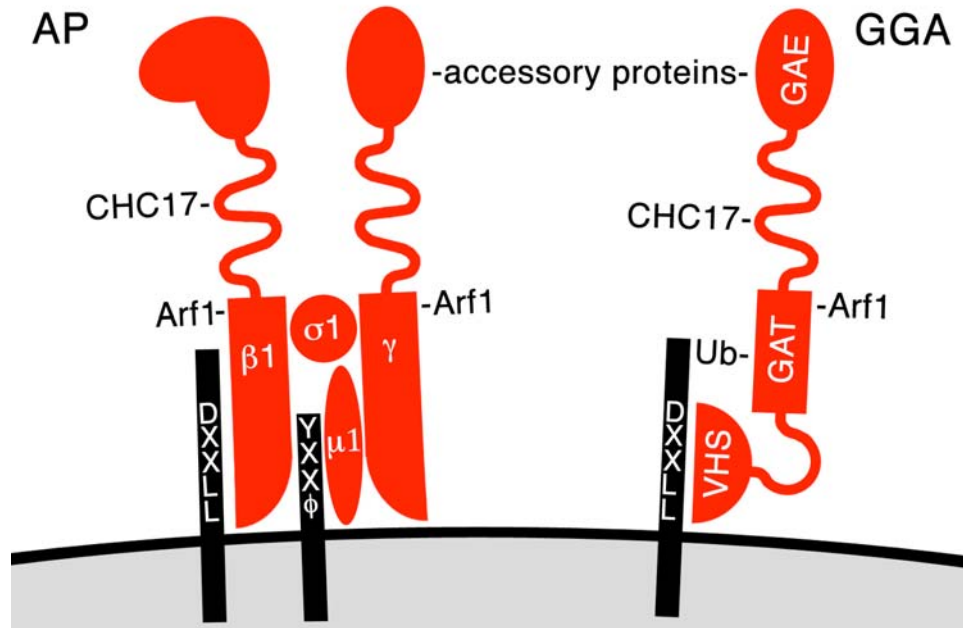
Fig. 1-2: Classes of adaptors: left: tetrameric adaptor protein complex exemplified by AP1. right: monomeric GGA adaptor. Note the similarities in clathrin binding region

The adaptor proteins AP1-3 consist of four subunits each that all display high homology among each other. All three adaptors recognize cargo, bind specific lipids and interact with CHC17. Their respective specificities for cargo and lipids result in differing localization within the cell. AP1 and AP3 act in clathrin-mediated sorting at the TGN and endosomes, while AP2 acts in clathrin-mediated endocytosis from the plasma membrane. AP2 function is best understood, but AP1 and AP3 are thought to act in similar fashion at their respective localizations. Adaptor proteins not only interact with cargo and membranes on the one hand and clathrin on the other, but they also interact with several accessory proteins. Accessory proteins are required for recognition of specific subsets of cargo and regulation of clathrin coat formation. At least some functions of adaptor proteins are regulated by phosphorylation resulting in affinity changes for various binding partners. The interplay of numerous weak interactions surrounding adaptor proteins are thought to result in initiation of a vesicle trafficking event. Interestingly, a fourth adaptor protein complex, AP4, has been described but this

complex does not bind CHC17 and is thought to be required for clathrin-independent trafficking steps.

GGAs are a separate class of adaptor proteins found at the TGN and endosomes. They qualify as adaptor proteins since they bind both cargo and CHC17 (Bonifacino, 2004). There are three GGAs in humans (GGA1-3) but few differences have been described between them. GGA1 and GGA3 can be autoinhibited, while GGA2 seems to be in a constitutively active form. GGAs have been shown to act cooperatively in cargo sorting at the TGN and GGA1 also interacts with AP1 (Bai et al., 2004; Ghosh et al., 2003b). However, both GGAs and AP1 bind the same motifs in cargo molecules and it is unknown if they act synergistically in cargo sorting or if they compete for cargo binding. An interesting feature of GGAs is their ability to recognize ubiquinated cargo at the endosome (Puertollano and Bonifacino, 2004). This demonstrates that GGAs may act independently of AP1 in endosomal sorting of ubiquitinated cargo.

Cargo in membrane traffic

As mentioned previously, membrane traffic occurs between various organelles and compartments. Therefore extensive sorting occurs at the site of emanating vesicles, since vesicles need to contain not only cargo but also factors required for the subsequent fusion (Bonifacino and Rojas, 2006; Maxfield and McGraw, 2004). Fusion specificity and the recognition of correct target membranes by vesicles is as complex as the initial sorting (Pfeffer, 2007). However, one commonly used approach to distinguish between individual transport routes is to characterize the cargo being transported. Using this approach, proteins that influence specific cargoes can be located in specific

transport routes. Model cargoes include transferrin-receptor (TfrR), epidermal growth factor receptor (EGFR) and Shiga-toxin subunit B (STxB) at the plasma membrane, as well as TGN46 and mannose-6-phosphate receptors (M6PR) emanating from the TGN. All of these cargoes traffic via endosomes and use distinct sets of proteins for their correct transport. CHC17 has been demonstrated to be part of individual sorting steps for all of the mentioned cargoes, except TGN46. TfrR and EGFR are internalized from the plasma membrane by means of CHC17-mediated endocytosis and subsequently recycled to the plasma membrane (TfrR) or degraded in the lysosome (EGFR). STxB is internalized in a clathrin-independent manner, however its endosomal sorting requires CHC17 (Saint-Pol et al., 2004). Although it has been demonstrated that TGN46 cycles between endosomes and TGN (unlike its murine counterpart TGN38, which also cycles via the plasma membrane) (Banting et al., 1998), very few proteins associated with its trafficking are known, one of them being Syntaxin 6 (Ganley et al., 2008). M6PR in contrast has been extensively studied as a receptor for hydrolases destined for lysosomes (Ghosh et al., 2003a). M6PR exit from the TGN and possibly also its sorting at the endosome is CHC17-dependent. There is some debate in the literature, however, regarding the nature of the endosomal compartment from which M6PR retrograde sorting is accomplished (Ganley et al., 2008; Rojas et al., 2007). It remains to be seen whether M6PR return to the TGN via early or late endosomes. Taken together, these model cargoes offer a toolbox with which individual trafficking routes can be distinguished, even though CHC17, possibly using distinct sets of adaptors, may be involved in multiple sorting steps.

Clathrin heavy chains

While much has been learned about the biology of CHC17 since its initial description (Pearse, 1976), the second isoform of clathrin heavy chain in humans remains largely a mystery. The encoding gene, CLTCL1 (old name: CLTD), was described by several groups over 10 years ago (Kedra et al., 1996; Long et al., 1996; Sirotkin et al., 1996). Expression of encoding RNA was found at low levels in all tissues with increased expression in testis and heart muscle. The highest expression levels were seen in skeletal muscle. The encoded protein has also been detected in a variety of cell lines and tissues (Liu et al., 2001; Towler et al., 2004a). Subsequent analysis and comparisons of the two clathrin heavy chain genes revealed that they are highly homologous, the resulting proteins showing 85% amino acid identity (Wakeham et al., 2005). The two clathrin heavy chains were separated during a gene dublication event that occurred 510-600 million years ago. This study also revealed that CHC22, while present in most vertebrates, is absent from mice. Instead, a pseudogene was discovered in the mouse genome indicating that mice lost the CLTCL1 gene later in evolution. Divergence analysis indicated that there are only 12 amino acid changes, that are evolutionarily conserved between the two clathrin heavy chain genes (Wakeham et al., 2005). Suspiciously, they are concentrated in the n-terminal domain required for adaptor protein interaction and the proximal leg domain required for binding CLCs. Indeed, previous work indicated that CHC22 does not bind CLCs in cells and it further differs from CHC17 by not binding the endocytic adaptor protein AP2 (Liu et al., 2001). However, CHC22 does bind the adaptor proteins AP1 and AP3, localizing CHC22 function in the vicinity of TGN and endosomes. To date, only one protein has been

described that interacts with CHC22 but not CHC17. The sorting nexin family member

SNX5 binds CHC22 in the proximal leg domain. Interestingly, this is the same region that

is occupied on the CHC17 molecule by CLCs (Towler et al., 2004a). An important

characteristic of CHC22 is its high expression in skeletal muscle. Indeed, in contrast to

CHC17, CHC22 is upregulated during muscle differentiation, suggesting that it could play

a specialized role in muscle biology (Liu et al., 2001).

Skeletal muscle differentiation

Skeletal muscle is a highly specialized tissue with the principal function of generating

movement. Its regular cellular functions are highly specialized and adapted to serve this

purpose. Mature muscle is generated in a complicated differentiation process

encompassing several characteristic steps (Le Grand and Rudnicki, 2007) (Fig. 1-3).
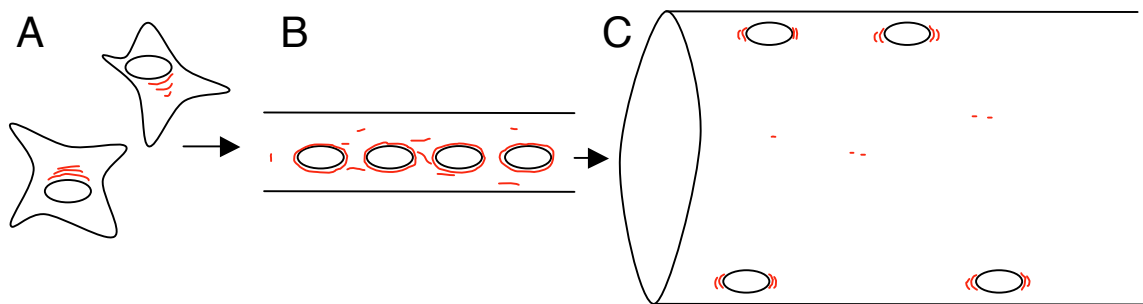
Fig. 1-3: Skeletal muscle differentiation: (A): mononucleated precursor myoblasts with regular Golgi localization. (B) multinucleated myotubes with centrally located nuclei surrounded by Golgi membranes. (C) multinucleated myofibers with nuclei and Golgi membranes located in close proximity to the plasma membrane. Also, Golgi membranes are found in the core of fibers

I will briefly discuss muscle differentiation with an emphasis on membrane

compartments (Towler et al., 2004b). Precursor cells to mature musclefibers are

mononucleated myoblasts that display regular Golgi morphology (Fig. 1-3A). Upon differentiation myoblasts fuse and elongate to form myotubes (Fig. 1-3B). Golgi membranes show a very characteristic localization in these cells as they are surrounding myonuclei. Interestingly, centrosomal markers such as pericentrin and γ-tubulin are also found surrounding nuclei (Bugnard et al., 2005). Further maturation of myotubes leads to establishment of the contractile apparatus. In this process membranes and nuclei are relocated in close proximity of the plasma membrane, resulting in the formation of mature myofibers (Fig. 1-3C). Myofibers exhibit specialized membrane domains such as T-tubules and myotendinous and neuromuscular junctions connecting fibers with other fibers and neurons respectively. Furthermore myotubes and myofibers exhibit specialized membrane pathways and compartments supporting their physiological function. One such compartment is the GLUT4 storage compartment.

The GLUT4 storage compartment

Skeletal muscle generates movement. This requires large amounts of energy that muscle takes up from the blood stream in the form of glucose. All tissues including skeletal muscle express glucose transporters for constitutive glucose uptake at their surface. However, skeletal muscle and adipose tissue have developed a second, inducible system in addition to the ubiquitous uptake of glucose from the bloodstream. In skeletal muscle this regulated glucose-uptake system is activated under conditions of high glucose levels in the bloodstream, indicated by increased insulin levels, or under conditions of high glucose requirement in the muscle, namely exercise. The system works by increasing the number of glucose transporter molecules on the cell surface.

The glucose transporter that is inducible in this way is isoform GLUT4, and the compartment from where GLUT4 is translocated to the plasma membrane is termed GLUT4 storage compartment (GSC). Failures in this system have been implicated in type II diabetes (Bryant et al., 2002; Huang and Czech, 2007).

The GSC is a specialized compartment storing GLUT4 under basal conditions (Fig 1-4).
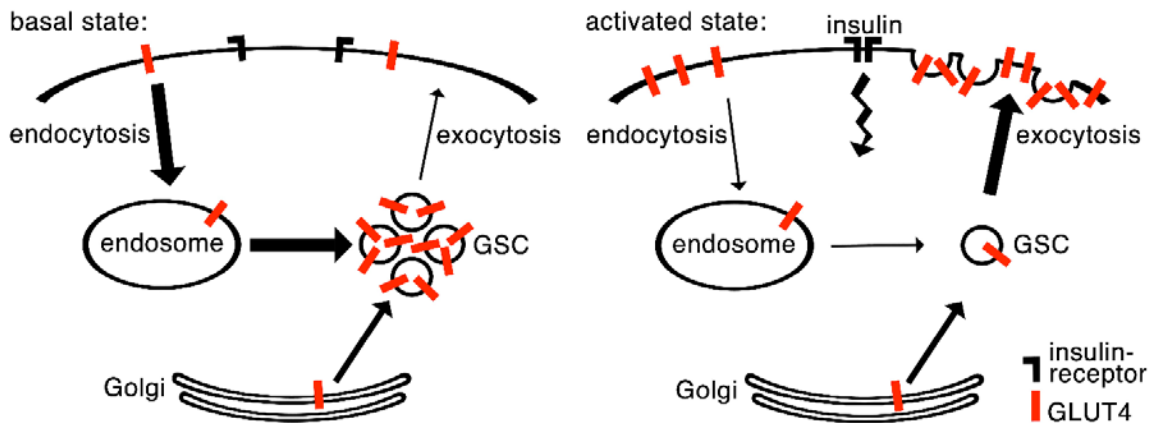
Fig. 1-4: The GLUT4 storage compartment: left: GLUT4 accumulation in the GSC under basal conditions. Note the high rates of GLUT4 endocytosis and sorting into the GSC depicted by thick arrows. Right: upon insulin activation a reversal in the rates of endo- and exocytosis occurs resulting in net accumulation of GLUT4 at the plasma membrane

Under basal conditions, characterized by low blood glucose and hence low insulin levels, the rate of GLUT4 endocytosis and sorting into the GSC is high. Upon activation of the GSC by means of exercise or high blood glucose levels resulting in increased insulin levels, a reversal in the rates of GLUT4 endo- and exocytosis is induced. This results in translocation of GLUT4 to the plasma membrane, where an increased amount of glucose transporters leads to increased glucose influx.

The molecular mechanism underlying this complex system and possible involvement of clathrin heavy chains are only beginning to be unveiled. CHC17 has been demonstrated to at least partially mediate GLUT4 endocytosis and recycling back to the plasma

membrane from endosomal membranes (Antonescu et al., 2008; Huang et al., 2007; Li et al., 2007). In addition, members of the GGA-family of monomeric clathrin adaptors have been implicated in exporting newly synthesized GLUT4 from the TGN and possibly the endosome, although data is conflicting in this regard. (Li and Kandror, 2005; Watson et al., 2004; Watson and Pessin, 2008). Several other proteins have been identified that play roles in the generation and function of the GSC as well as trafficking of GLUT4, among them the SNARE-proteins VAMP2 and Syntaxin 6 (Williams and Pessin, 2008). Notably, the vast majority of this data was gathered in an adipocyte cell line generated from mice (3T3-L1). Importantly, fundamental differences have been described in glucose homeostasis between mice and humans. Generally, blood glucose levels are controlled to a much higher degree by the release of glucose from the liver in mice, whereas humans control their blood glucose levels primarily through the regulated uptake of glucose from the bloodstream by skeletal muscle as described here (Bruning et al., 1998; Michael et al., 2000).

Aim

The overall aim of this work is to establish the function of CHC22. To this end comparative studies between CHC17 and CHC22 are carried out concentrating on cell culture approaches. Model systems include the epithelial-derived cell line HeLa for analysis of ubiquitous CHC22 functions and the human skeletal muscle cell line LHCNM2 for analysis of CHC22 in this specialized cell type exhibiting highest levels of CHC22 expression.

The studies that will be described show a role for CHC22 independent of CHC17 in

endosomal sorting. One cargo depending on CHC22 is characterized in GLUT4.

Chapter 2 - Distinct functions for clathrin heavy chain isoforms in endosomal sorting

The text of this chapter is a manuscript in preparation. Some additional data will be incorporated pending outcome of experiments as discussed at the end of the chapter.

Authors contributions:

CE designed and conducted research and wrote the manuscript. CYC first described the phenotype presented in figure 2-3c. FMB designed research and gave editorial input on the manuscript.

Specifically, I generated all figures, with CYC first describing the finding presented in figure 2-3c. Also, I wrote the manuscript with editorial advice from FMB.

Distinct functions for clathrin heavy chain isoforms in endosomal sorting

Christopher Esk[1], Chih-Ying Chen[1] and Frances M. Brodsky[1,2]

[1]The G.W. Hooper Foundation, Departments of Biopharmaceutical Sciences,

Pharmaceutical Chemistry and Microbiology and Immunology, University of California,

San Francisco, CA 94143, USA

[2]To whom correspondence should be addressed. Email: Frances.Brodsky@ucsf.edu

Abstract

The ubiquitious clathrin heavy chain, CHC17, is well characterized as a vesicle coat component and has recently been implicated in Golgi biogenesis and mitosis. The 85% sequence identity between CHC17 and its isoform CHC22 does not predict the extent to which CHC22 shares CHC17 functions. The comparative intracellular roles of the two clathrin heavy chains were analyzed in HeLa. CHC22 was not recruited to the mitotic spindle nor did its depletion affect endocytosis, demonstrating that these are unique functions of CHC17. However, upon siRNA depletion of CHC17, CHC22 showed increased membrane association and depletion of either CHC resulted in distinct trafficking defects of various cargoes between endosome and TGN. Depletion of both clathrin heavy chains had a more pronounced effect on Golgi compartments than depletion of CHC17 alone, indicating that Golgi biogenesis is influenced by the distinct trafficking pathways of both clathrins. In differentiated human myoblast cultures, similar segregation of CHC functions was detected, revealing the endosome-TGN transport as the pathway in which CHC22 exerts its muscle-specific function.

Introduction

Clathrin heavy chain 17 (CHC17) is well characterized as a coat protein required for vesicle formation at the plasma membrane, the *trans*-Golgi network and endosomes (Brodsky et al., 2001; Conner and Schmid, 2003). Most vertebrates and mammals have a second clathrin heavy chain isoform (CHC22; names are designated in accordance with the genes' position on human chromosomes) with *mus musculus* being the notable exception having only a pseudogene (Wakeham et al., 2005). CHC22 exhibits limited expression in all tissues with high expression in cardiac and skeletal muscle (Sirotkin et al., 1996). Comparisons between CHC17 and CHC22 show 85% amino acid identity, with amino acid changes occurring throughout the whole gene. Interestingly however, several amino acid changes, predominantly in the n-terminal domain and the proximal leg domain, are evolutionarily conserved, indicating that they are functionally relevant (Wakeham et al., 2005).

CHC17 forms trimers, so-called triskelia that serve as the functional unit to assemble into flat lattices on membranes and eventually coats on vesicles. It has been demonstrated that vesicle formation requires CHC17 for invaginating the membrane (Hinrichsen et al., 2006). CHC17 binds clathrin light chains (CLC) that act in a regulatory fashion on coat formation (Liu et al., 1995), although recent data suggest CLC are not essential in this process (Poupon et al., 2008). CHC17 is recruited onto membranes by adaptor proteins that bind to cargo destined for trafficking. Also, there are several accessory proteins required for cargo selection. The interplay between these factors determines the fate of the cargo (Benmerah and Lamaze, 2007; Ungewickell and Hinrichsen, 2007). Recently

CHC17 has been shown to be required in additional processes, namely spindle formation in mitosis (Royle et al., 2005), and Golgi reassembly after drug-induced fragmentation (Radulescu et al., 2007). Depletion of CHC17 leads to malformation of the mitotic spindle and incomplete stack separation within the Golgi.

We previously demonstrated that CHC22 forms trimers but it does not stably associate with CLC. Also, CHC22 does not bind the adaptor protein AP2 – the main regulator of clathrin-mediated endocytosis at the plasma membrane. However, it has been shown that CHC22 can associate with the adaptor proteins AP1 and AP3, which are localized at the TGN and endosomes, suggesting a role in transport processes in these compartments. A unique interaction partner of CHC22 has been found in sorting nexin 5 (Liu et al., 2001; Towler et al., 2004a). Sorting nexin 5 has been implicated in macropinocytosis and may act as part of the retromer complex (Kerr et al., 2006; Wassmer et al., 2007). Still, a pathway for CHC22 function has yet to be defined.

Early endosomal sorting is a complex process, as numerous cargo molecules have to be destined for a variety of targets (Bonifacino and Rojas, 2006; Maxfield and McGraw, 2004). Several cargo molecules have been shown to traffic at least partly through the early endosome en route from and to other destinations within the cell and they serve as markers for distinct trafficking routes. Cargoes that are sorted at the endosome upon arrival from the plasma membrane include the transferrin receptor (Harding et al., 1983), which is recycled back to the plasma membrane, Shiga-Toxin, which traverses the endosome en route to the TGN and subsequently the endoplasmatic reticulum (Mallard et al., 1998) and EGF, which upon endocytosis is trafficked via the early endosome to lysosomes for degradation (Hanover et al., 1984). Cargoes arriving from the TGN

include mannose-6-phosphate receptors (M6PR) and TGN46 both of which are ultimately recycled to the TGN (Banting et al., 1998; Geuze et al., 1985). However, while TGN46 is thought to recycle back to the TGN directly from early endosomes, a significant portion of M6PR is trafficking via the late endosome (Ganley et al., 2008). Elucidating CHC17's role in these sorting events has been complicated by the fact that at least some of these cargoes also require CHC17 for trafficking from their respective origins.

Here we compare properties of the two clathrin heavy chain isoforms using siRNA-mediated depletion. We show that CHC22 does not act together with CHC17 but instead has an independent role in sorting specific cargo at the early endosome. Both clathrin heavy chains contribute to Golgi morphogenesis by means of their independent functions.

Results

CHC22 associates with peripheral membranes but does not partake in CHC17 function

We were interested in the relationship between the two clathrin heavy chains CHC17 and CHC22. While the ubiquitous CHC17 is well characterized, very little is known about its homologue CHC22. Polyclonal antibodies against CHC22 were raised in rabbits against the trimerization domain of CHC22 (aa 1521-1640) as well as a peptide (aa 1549-1563). Both antibodies were purified to recognize CHC22 but not CHC17 and gave identical results in subsequent studies. Immunofluorescence analysis revealed a number of vesicles carrying CHC22 scattered throughout the cytoplasm, with a slight focus in the perinuclear area (Fig. 2-1). Some of these vesicles also seemed to carry CHC17 although very little direct colocalization was observed (Fig. 2-1a).
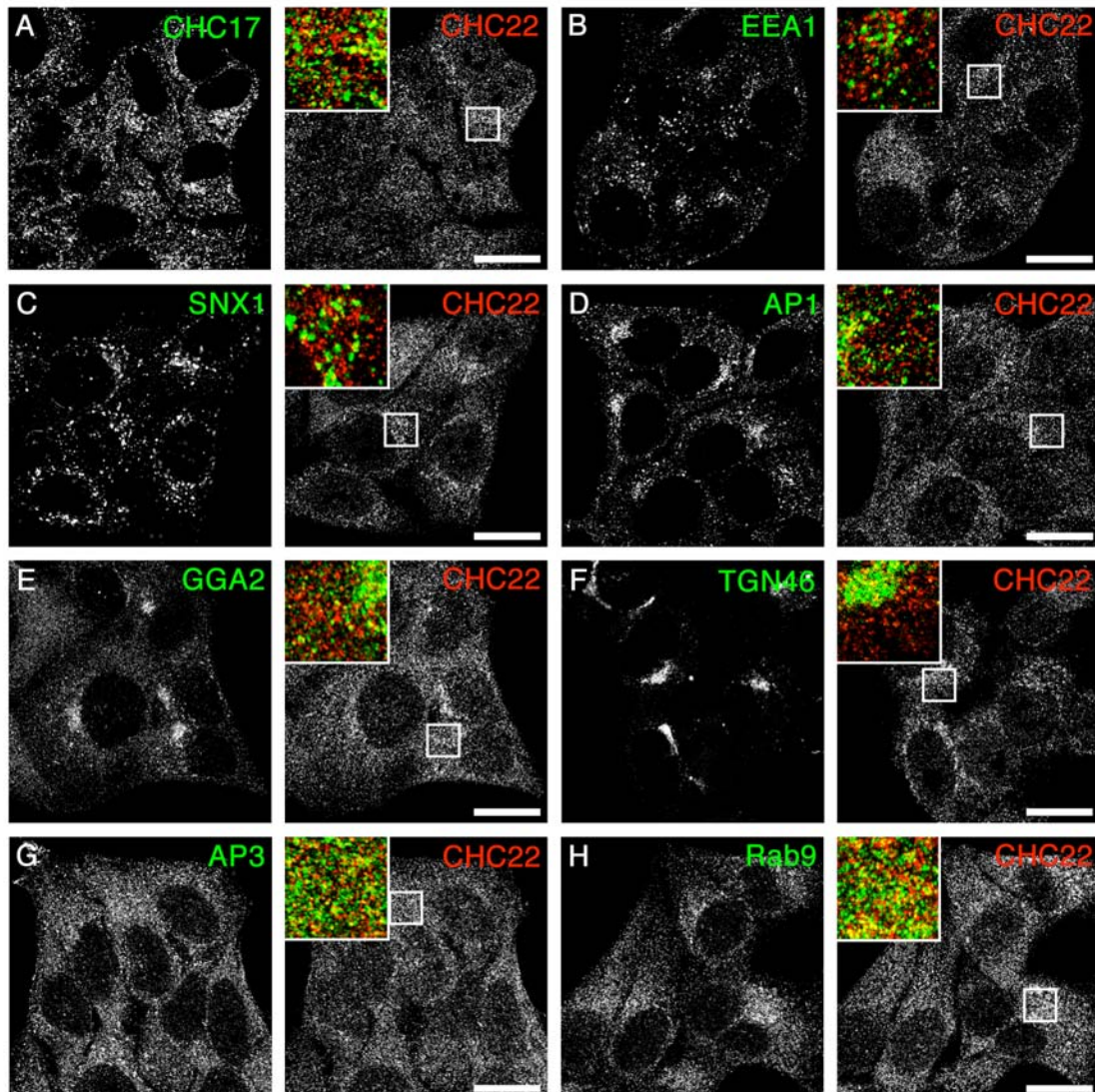
Figure 2-1: CHC22 colocalizes partially with late endosomes but not early endosomes or the TGN: HeLa cells were grown on coverslips, processed for immunofluorescence and stained using a polyclonal antibody against CHC22 (right row, red in merge). Simultaneous staining were performed using monoclonal antibodies (left row, green in merge) against CHC17 (A), EEAI (B), SNX1 (C), γ-adaptin (D) GGA2 (E), AP3 (G), Rab9 (F) and a sheep polyclonal antibody against TGN46 (E).

The intracellular distribution of endogenous CHC22 was further characterized regarding known cellular markers for various organelles. Previous results indicated that CHC22 does not associate biochemically with either CHC17, clathrin light chains or the clathrin adaptor protein AP-2 directly, however, it co-immunoprecipitates with the clathrin adaptor proteins AP-1 and AP-3. Also, overexpressed CHC22 partially colocalized with both AP-

1 and AP-3 (Liu et al., 2001). This suggested that CHC22 acts in the TGN and early endosomes. Contrary to this hypothesis, at steady state endogenous CHC22 does not colocalize with the early endosome as indicated by costaining with EEAI (Fig. 2-1b) or SNX1-positive transport vesicles (Fig. 2-1c). Neither does it seem to be accumulated in a significant manner at the TGN as marked by the clathrin adaptors AP1 (Fig. 2-1d) and GGA2 (Fig. 2-1e) or TGN46 (Fig. 2-1f). However, some colocalization along with a related staining pattern for CHC22 was observed with AP3 (Fig. 2-1g) and Rab9 (Fig. 2-1h), a marker for the late endosome (Lombardi et al., 1993). In contrast, CHC17 does not colocalize with Rab9 (data not shown). This data suggests that CHC22 is concentrated on vesicular membrane structures, some of which also carry at least partially CHC17, AP3 and Rab9.

We used siRNA-mediated depletion of clathrin heavy chains to gain further insight into their relationship and potential differing functions. Transfecting siRNAs specific for either clathrin heavy chain resulted in strong downregulation of the respective targets. (Fig. 2-2a). Interestingly, CHC22 was stabilized in CHC17-KD cells, while the reverse was not true. Also, stabilities of clathrin light chains were monitored. CHC17 is required for CLC stability, while CHC22 is not, in accordance with earlier data that CLC do not bind CHC22 (Liu et al., 2001). Preparations of heavy and light membrane fractions as well as a cytosolic fraction from cells treated with siRNA against CHC17 revealed that in these cells CHC22 is accumulated on light membranes as CHC22-levels in these fractions increase while CHC22-levels in the cytosol are decreased (Fig. 2-2b). This argues for a
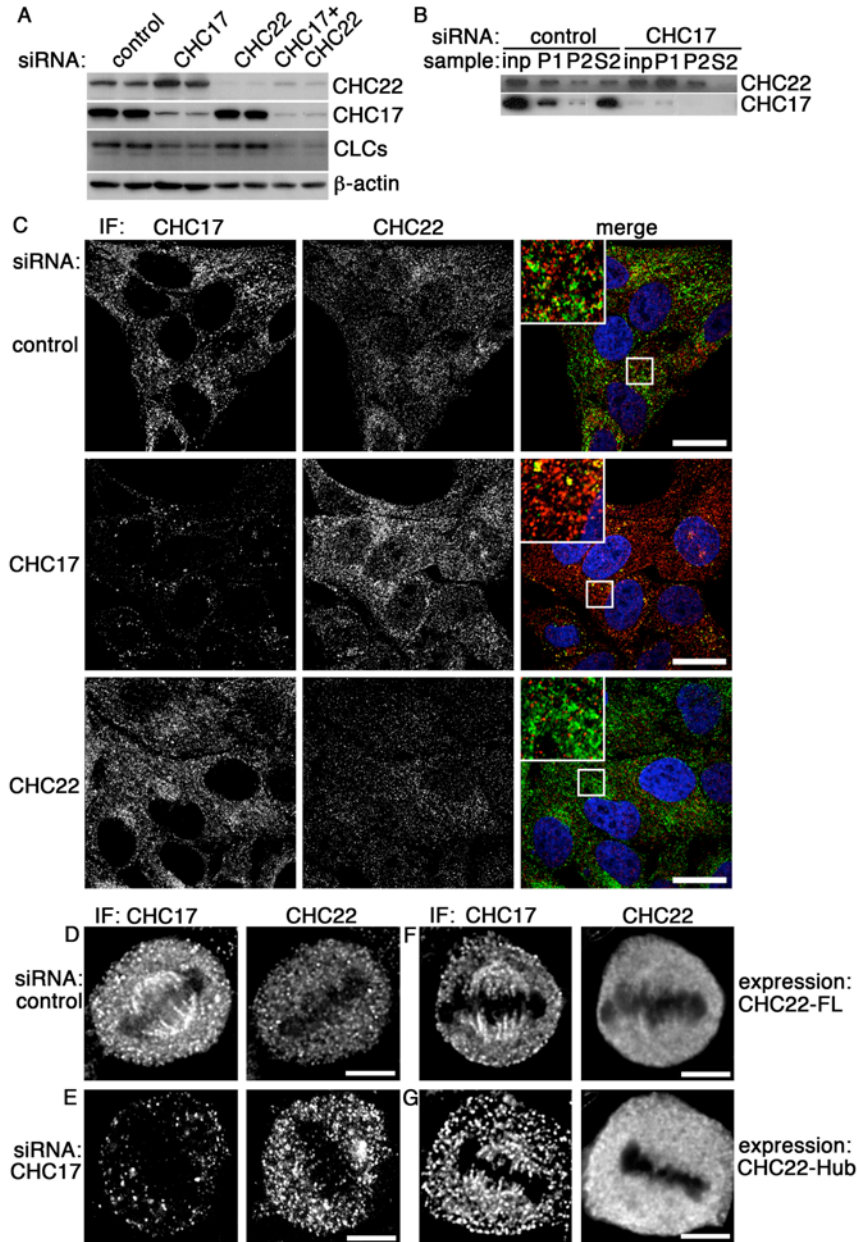
Figure 2-2: CHC17 downregulation leads to stabilization of CHC22 on membranes but not on mitotic spindles. (A) HeLa cells were treated with control siRNA or siRNA against CHC17, CHC22 and CHC17 together with CHC22 as described in material and methods. Whole cell lysates were prepared, separated in SDS-PAGE and transferred onto nitrocellulose membrane. Membranes were probed with the indicated antibodies. β-actin serves as a loading control. (B) HeLa cells were treated with either control siRNA or siRNA against CHC17. Whole cell lysates were fractionated in a nuclear fraction (P1, 3000 x g), a membrane fraction (100.000 x g) and a soluble fraction (S) and analyzed in immunoblotting with the indicated antibodies. (C) HeLa cells treated with siRNA as indicated were processed for immunofluorescence and stained for CHC17 and CHC22. (D) WT HeLa cells were processed for immunofluorescence. Mitotic cells were imaged as determined by condensed chromatin. (E) Experiment as in D using HeLa cells depleted of CHC17 using specific siRNA. (F) Experiment as in D using HeLa cells expressing full-length CHC22 under the control of inducible T7 promotor. (G) Experiment as in D using HeLa cells expressing CHC22-Hub fragment under the control of inducible T7 promotor.

stabilization of CHC22 in cells depleted of CHC17 due to increased membrane association. Interestingly, even in control cells the ratio of membrane-bound to soluble CHC22 is higher than for CHC17. Similar results were obtained in immunofluorescence experiments (Fig. 2-2c). We note an accumulation of CHC22 in the perinuclear area in CHC17-depleted cells when compared to control transfected cells. Vice versa, CHC17 is not affected by depletion of CHC22 either in membrane association (data not shown) or immunofluorescence (Fig. 2-2c). Recently an additional function of CHC17 has been revealed in spindle assembly of mitotic cells (Royle et al., 2005). In contrast to CHC17, CHC22 was not found on spindles in mitotic cells (Fig. 2-2d). Depletion of CHC17 did not lead to spindle recruitment of CHC22 either (Fig. 2-2e). Furthermore, overexpressing a T7-CHC22 full-length construct (Liu et al., 2001) in an attempt to force CHC22 onto spindles resulted in a similar distribution as a c-terminal T7-CHC22-Hub construct (aa 1074-1640) (Fig. 2-2f, g). This construct was used as a control, as the corresponding CHC17-fragment cannot be recruited to the spindle, due to the lack of the n-terminal domain despite its ability to trimerize (Royle et al., 2005). These results indicate that CHC22 does not partake in spindle association as CHC17 does. A notable difference in CHC22-decorated membranes and Golgi membranes coated by CHC17 was the sensitivity to Brefeldin A (BFA), a drug that inhibits Golgi-formation (Lippincott-Schwartz et al., 1989). Whereas CHC17 staining is perturbed in the perinuclear area in cells treated with BFA, CHC22-staining appears normal, indicating that CHC22 recruitment is Arf1-independent (Fig. 2-3a). Also, clathrin-mediated endocytosis of transferrin-receptor, which is strongly inhibited in CHC17-depleted cells (Hinrichsen et al., 2003), (Motley et al., 2003) is not affected in CHC22-depleted cells (Fig. 2-3b). This finding is consistent with CHC22 not binding AP-2, the main adaptor protein required for receptor-mediated endocytosis.
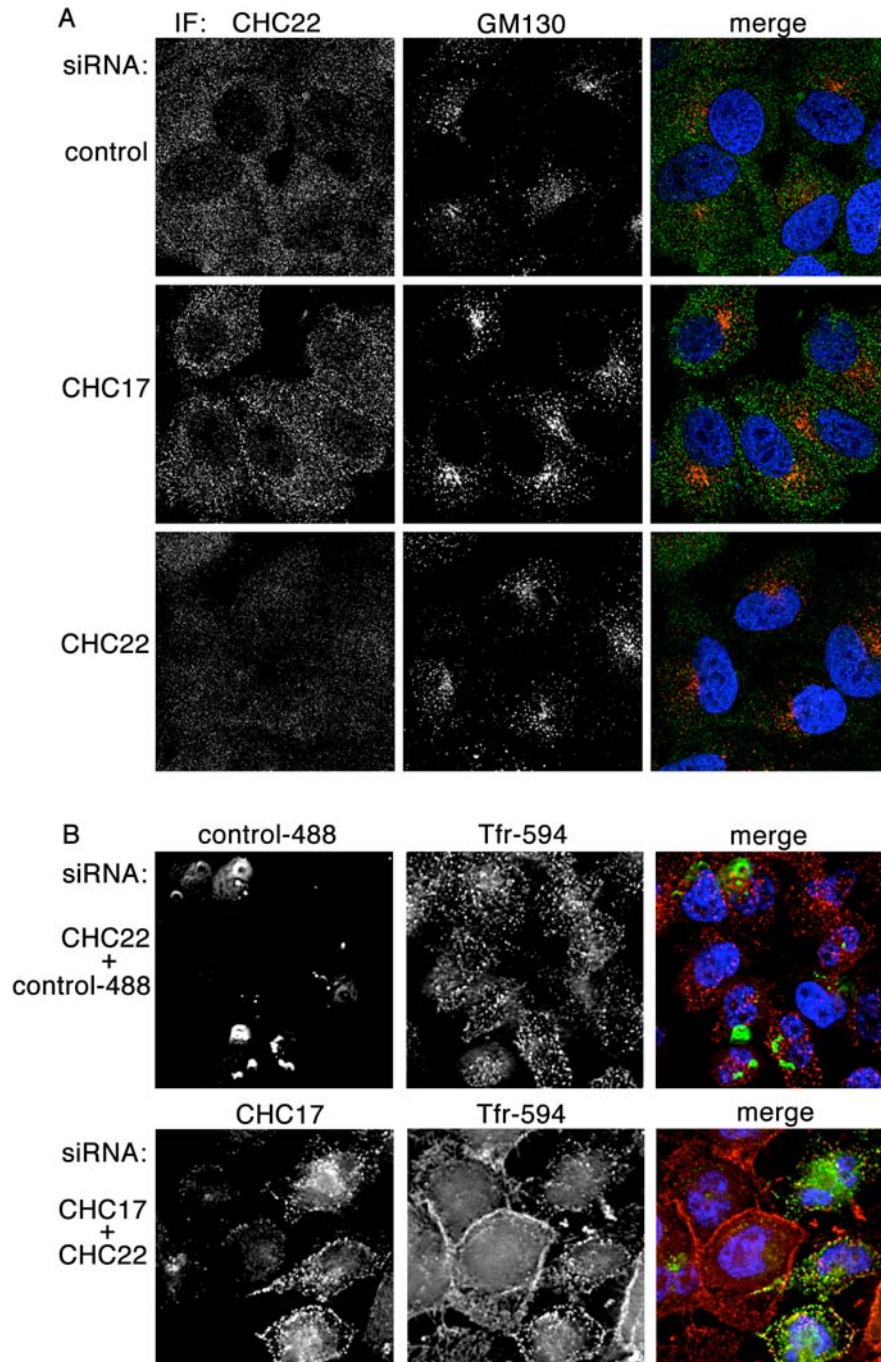
Figure 2-3: BFA-treatment does not prevent CHC22 membrane association and depletion of CHC22 does not affect endocytosis. HeLa cells were depleted of CHC17 and CHC22 using specific siRNAs as indicated, incubated in the presence of BFA for 45 min., processed for immunofluorescence and stained using antibodies against CHC22 and GM130 as indicated. GM130 served as an internal control for Golgi fragmentation. (B) HeLa cells were grown on coverslips and transfected with combinations of fluorescence-labelled control siRNA and siRNA targeting CHC22 or siRNAs targeting CHC17 and CHC22. Cells were incubated with fluorescent transferrin as described in material and methods and internalization was allowed for 20 min. Cells were then fixed and processed for immunofluorescence using the indicated markers.

Taken together, we found no evidence for CHC22 acting together with or substituting for CHC17.

CHC17 and CHC22 act independently in endosomal sorting

We previously showed that overexpression of a c-terminal T7-CHC22-Hub construct (aa 1074-1640) affects mannose-6-phosphate receptor localization in that it is dispersed from its normal perinuclear focus throughout the cell (Liu et al., 2001). Overexpression of either a T7-CHC22 full-length construct (Liu et al., 2001) or a n-terminal GFP-CHC22-TD construct (aa 1-450, data not shown) did not have the same effect. Interestingly the corresponding CHC17-Hub fragment has an inhibitory effect on receptor-mediated endocytosis, acting as a dominant-negative mutant in this process (Bennett et al., 2001; Liu et al., 1998). Therefore we assessed the roles of clathrin heavy chains in M6PR-trafficking in cells depleted of clathrin heavy chains. M6PRs are exported from the TGN, where they bind hydrolases destined for the lysosome, in a CHC17 and AP-1 dependent manner (Meyer et al., 2000). Whereas M6PR was localized loosely in the perinuclear area in control cells, CHC17-depletion lead to a very tight perinuclear localization of M6PR, presumably the TGN (Fig. 2-4a). This is consistent with previous data (Hinrichsen et al., 2003). In contrast, depletion of CHC22 led to a different phenotype in that M6PR was dispersed throughout the cytosol in small vesicular structures (Fig. 2-4a). We note that membranes carrying M6PR in CHC22-depleted cells do not carry CHC17. To test whether the redistribution of M6PR in cells depleted of either clathrin heavy chain had effects on M6PR-function we measured the secretion of the lysosomal hydrolase
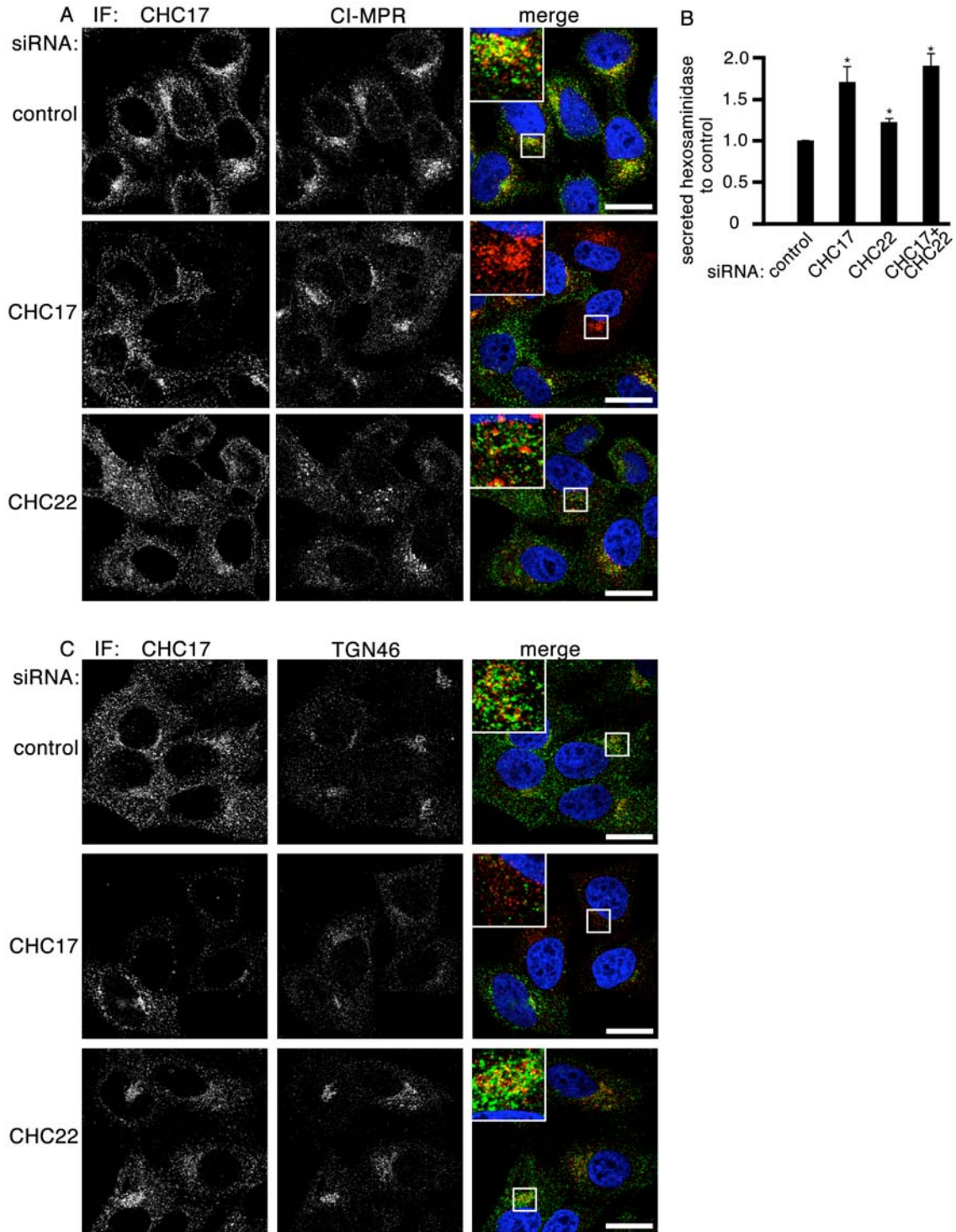
Figure 2-4: CHC17 and CHC22 affect CI-MPR- and TGN46 function in differential ways. (A) HeLa cells were depleted of CHC17 and CHC22 using specific siRNAs as indicated, processed for immunofluorescence and stained using antibodies against CHC17 and CI-MPR as indicated. (B) HeLa cells were treated with indicated siRNAs and intra- and extracellular Hexosaminidase activity was measured as described in material and methods. Depicted are ratios of extracellular to intracellular Hexosaminidase activities normalized against control ratios (n=5). (C) HeLa cells were depleted of CHC17 and CHC22 using specific siRNAs as indicated, processed for immunofluorescence and stained using antibodies against CHC17 and TGN46 as indicated.

hexosaminidase (Fig. 2-4b) Newly synthesized hexosaminidase is trafficked to the lysosomes by means of M6PR. Impairment of this pathway leads to increased secretion of hexosaminidase due to missorting at the TGN (Riederer et al., 1994). Secreted hexosaminidase-levels were measured in CHC17- and CHC22-depleted cells and normalized to control levels. Cells depleted of CHC17 exhibited a 70% increase in secreted hexosaminidase, while CHC22-depleted cells exhibited a 22% increase. Therefore the effect of CHC17-depletion was much stronger than the effect of CHC22-depletion, however both were statistically significant. Interestingly, in cells treated with siRNA against both CHC17 and CHC22 secreted hexosaminidase increased by 90% suggesting additional effects of depleting both clathrin heavy chains, although the difference between CHC17- and CHC17 + CHC22-depleted cells was not statistically significant in this set of experiments. The vesicular staining pattern of M6PR in CHC22-depleted cells was reminiscent of endosomal staining. To test the possibility of M6PR being retained in early endosomes, we costained clathrin heavy chain depleted cells for M6PR and the early endosome antigen I (EEAI). It has been reported that M6PR localize to early endosomes in cells depleted of retromer, a protein complex required for M6PR-trafficking out of early endosomes (Arighi et al., 2004), (Seaman, 2005). Therefore we used depletion of the retromer-subunit sorting nexin 1 (SNX1) as a control. In CHC17-depleted cells EEAI-localization seemed shifted from its normal staining pattern throughout the cell towards a perinuclear localization (Fig. 2-5). This, again, is in accordance with previous observations (Hinrichsen et al., 2003). CHC22-depleted cells, however, showed little overall change in EEAI localization, although we frequently noted extended, tubular structures. Importantly, M6PR did not colocalize with EEAI, despite a similar staining pattern, implying that M6PR is retained in a compartment other than the early endosome. In contrast, SNX1-depleted cells showed colocalization of M6PR and
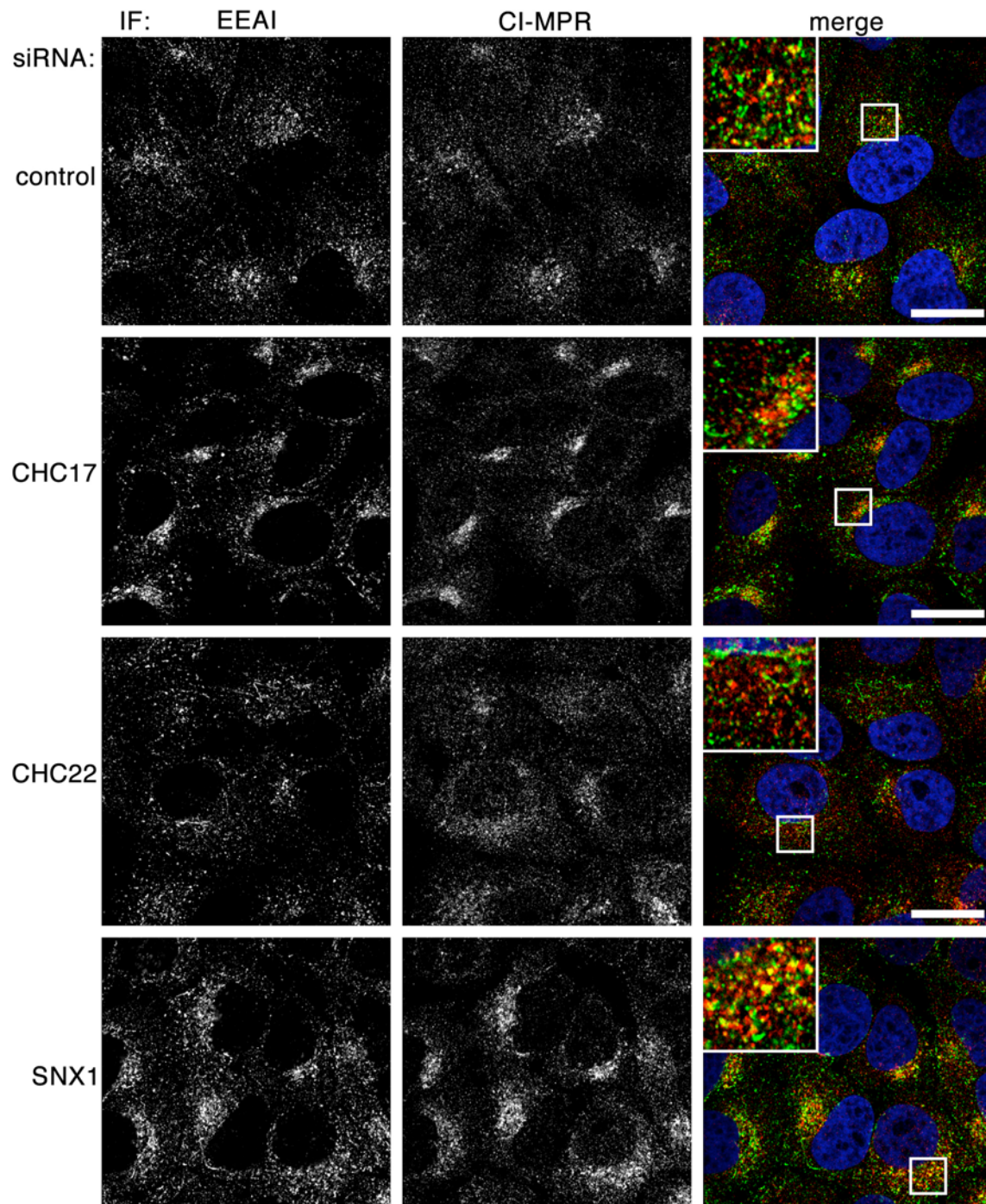
Figure 2-5: M6PR is not retained in early endosomes in cells depleted of CHC22. HeLa cells were depleted of CHC17, CHC22 and SNX1 using specific siRNAs as indicated, processed for immunofluorescence and stained using antibodies against EEAI and CI-MPR as indicated.

EEAl mirroring literature data (Seaman, 2004). This data indicates that both CHC17 and CHC22 are implicated in the trafficking of M6PR acting at different steps in M6PR cycling. Also, CHC17 and CHC22 may not compensate their respective roles for one another.

To compare the findings on M6PR-trafficking with other molecules that traffic between the TGN and endosomes we assessed TGN46 in clathrin heavy chain depleted cells. Differences in M6PR and TGN46 transport have recently been exploited to distinguish retrograde pathways from the endosome to the TGN (Ganley et al., 2008). TGN46 cycles between the TGN and the early endosome with the vast majority being localized to the TGN at steady state. However, unlike its rodent homologue TGN38, TGN46 does not traffic via the plasma membrane (Banting et al., 1998). Immunofluorescent analysis of TGN46 in control cells showed strong perinuclear staining indicative of the TGN-localized pool of TGN46 (Fig. 2-4c). In contrast, CHC17-depletion leads to a dispersal of TGN46 throughout the cytoplasm. Also, the fluorescent intensity appeared diminished when compared to control cells. This effect seemed to be CHC17-specific, since cells depleted of CHC22 exhibited normal TGN46 localization. Immunoblotting of lysates from siRNA-treated cell revealed that TGN46-levels were drastically reduced in CHC17-depleted cells, matching immunofluorescence (data not shown). CHC22-depleted cells contained TGN46-levels resembling control levels. This demonstrates that unlike M6PR, TGN46 trafficking is independent of CHC22.

Since both TGN46 and M6PR cycle between TGN and endosomes, it is difficult to assess the potential roles clathrin heavy chains play in trafficking cargo from both compartments. Therefore we used Shiga-Toxin B (STxB) as a cargo probe since its

trafficking is unidirectional (Mallard et al., 1998). Upon clathrin–independent entry into cells, STxB is trafficked via EEAI-positive early endosomes in a CHC17- and retromer-dependent step to the TGN (Bujny et al., 2007; Saint-Pol et al., 2004). Interestingly, it has been proposed that CHC17 and retromer act in a sequential manner, although both are required for exit of STxB from the early endosome with CHC17 coating defining microdomains, which are subsequently tubulated by retromer (Popoff et al., 2007). We tested the transport of STxB in cells depleted of clathrin heavy chains. After internalizing for 15 min in control cells or cells depleted of either clathrin heavy chain, STxB was found to colocalize with EEA (Fig. 2-7) and after 60 minutes STxB showed Golgi-localization in control cells (Fig. 2-6), resembling described kinetics (Saint-Pol et al., 2004). In contrast, CHC17-depleted cells showed STxB to be dispersed and colocalized with EEAI (Fig. 2-6, Fig. 2-7), even after 60 minutes of internalization again mirroring published data (Saint-Pol et al., 2004). To our surprise, under the same uptake-conditions CHC22-depleted cells also exhibited dispersed STxB-staining (Fig. 2-6). Importantly though, in case of CHC22-depleted cells, STxB was not colocalized with EEAI-positive structures (Fig. 2-7) suggesting that STxB is retained in a post- early endosome compartment, since STxB trafficks through an EEAI-positive compartment after 15 min. of internalization.
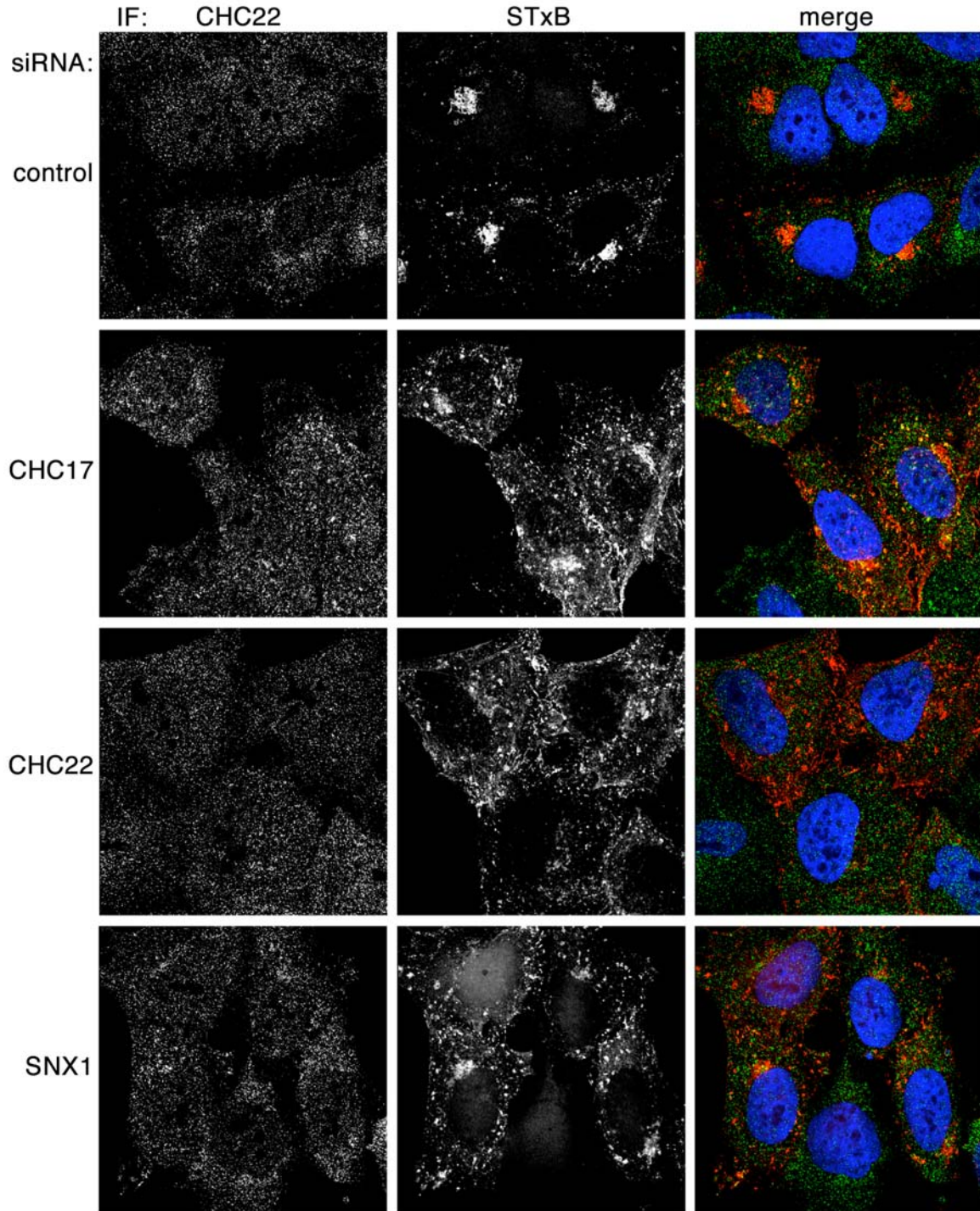
Figure 2-6: CHC17, CHC22 and SNX1 affect Shiga-toxin trafficking: HeLa cells were depleted of CHC17, CHC22 and SNX1 using specific siRNAs as indicated. Fluorescent Shiga-toxin in fresh media was bound to cells for 30 min on ice, washed in PBS and chased for 60 min. in fresh media at 37C. Cells were fixed, processed for immunofluorescence and stained using an antibody against CHC22.
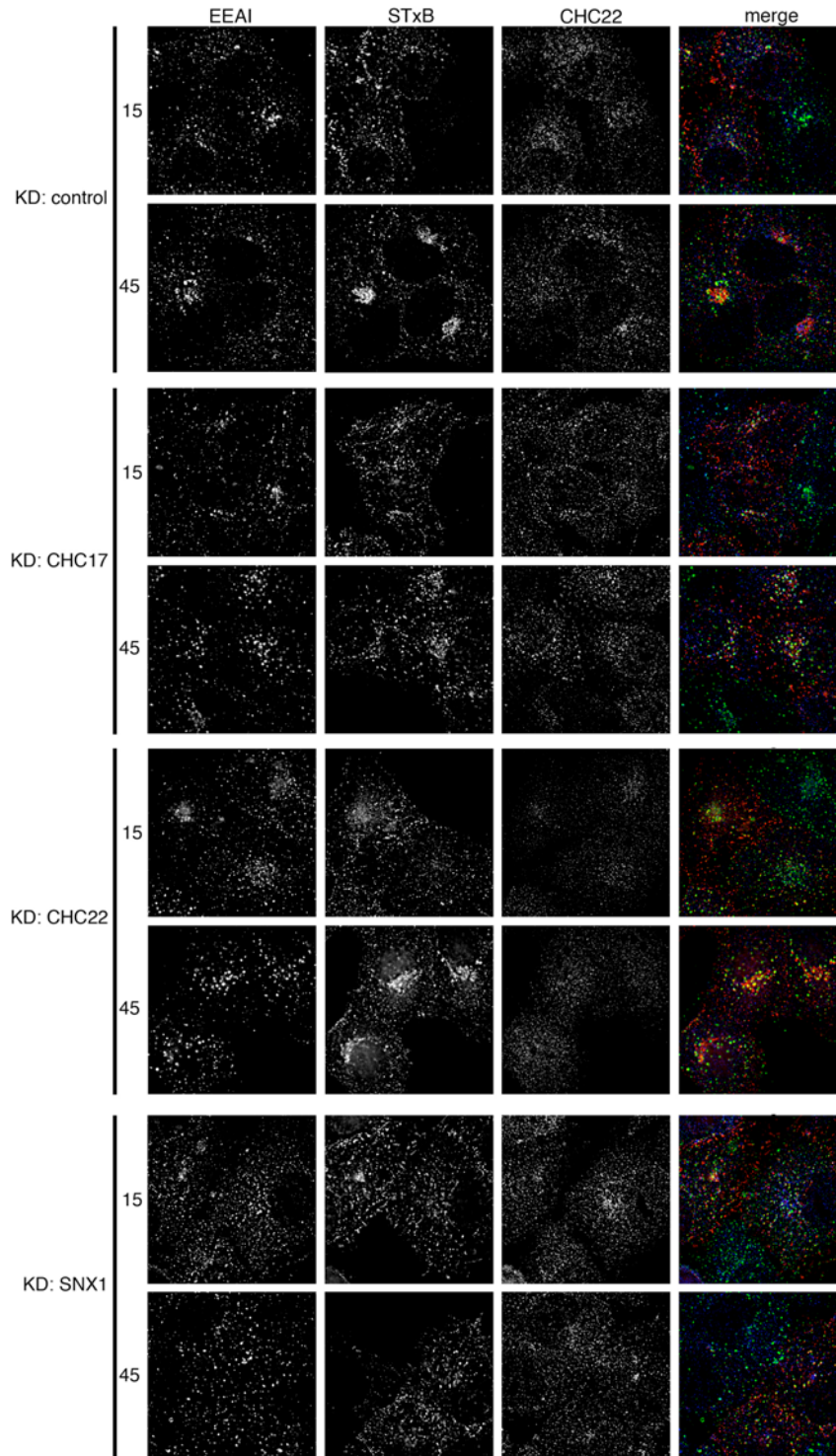
Figure 2-7: STxB retrograde trafficking is impaired in CHC17, CHC22 and SNX1-depleted cells: (A) HeLa cells were depleted of CHC17, CHC22 and SNX1 using specific siRNAs as indicated. Fluorescent Shiga-toxin in fresh media was bound to cells for 30 min on ice, washed in PBS and chased for 15 or 45 min. in fresh media at 37C. Cells were fixed, processed for immunofluorescence and stained using antibodies against CHC22 and EEAI as indicated.

Since both M6PR and STxB have been reported to be retromer-dependent in their exit from the early endosome, we assessed whether they traffic together in a clathrin heavy chain dependent way. Staining simultaneously for EEAI and M6PR in cells undergoing STxB internalization, showed that all three markers accumulate in the same structures in CHC17- and to some extend in SNX1-depleted cells (Fig. 2-7). In contrast, both M6PR and STxB are trafficked away from EEAI-positive early endosomes and accumulate together in downstream vesicles in CHC22-depleted cells. Together this data suggest a role for CHC22 in trafficking from early endosomes, downstream of both CHC17 and retromer function. Interestingly, pathways for M6PR and STxB must diverge even further downstream of CHC22-function, since M6PR is thought to traffic to late endosomes, while STxB traffics straight to the TGN (Ganley et al., 2008).

We tested the effect of clathrin heavy chain depletion on the late endosome using the GTPase Rab9 as a marker (Lombardi et al., 1993) as we were interested in a compartment potentially depending on membrane flow from upstream trafficking events involving clathrin heavy chains. Rab9 is recruited selectively onto late endosomes and is required for transport of M6PR from late endosomes to the TGN. Loss of Rab9 leads to a reduction in size and number of late endosomes. Also, their localization is shifted to a perinuclear position (Ganley et al., 2004). CHC17-depleted cells showed no obvious defect in Rab9 localization when compared to control cells (Fig. 2-8). In contrast, cells depleted of CHC22 showed Rab9-positive membranes much more tightly associated with the nucleus (Fig. 2-8). This result emphasizes the importance of CHC22 for correct late endosome generation.
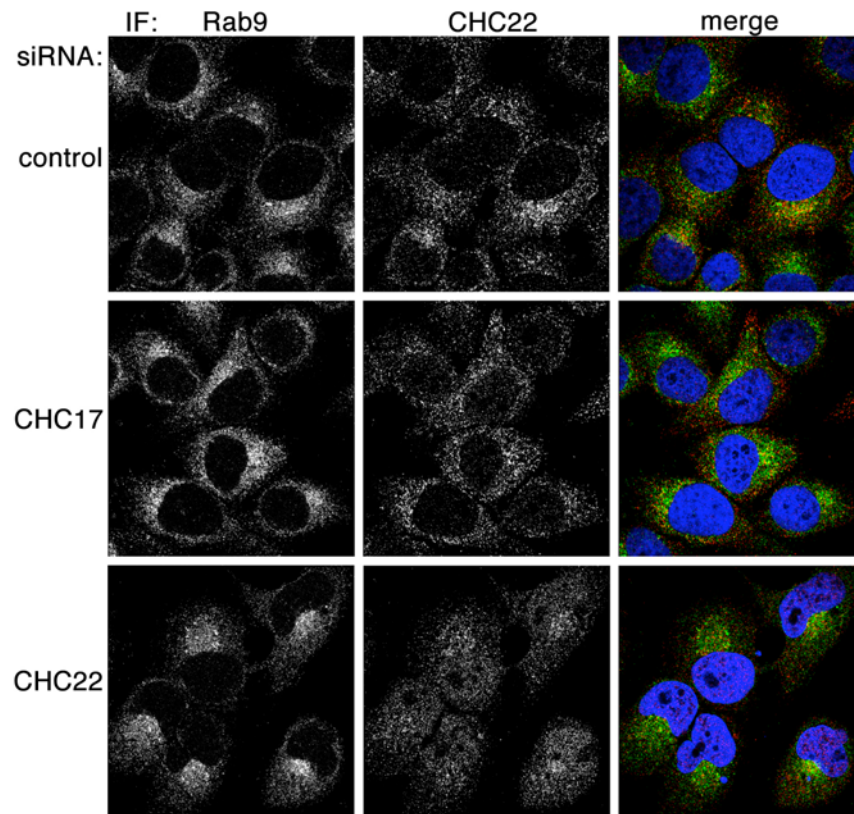
Figure 2-8: CHC22 but not CHC17 affects Rab9 localization: HeLa cells were depleted of CHC17 and CHC22 using specific siRNAs as indicated, processed for immunofluorescence and stained using antibodies against CHC22 and Rab9 as indicated.

Both CHC17 and CHC22 contribute to Golgi morphogenesis

CHC17 has recently been implicated in reassembly of the Golgi apparatus after drug-induced fragmentation (Radulescu et al., 2007). Golgi fragments containing *Cis*- and *medial*-marker proteins did not separate correctly in CHC17-depleted cells recovering from Brefeldin A or butanol treatment. This finding was attributed to a lack of unmixing of membranes resulting in a "tight" phenotype. A similar situation of a fragmented Golgi followed by reassembly, occurs in cell division as Golgi membranes are redistributed throughout the mitotic cell and reassembled in cytokinetic cells via so-called "Golgi twins"

(Colanzi and Corda, 2007; Gaietta et al., 2006). We probed cells depleted of CHC17, CHC22 or CHC17 and CHC22 for Golgi morphology using markers for the *cis*- and *medial*-Golgi compartment. We concentrated on cytokinetic cells as defined by still condensed chromatin. Golgi-twin formation was clearly visible in control cells (Fig. 2-9). While cells depleted of CHC22 alone did not exhibit an obvious phenotype (data not shown), cells depleted of CHC17 and even stronger CHC17 in combination with CHC22 showed Golgi-fragmentation in cytokinetic cells. This is true for both *cis*- and *medial*-markers GM130 and GS27 (Fig. 2-9a, b). CHC17-depletion leads to some vesicles carrying the markers being localized away from the emerging Golgi, while the additional downregulation of CHC22 enhances this effect dramatically, resulting in Golgi membranes being dispersed throughout the whole cell.
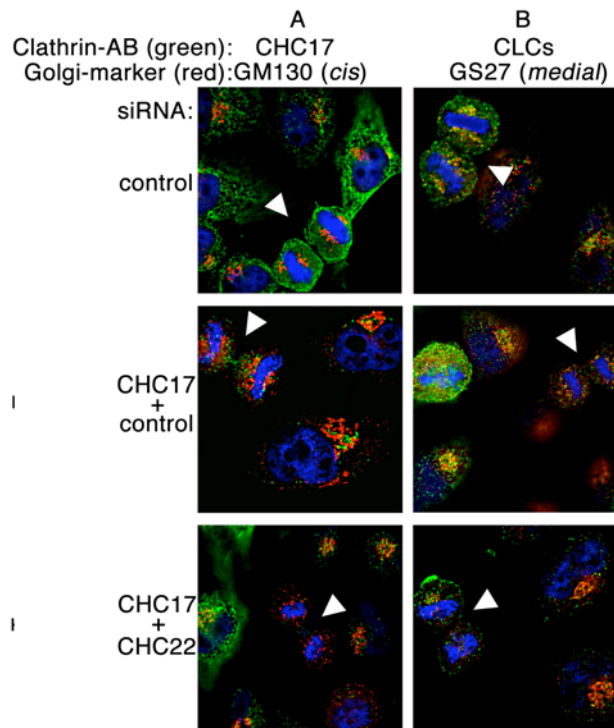
Figure 2-9: Mild and severe effect of CHC17- and CHC17+CHC22-depletion on Golgi morphology in cytokinetic cells: HeLa cells were depleted of CHC17 and CHC17 + CHC22 using specific siRNAs as indicated, processed for immunofluorescence and stained using antibodies against CHC17 (A, green) and clathrin light chains (B, green) in combination with GM130 (A, red) and GS27 (B, red). Cytokinetic cells as determined by condensed chromatin and characteristic shape are identified by arrowheads.

One could expect this effect to last in interphase cells. However, only rarely did we detect dispersed GM130 and GS27-staining in interphase cells (Fig. 2-10). Also, a "tight" Golgi phenotype characteristic of mixed *cis*- and *medial*- Golgi stacks (Radulescu et al., 2007) was rarely visible. Notably, the Golgi is not required to exhibit perfect stack separation to perform its function at moderate levels (Puthenveedu et al., 2006).
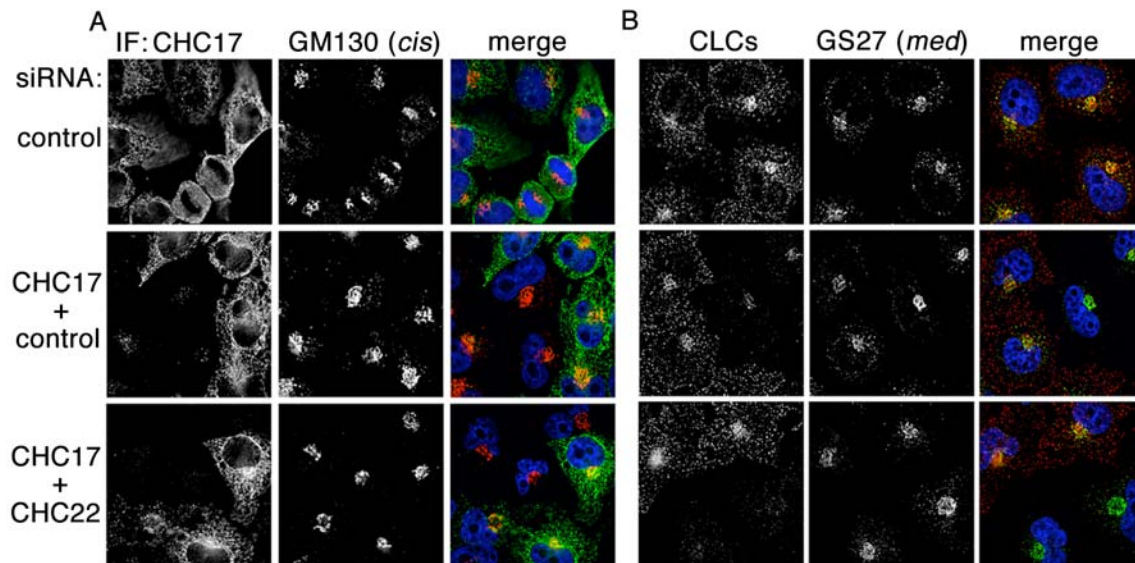
Figure 2-10: Golgi integrity is mildly affected in CHC17 and CHC17 + CHC22-depleted interphase cells. HeLa cells were depleted of CHC17 and CHC17 + CHC22 using specific siRNAs as indicated, processed for immunofluorescence and stained using antibodies against CHC17 (A, green) clathrin light chains (B, green) in combination with GM130 (A, red) and GS27 (B, red).

CHC22 plays a similar role in endosomal sorting in human skeletal muscle

Expression analyses in human tissue samples revealed that CHC22 is present at low levels in all tissues tested with moderate expression in testis and high expression in cardiac and skeletal muscle (Sirotkin et al., 1996). Skeletal muscle maintains a unique membrane system that is required for function of this specialized tissue. Several isoforms of ubiquitous trafficking molecules have been identified, that confer specific functions in skeletal muscle (Towler et al., 2004b). To confirm that the data generated in

HeLa also applies to tissues with high CHC22 expression, we analyzed clathrin heavy chains in a human skeletal muscle cell line. LHCNM2 cells are comparable in their growth and differentiation properties to the commonly used rodent cell lines C2C12 and L6 (Zhu et al., 2007). Immunofluorescence analysis of LHCNM2 depleted of clathrin heavy chains and differentiated to form myotubes revealed a similar phenotype for M6PR as in HeLa cells (Fig. 2-11a). Due to the Golgi being localized around myonuclei in skeletal myotubes, differences in M6PR-localization in CHC17-depleted cells is diffcult to score, but in CHC22-depleted cells a dispersal similar to the situation in HeLa is evident. Furthermore, we compared protein levels in CHC17- and CHC22-depleted cells (Fig 2-11b). CHC17-depletion resulted in increased CHC22-levels, while CHC17 was not significantly affected by CHC22-downregulation. We also monitored M6PR-levels (Fig. 2-11b, c). Both CHC17- and CHC22-depletion lead to a decrease of total M6PR, to 83 % and 61 % of control cells respectively. Cathepsin D, a hydrolase trafficked to lysosomes by M6PR, matures proteolytically from a premature form leaving the TGN (53 kDa) and an intermediate form (47 kDa) into a mature form (31 kDa). Levels of the respective Cathepsin D forms may be used to assess trafficking towards the lysosome (Mardones et al., 2007). Interestingly, when compared to control cells, the ratio of pro- to mature forms of Cathepsin D in CHC17-depleted cells was not significantly altered (Fig. 2-11d). In CHC22-depleted cells however, there was a significant increase in the proforms of Cathepsin D, strongly arguing for a defect in its delivery to the lysosomes.
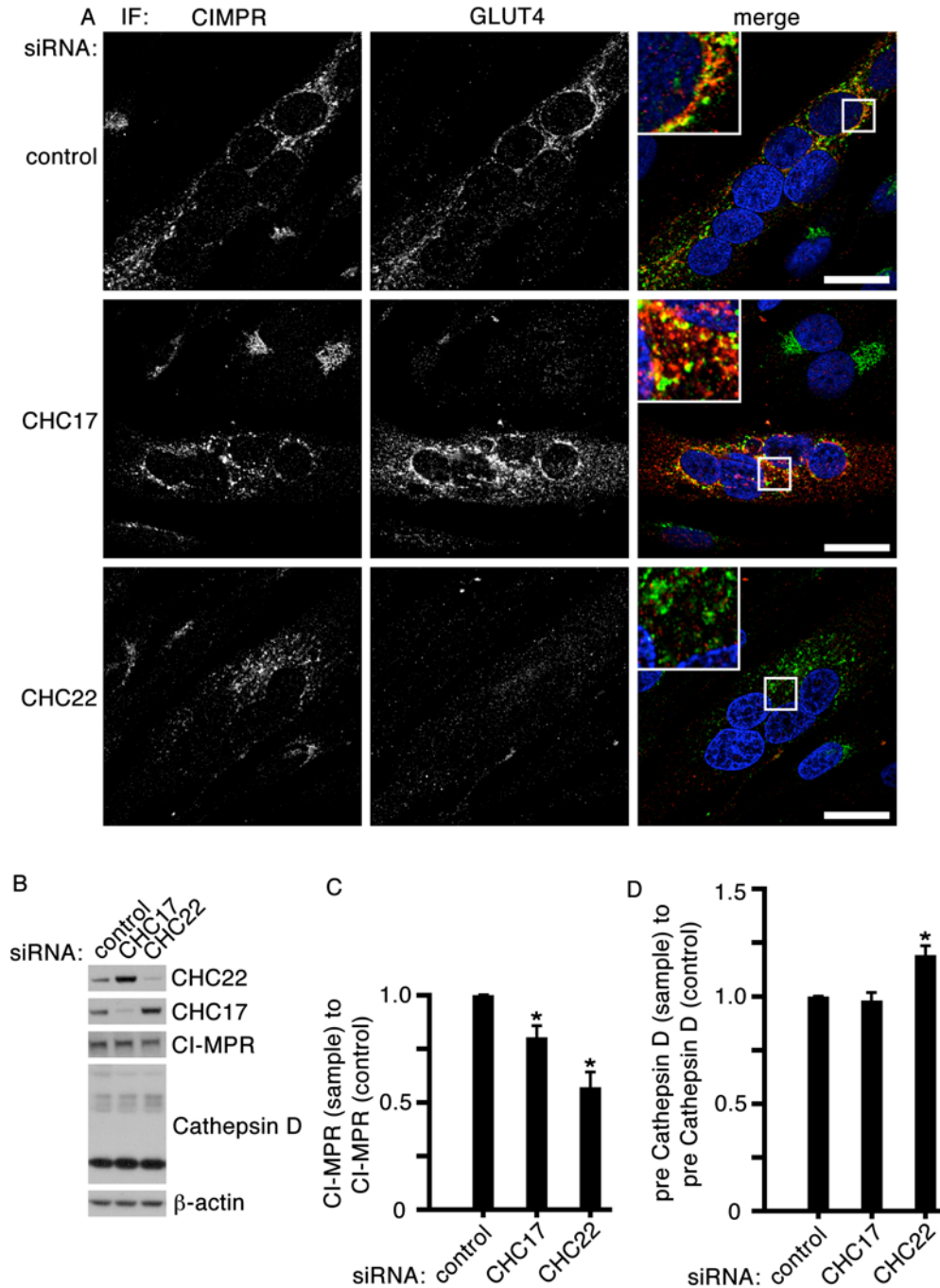
Figure 2-11: Specific effects of CHC17 and CHC22-downregulation on CI-MPR trafficking are observed in human skeletal muscle. (A) LHCNM2 human skeletal muscle myoblast were differentiated, depleted of CHC17 and CHC22 using specific siRNAs and processed for immunofluorescence. Cells were stained using antibodies against CI-MPR and GLUT4. (B) LHCNM2 cells were differentiated and depleted of CHC17 and CHC22. Whole cell lysates were prepared, separated in SDS-PAGE and transferred onto nitrocellulose membrane. Membranes were probed with the indicated antibodies. (C) quantification of CI-MPR levels in whole cell lysates generated as in (B). Shown are ratios compared to control (n=5). (D) quantification of Cathepsin D levels. Shown are ratios of precursor form to mature Cathepsin D relative to control (n=5).

Taken together this data shows that one of the key functions of CHC22 is required in skeletal muscle cells. Also, it confirms the operational localization in endosomes as defined in Hela cells for skeletal muscle cells.

Discussion

In this study we compare the two clathrin heavy chain isoforms found in humans, CHC17 and CHC22. While both isoforms share some key characteristics such as the ability to trimerize and the ability to partake in membrane trafficking events, we show that the less understood isoform CHC22 does not directly act together with CHC17 and may not substitute for CHC17 absence. Instead, CHC22 is involved in a discrete sorting step of M6PR and STxB at the early endosome. This function was observed in both epithelial and skeletal muscle cells.

CHC22 not acting together with or substituting for the ubiquitous CHC17 is true for three known functions of CHC17, namely vesicle formation, spindle formation and Golgi stack separation. This is remarkable since CHC17 and CHC22 are highly homologous, 85% percent at the amino acid level (Wakeham et al., 2005). However, comparisons of amino acid changes across several species demonstrated that there are a number of amino acid changes that are evolutionary conserved, accumulated primarily in the n-terminal and proximal leg domain.

The n-terminal domain of CHC17 mediates its interaction with adaptor proteins and indeed we previously showed, that CHC22 does not bind AP2, the main adaptor for endocytosis (Liu et al., 2001). Here we demonstrate that CHC22 does not partake in endocytosis, even in the absence of CHC17. Also, CHC22 may not rescue CHC17-mediated export from the TGN of M6PR, which depends on adapting by AP1.

We also showed that CHC22 is not recruited to the spindle in mitotic cells, contrasting with the behaviour of CHC17 (Royle et al., 2005). Depletion of CHC17 or overexpression of CHC22, which was previously shown to result in recruitment of CHC22 onto the TGN (Liu et al., 2001), possibly by shifting binding affinities for AP1 and AP3, does not result in spindle recruitment either. In reverse, our data suggests that neither AP1 nor AP3 are involved in spindle recruitment of CHC17.

A third role for CHC17 has been been demonstrated to be organizing *cis*- and *medial*-Golgi stack formation after drug-induced fragmentation (Radulescu et al., 2007). We show that, while a subset of CHC17 bearing membranes presumably representing Golgi membranes are fragmented in BFA-treated cells, CHC22 staining seems normal, indicating that membrane association of CHC22 is Arf1-independent. Nonetheless, CHC22-depletion added to the severity of CHC17-depletion in a physiological situation in which Golgi assembly is required, cytokinesis. While we cannot rule out, that CHC22 partially rescues CHC17-function in this process, we believe it to be unlikely, given CHC22's inability to rescue other functions of CHC17. Rather, we believe that a unique function of CHC22 in retrograde traffic from endosomes to the Golgi adds to the phenotype. This function is presumably to traffic Golgi proteins that have escaped the Golgi back to its origin. A similar mechanism of retrieval of escaped cargo has been demonstrated in ER to Golgi transport, where a balance of anterograde and retrograde traffic of escaped proteins results in concentration of proteins in their respective compartments (Appenzeller-Herzog and Hauri, 2006).

Interestingly, mass spectrometric analyses of clathrin-coated vesicles identified CHC22 being depleted from this fraction in CHC17 depleted cells suggesting that CHC22 may be associated with CHC17 on coated vesicles (Borner et al., 2006). However, based on

our findings we believe CHC22 is not associated with CHC17. Presumably, CHC22-coated vesicles were copurified with CHC17-coated vesicles. We show in this study, that CHC22 acts downstream of CHC17 in endosomal sorting of M6PR and STxB. Hence, if trafficking of these cargoes is inhibited in CHC17-depleted cells, less CHC22-coated vesicles would be expected in the cell. Indeed we show that CHC22 is stabilized and potentially immobilized on membranes in CHC17-depleted cells.

So, where does CHC22 function? Immunofluorescence showed, that most CHC22 bearing structures did not carry CHC17, although some showed both CHC17 and CHC22 staining. CHC22 staining resembled endosomal staining, partly overlapping with AP3 and Rab9 but not EEAI. We note that despite considerable efforts we did not achieve immuno-electron microscopy with either antibody against CHC22. Therefore the exact morphology of CHC22 carrying vesicles is still unknown.

Both clathrin heavy chains are required for M6PR trafficking. The function of CHC22 in this process is independent of CHC17 as staining patterns of M6PR in cells downregulated for either clathrin heavy chain were different. Also, downregulation of both CHC17 and CHC22 seemed to have an additive effect on secretion of hexosaminidase. CHC22-depletion led to a dispersed staining for M6PR, suggesting M6PR is trapped in an endosomal trafficking step.

We used TGN46 as an alternative molecule cycling between TGN and endosomes. Recently, TGN46 has been used as a marker for retrograde trafficking from early endosomes to the TGN in comparison to M6PR-trafficking from the late endosome to the TGN (Ganley et al., 2008). We found that TGN46 trafficking does not depend on CHC22

at all, whereas it strongly depended on CHC17 for correct endosomal sorting. While it is difficult to rule out CHC17-mediated trafficking of TGN46 from the TGN, we find it unlikely, as M6PR accumulates in the TGN upon CHC17-depletion. Since CHC17 but not CHC22 affects TGN46 we interpret this finding as CHC17 and CHC22 being involved in discrete sorting steps at the endosome with CHC17 acting upstream of CHC22.

We also used STxB as a marker molecule. One of the main advantages of STxB is its unidirectional trafficking pathway from the plasma membrane, via early endosomes to the TGN. CHC17 is only required for one sorting step of STxB at the early endosome (Mallard et al., 1998; Saint-Pol et al., 2004). Furthermore, it has recently been demonstrated that both M6PR and STxB are sorted by retromer at the early endosome (Arighi et al., 2004; Bujny et al., 2007; Popoff et al., 2007; Seaman, 2004). Surprisingly, we found that both CHC17 and CHC22-depletion result in a block of retrograde traffic of STxB from endosome to the TGN after 60 min of internalization. Interestingly though this block of STxB seemed to appear in different vesicles, as STxB-positive vesicles in CHC17-depleted cells were EEAI-positive, while STxB-positive vesicles in CHC22-depleted cells were not. Of note, after 15 min. of internalization STxB was found in EEAI-positive early endosomes in cells depleted of either clathrin heavy chain. This strongly argues that CHC22 acts downstream of CHC17 in endosomal sorting.

It has previously been shown, that CHC17 and retromer act cooperatively in sorting of STxB (Popoff et al., 2007). It was proposed that while CHC17 concentrates STxB in microdomains within EEAI-positive endosomes and initiates membrane deformation, retromer may bind to deformed membranes and tubulate them. CHC17-dependent invagination of membrane has been demonstrated in case of the plasma membrane

(Hinrichsen et al., 2006). Subunits of retromer may include sorting nexin family members 1,2,5 and 6 (Rojas et al., 2007; Wassmer et al., 2007), which include membrane curvature sensing BAR-domains (Carlton et al., 2004). Recently, the structure of retromer has been described (Hierro et al., 2007). Retromer leads to tubulation of membranes. However, it is unknown if these tubules connect early endosomes with the TGN directly or if they collapse and therefore form vesicles or both. So far, no reports on tubules directly connecting endosomes and TGN are available.

We propose that CHC22 may traffic both M6PR and STxB in a novel sorting step after these cargoes have been sorted away from EEAI-positive early endosomes by CHC17 and retromer (Fig. 7).
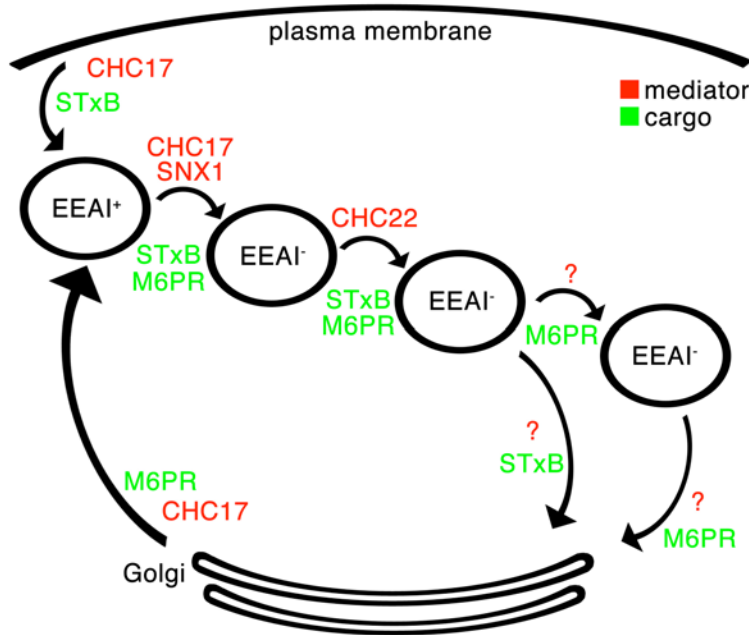
Figure 2-12: model for CHC17 and CHC22 function in retrograde endosomal trafficking. Red indicates mediators of membrane trafficking steps including clathrin heavy chains, green indicates cargo molecules

CHC22 could be recruited to collapsing retromer-derived tubules via interaction with SNX5 (Towler et al., 2004a). CHC22 may act purely to stabilize membranes, but the fact

that CHC22-depletion results in dispersed staining of M6PR and STxB suggests, that the CHC22 coated vesicles may not be processed further. CHC22 may be involved in further processing of these transport vesicles by recruiting factors required for downstream processing. Alternatively, CHC22 could sort proteins other than M6PR and STxB. We emphasize that although our model displays vesicular transport of cargo (Fig. 7), this is only to display functionally independent sorting events. Similar mechanism could apply to the endosomal model described by Bonifacino and Rojas, termed the "tubular endosomal network" in which the endosome is described as distinguishable domains, carrying differential sets of proteins, that are nonetheless connected (Bonifacino and Rojas, 2006). Of note, while STxB traffics directly from early endosomes to the TGN (Mallard et al., 1998), M6PR is thought to traffic via late endosomes (Lombardi et al., 1993). That would require sorting of these cargoes into vesicles destined for the respective target membrane, molecular mechanism of which remain elusive. Further investigation will be required to solve this interesting problem.

Lastly, we demonstrated that CHC22 acts in the same pathways in HeLa cells and human skeletal muscle. This is important, since CHC22 shows its highest expression in skeletal muscle and there are several specialized membrane pathways in muscle. Several isoforms of membrane trafficking proteins are found in skeletal muscle, that act in specialized ways in this tissue (Towler et al., 2004b). However, CHC22 is required for M6PR trafficking in skeletal muscle, indicating that its function is conserved in various tissues.

In conclusion, we show in this work, that two clathrin heavy chain isoforms in human act independently from one another. Nonetheless, both are required for distinct cellular

functions, demonstrating how diversification of a common ancestor in evolution may lead

to independent functions.

Material and Methods

Antibodies, recombinant proteins and siRNAs

One monoclonal and one polyclonal antibody that specifically recognize CHC22 and not CHC17 have been described (Liu et al., 2001). A second polyclonal antibody against amino acids 1549-1563 from human CHC22 was raised by contract (New England Peptides). The antibody was purified negatively and positively, using recombinantly expressed trimerization domain fragments of human CHC17 and CHC22, respectively, coupled to NHS-Hi-Trap columns (Amersham) and specificity for CHC22 was confirmed by immunoblotting the recombinant fragments. Anti-CHC17 (mouse monoclonals X22 and TD.1) and rabbit polyclonal against clathrin light chains) were generated in our laboratory (references available upon request). Commercial sources of antibodies were as follows: TGN46 (sheep polyclonal, Serotec), EEA1, AP1, SNX1, GM130 (mouse monoclonal, BD Transduction Laboratories), β-actin (mouse monoclonal, Sigma), GM130 (rabbit polyclonal, Sigma), CI-MPR (mouse monoclonal, Calbiochem) Cathepsin D (rabbit polyclonal, Calbiochem). Monoclonal anti-GGA2 antibody was a gift from Juan Bonifacino (NIH, Bethesda) with permission from John Hopwood (Women's and Children's Hospital, Adelaide), and monoclonal anti-Rab9 antibody was a gift from Suzanne Pfeffer (Stanford). Polyclonal anti-CI-MPR was a gift from Linton Traub (University of Pittsburgh). Secondary antibodies for immunofluorescence were from Molecular Probes (Alexa488, Alexa568, Alexa647 conjugates) and Jackson Immunoresearch (Cy3-conjugates). Secondary antibodies coupled to HRP were from Zymed Laboratories.

Recombinant Shiga-Toxin subunit B coupled to Cy3 was a gift from Ludger Johannes (Institute Pasteur, Paris). siRNAs were synthesized by Qiagen. DNA sequences targeted were AAGCAATGAGCTGTTTGAAGA for CHC17, AAGAACAAGACCAAGAGCCAC for SNX1 (Bujny et al., 2007) and TCGGGCAAATGTGCCAAGCAA and AACTGGGAGGATCTAGTTAAA for CHC22 (1:1 mixture of siRNAs were used).

Cell culture, transfection, Brefeldin A treatment and STxB-internalization

HeLa cells were grown in DMEM supplemented with 10% FBS, 50 U/ml penicillin, 50 µg/ml streptomycin and 0.625 µg/ml fungizone. Tetracycline-inducible T7-CHC22-FL and T7-CHC22-Hub expressing HeLa cells were described previously (Liu et al., 2001). LHCNM2 human skeletal muscle cells (Zhu et al., 2007) were maintained in tissue culture flasks coated with rat-tail collagen in basal medium (4:1 DMEM:M199, 0.02 M HEPES, 0.03 µg/ml ZnSO4, 1.4 µg/ml Vitamin B12) with 10% fetal bovine serum (FBS), 55 ng/ml dexamethasone, 2.5 ng/ml hepatocyte growth factor (Sigma), 50 U/ml penicillin, 50 µg/ml streptomycin, 0.625 µg/ml fungizone (growth medium). Differentiation was induced by culturing in fusion medium (basal medium with 0.5 % FBS, 10 µg/ml insulin, 50 µg/ml apo-transferrin and 5.5 ng/ml dexamethasone) followed by differentiation medium (basal medium with 0.5% FBS, 55 ng/ml dexamethasone).

Cells were transfected with 0.8 µg/24-well expression vector using Lipofectamine 2000 (Invitrogen) and assayed after 48 h following a 24 h period in the presence of 50 ng/ml tetracycline. Cells were transfected with 10 nM siRNA using HiPerfect (Qiagen) according to the manufacturer's instructions. HeLa cells were split, reseeded 24 h post transfection and retreated with siRNA 24 h later. Cells were used for experimentation 72 h post the second round of transfection. LHCNM2 cells were transfected twice 72 h apart

and used 72 h later.

For some experiments cells were treated with 5 μg/ml Brefeldin A in growth media for 60 min. prior to fixation.

STxB-internalization was performed essentially as described (Popoff et al., 2007). Briefly, cells were washed in cold PBS and incubated on ice in media containing 2 μg/ml STxB coupled to Cy3 for 30 min. Cells were washed in cold PBS and warm media was added. Internalization was carried out for various times at 37°C.

Hexosaminidase secretion

Hexosaminidase secretion was measured based on previously described protocols (Riederer et al., 1994). Briefly, cells treated with siRNA as described above were washed in PBS and incubated in DMEM supplemented with 10mM mannose-6-phosphate for 8 h at 37°C. Secreted hexosaminidase activity was assayed in 0.5 ml media by addition of 120 μl 5x hexosaminidase substrate buffer (0.5 M NaAcetate, pH 4.4, 0.5 % Triton X-100, 5 mM p-nitrophenyl-N-acetyl-β-D-glucosaminide). After shaking at 37°C for 1 h, reactions were stopped by addition of 0.6 ml stop buffer (0.5 M glycine, 0.5 M Na_2CO_3, pH 10.0). Release of p-nitrophenol was measured spectrophotometrically at 405 nm. Intracellular hexosaminidase was measured by washing the cells twice in cold scraping buffer (10 mM phosphate buffer, pH 6.0, 0.15 M NaCl), scraping them into scraping buffer supplemented with 0.5 % Triton X-100 followed by centrifugation at 100,000g for 15 min at 4°C. 50 μl of he resulting supernatant were assayed in 570 μl 1x hexosaminidase substrate buffer. Secreted hexosaminidase was determined as the percentage of the whole hexosaminidase for each sample. Secreted hexosaminidase of

samples was then compared to control samples and ratios were calculated.

Cell fractionation and immunoblotting

Cells grown and treated with siRNA as indicated above were washed in lysis buffer (100 mM NaCl, 50 mM HEPES, pH 7.4, 5 mM MgCl$_2$) and scraped into lysis buffer supplemented with protease inhibitor cocktail (1 tablet / 10 ml buffer, Roche). Cells were broken by subjecting them 10x to a motorized dounce homogenizer and subsequently shearing them four times using a 22.5 Gauge needle. Lysates were spun at 5000g to generate low-speed pellets (P1). The resulting supernatants were centrifuged at 100000g to generate a high-speed pellet (P2) and a cytosolic fraction (S2). Fractions were taken up in reducing sample buffer and subjected to SDS-PAGE.

Protein samples were separated by SDS-PAGE (4-12% acrylamide gel, Invitrogen), transferred to nitrocellulose (Millipore) and labeled with primary antibodies at 1-5 µg/ml and secondary antibodies. The presence of antibody-labelled proteins in samples was detected using Western Lightning Chemiluminescence Reagent (Amersham). Quantification was performed using Quantity One software (Biorad).

Immunofluorescence

Cells grown on coverslips were washed in warm PBS, fixed in warm PFA (3.7% in PBS, 10min), then washed (2X, 5 min, PBS), permeabilized (4 min. 3% BSA, 0.5% Triton X-100 in PBS) and blocked in blocking solution (3% BSA in PBS, 30 min). Antibody labeling was performed by inversion of coverslips on 20µl blocking solution with primary or secondary antibodies (1-5µg/ml) or DAPI (300nM) on parafilm and washing with PBS.

Samples were mounted in Prolong Antifade Kit (Invitrogen). Some images were acquired on an Olympus IX80 microscope equipped with Deltavision Restoration microscope technology (Applied Precision Instruments, Issaquah, WA and running SoftWoRx (Applied Precision) deconvolution and data analysis software. Other samples were analyzed by confocal laser scanning microscopy using a Nikon EZ-C1Si microscope system equipped with an ApoPlan 100x, 1.40NA oil lens. DAPI, Alexa-488 and Alexa-568 fluorescence was sequentially excited using lasers with wavelengths of 405 (DAPI), 488 (Alexa 488) and 561 nm (Alexa 568). Image analysis was performed using NIS Elements software (Nikon) and Metamorph software (Molecular Devices). Data for this study were acquired at the Nikon Imaging Centers at UCSF.

Additional information

Some data is still missing from this manuscript. These changes will be incorporated pending the outcome.

- Fig. 2-4) immunoblot of HeLa cells downregulated for CHC17 and CHC22 probed with antibodies against CHC17, CHC22, TGN46, β-actin
- Fig. 2-6) will be replaced by the same experiment stained for CHC17, CHC22, STxB
- Fig. 2-7) will be replaced with
    1. Fig. 2-7a: STxB uptake for 15 min. in CHC17, CHC22, SNX1-depleted cells stained for CHC17, CHC22, SNX1 in combination with EEAI, STxB
    2. Fig. 2-7b: STxB-uptake for 60 min in CHC17, CHC22, SNX1-depleted cells stained for CI-MPR, EEAI, StxB
- Fig. 2-11a) will be replaced by the same experiment stained for CHC17, CI-MPR

Chapter 3 - A role for the CHC22 clathrin heavy chain isoform in glucose metabolism by human skeletal muscle

The text of this chapter is a manuscript in review.

Authors contributions:

SV, CE, SH and FMB designed research. SV, CE and SH conducted research. BHF, AMP and RK created CHC22-transgenic mice. CYC designed siRNA targeting CHC22. WEW created LHCNM2 cells. SV, CE and FMB wrote the manuscript.

Specifically, I performed research for and created figures 3-3, 3-4 and 3-9. Also, I wrote the corresponding passages in the manuscript, later edited and partly rewritten by FMB. Furthermore, I gave and received input on the rest of the figures and manuscript. The manuscript is presented here as a whole, as it has been a very close collaboration with the other authors. The work as a whole is discussed in greater context in chapter 4, with an emphasis on the data generated by me.

A role for the CHC22 clathrin heavy chain isoform in glucose metabolism by human skeletal muscle

Stéphane Vassilopoulos[1*], Christopher Esk[1*], Sachiko Hoshino[1*], Birgit H. Funke[2], Chih-Ying Chen[1], Alex M. Plocik[2], Woodring E. Wright[3], Raju Kucherlapati[2] and Frances M. Brodsky[1+]

[1]The G.W. Hooper Foundation, Departments of Biopharmaceutical Sciences, Pharmaceutical Chemistry and Microbiology and Immunology, University of California, San Francisco, CA 94143, USA

[2]Harvard Medical School-Partners Healthcare Center for Genetics and Genomics

77 Ave. Louis Pasteur, Boston, MA 02115, USA

[3]Department of Cell Biology, UT Southwestern Medical Center, Dallas, TX 75390, USA

[*]These three authors contributed equally to the work described in this manuscript.

[+]To whom correspondence should be addressed. Email: Frances.Brodsky@ucsf.edu

Abstract

In humans, the CHC22 isoform of clathrin heavy chain is primarily expressed in skeletal muscle. Although present in many vertebrates, the gene encoding CHC22 is a pseudogene in mice. CHC22 is now revealed to associate with components of the membrane traffic pathway for the glucose transporter GLUT4 in humans. CHC22 down-regulation in cultured human myoblasts disrupted GLUT4 localization to an insulin-sensitive compartment. CHC22 expression in the muscle of transgenic mice caused aberrant localization of components of the GLUT4 transport pathway and induced symptoms of diabetes. These studies demonstrate a role for CHC22 in formation and stabilization of the GLUT4 compartment in human muscle and highlight differences in glucose metabolism between humans and mice. This novel function for CHC22 reveals a species-restricted mechanism for glucose homeostasis with potential significance to human type II diabetes.

Main text

Complex tissues, such as skeletal muscle, developed specialized transport pathways by diversification of membrane traffic proteins through evolutionary gene duplication. Here we define the tissue-specific and species-restricted function of a clathrin heavy chain isoform CHC22 that arose by gene duplication in the vertebrate lineage and is expressed in human skeletal muscle (Sirotkin et al., 1996; Wakeham et al., 2005). The ubiquitous clathrin heavy chain, represented by human CHC17 (each isoform is named for the encoding chromosome), is expressed in all eukaryotes and in all vertebrate tissues. In association with three clathrin light chain subunits, three CHC17 subunits form the well-characterized clathrin triskelion that assembles into a protein coat for intracellular membrane transport vesicles (Brodsky et al., 2001; Ungewickell and Hinrichsen, 2007) . This lattice-like clathrin coat facilitates vesicular sorting of membrane-associated proteins during endocytosis and organelle biogenesis. The CHC22 isoform also forms a trimer, but does not stably associate with clathrin light chains, nor interact with CHC17 by co-trimerization or co-assembly (Liu et al., 2001; Towler et al., 2004a). CHC22 has conserved features in the vertebrate lineage, indicating a conserved function, but the gene encoding CHC22 is a pseudogene in mice, a phenotype shared by sixteen strains of mice representing both laboratory and wild mice (Wakeham et al., 2005). These properties led to consideration of membrane traffic pathways with suggested differences between human and mouse muscle cells, and thereby to investigation of a role for CHC22 in the membrane traffic of the glucose transporter GLUT4 (Postic et al., 2004; Tortorella and Pilch, 2002). The CHC22 function reported here defines a species-restricted mechanism for regulation of GLUT4 membrane traffic, a novel feature of

human glucose homeostasis with potential significance to type II diabetes and development of better animal models for this disease.

CHC22 clathrin associates with the GLUT4 transport pathway

Skeletal and cardiac muscle and adipose tissue import glucose for acute metabolic needs in response to insulin. In these tissues, insulin stimulation induces cell surface expression of the GLUT4 transporter, causing its release from an intracellular GLUT4 storage compartment (GSC) by fusion of GLUT4 storage vesicles (GSVs) with the plasma membrane. (Bryant et al., 2002; Huang and Czech, 2007). This pathway enables rapid glucose clearance from the bloodstream and defects in GLUT4 membrane traffic are associated with type II diabetes in humans (Garvey et al., 1998). With the hypothesis that some human-mouse differences in skeletal muscle glucose metabolism (Postic et al., 2004; Sarabia et al., 1992; Tortorella and Pilch, 2002) might be explained by the presence of CHC22 in humans, the distribution of CHC22 relative to GLUT4 pathway markers was analyzed in human skeletal muscle (Fig. 3-1). CHC22 was detected using previously characterized monoclonal and polyclonal antibodies that do not recognize CHC17 (Liu et al., 2001; Towler et al., 2004a). The distribution of CHC22 was distinct from CHC17 and remarkably similar to that of GLUT4 (Fig. 3-1A). Co-localization between CHC22 and GLUT4 was extensive though not absolute, and was observed in the perinuclear region of myonuclei, below the sarcolemma and in internal vesicles characteristic of GSVs (Ploug et al., 1998; Sarabia et al., 1992) (Fig. 3-1, A and B). In the perinuclear region, CHC22 also co-localized with another marker of the GSC, insulin-responsive amino peptidase (IRAP) (Fig. 3-1C) (Kandror and Pilch, 1994).

Studies of GLUT4 membrane traffic in murine adipocytes and rodent myoblast culures have identified the v-SNARE VAMP2 (synaptobrevin) as a mediator of insulin-stimulated release of GSVs (Randhawa et al., 2000; Williams and Pessin, 2008). VAMP2 was extensively co-localized with CHC22 (Fig. 3-1C). Mouse and rat models have also implicated adaptor molecules that link vesicle cargo to the CHC17 clathrin coat in
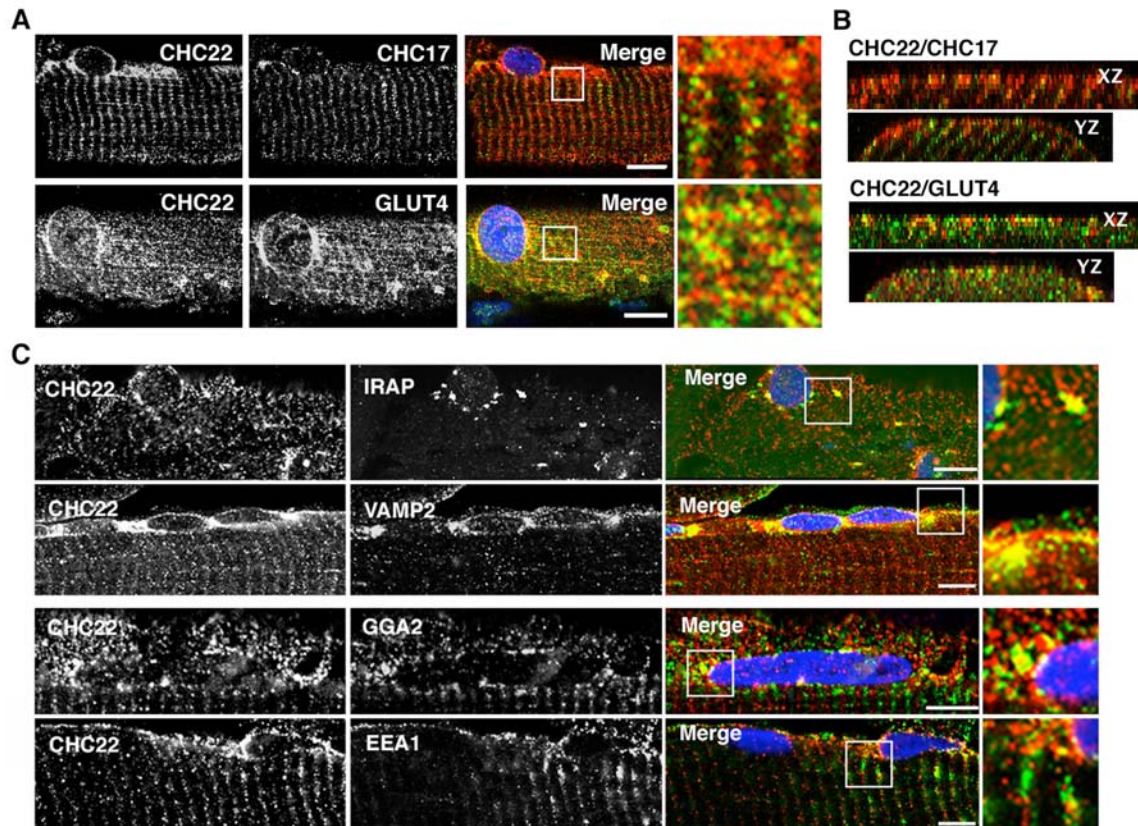
Fig. 3-1. Localization of CHC22 relative to components of the GLUT4 transport pathway in human skeletal muscle fibers. Longitudinal sections of human skeletal muscle were processed for double immunofluorescent labeling to detect the indicated proteins and analyzed by confocal microscopy. Polyclonal (rabbit) antibodies were detected with Cy3-conjugated-anti-rabbit immunoglobulin (Ig) and monoclonal (mouse) antibodies were detected with Alexa488-conjugated-anti-mouse Ig. In A and C, each row is the same sample with the black and white images showing staining for the individual proteins and the merge showing these images overlapped in color, with yellow indicating colocalization (scale bar represents 20μm). The far right panel in each row shows a magnified view of the region outlined in white on the merged image. **(A)** Top panels show staining with polyclonal antibody against CHC22 (red) and monoclonal antibody against CHC17 (green). Bottom panels show staining with monoclonal antibody against CHC22 (green) and polyclonal antibody against GLUT4 (red). **(B)** X-Z and Y-Z projections of the surface-proximal confocal images in A comparing CHC22 to CHC17 or GLUT4 distribution. **(C)** Each row shows a human skeletal muscle section labeled with a polyclonal antibody against CHC22 (red) and a monoclonal antibody against either IRAP, VAMP2, GGA2 or EEA1 (green).

biogenesis of the GSC, as well as in recapture of GLUT4 from the plasma membrane and in GSV recycling (Gillingham et al., 1999; Huang and Czech, 2007; Li et al., 2007; Watson et al., 2004). In human skeletal muscle, CHC22 partially localized with one of these adaptors, the Golgi-localized, gamma-ear-containing, Arf-binding adaptor-2 (GGA2) (Fig. 3-1C), suggesting that, in humans CHC22 might take over some of the functions mediated by CHC17 in mouse muscle. This is certainly feasible, as CHC22 shares 85% protein sequence identity with CHC17 and has previously been shown to bind the AP1 adaptor that interacts with GGA adaptors for sorting from the trans-Golgi network (TGN) by CHC17 (Bonifacino, 2004; Liu et al., 2001). Notably, our previous studies have also shown that CHC22 does not bind the endocytic AP2 adaptor for CHC17 and plays no detectable role in endocytosis from the plasma membrane (Liu et al., 2001). CHC22 also localized adjacent to intracellular structures marked by the early endosome protein EEA1 (Fig. 3-1C), suggesting CHC22 potentially functions in sorting from endosomes, as well as from the TGN. These morphological results localized CHC22 in human skeletal muscle to structures overlapping with the GSC, as well as with proteins involved in GLUT4 traffic and/or formation of the GSC from the TGN and endosomes.

Association between CHC22 and components of the GSC in human skeletal muscle was confirmed by biochemical analysis (Fig. 3-2). First, membrane microsomes comprising a mix of all intracellular membrane compartments were prepared from human skeletal muscle autopsy tissue. CHC22 fractionated predominantly with these membranes (Fig. 3-2A). In contrast, CHC17 and another vesicle coat protein b-COP were distributed between the cytosol and membrane fractions, representing disassembled and assembled states indicating that CHC22 is mainly in an assembled state. Microsome

fractions were then separated into large membrane fragments and coated vesicles, using a protocol for enrichment of CHC17 coated vesicles (Fig. 3-2B). Relative to total amounts of each clathrin in muscle, a smaller proportion of CHC22 (18±2.3%, n=3) was
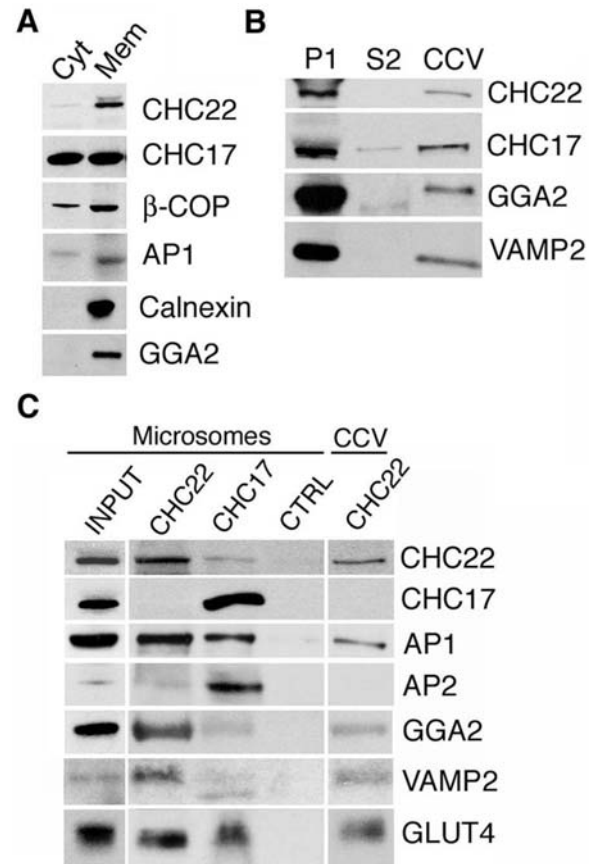
Fig. 3-2. Association of CHC22 with proteins involved in GLUT4 membrane traffic. Human skeletal muscle was homogenized and fractionated by differential centrifugation. Fractions were analyzed for the presence of the two clathrin isoforms and other membrane traffic markers including components of the GLUT4 transport pathway by direct immunoblotting following SDS-PAGE separation (A and B) or by immunoprecipitation and blotting (C). **(A)** Microsomal membrane (Mem, 20 μg) or the supernatant fraction (20 μg) corresponding to cytosolic (Cyt) proteins obtained during microsome preparation of were immunoblotted with antibodies recognizing the proteins indicated at the right. The migration shift for AP1 likely reflects known phosphorylation differences between the cytosolic and membrane-bound form of the detected β1 subunit. **(B)** A clathrin-coated vesicle (CCV) fraction was prepared from microsomes (Mem) in A using ficoll-sucrose centrifugation known to enrich for CHC17 CCVs. This preparation yields non-vesicular membranes (P1), CCVs and a supernatant (S2) after P1 and CCVs are sequentially removed. These fractions were analyzed with antibodies recognizing the indicated proteins. **(C)** Microsomes (Mem in A) or CCVs isolated as in B, were solubilized in detergent for immunoprecipitation with the antibodies indicated at the top. Resulting immunoprecipitates were analyzed by immunoblotting for the proteins indicated at the right. For microsome lysate, the input material (1-2%) and an immunoprecipitate using an isotype-matched control (CTRL) antibody are shown.

detected in the coated vesicle fraction compared to CHC17 (43±3.1%, n=3). This indicated that CHC22 can form coated vesicles but that it is more associated with large membrane compartments under steady state conditions compared to CHC17. The GLUT4 traffic mediators VAMP2 and GGA2 were both found in the pool of clathrin coated vesicles (CCVs) and associated with larger membranes (Fig. 3-2B). To determine whether these proteins were associated with CHC22 or CHC17, immunoisolation was performed from the microsomal or CCV fractions (Fig. 3-2C). GLUT4 was associated with both clathrins. Most of the VAMP2 and GGA2, but no AP2 adaptors were associated with CHC22. Thus CHC22 associates with GSC cargo and with proteins involved in GSC formation from the TGN and endosomes, including the AP1 adaptor. Lack of binding to AP2 further indicates that CHC22 is not involved in classical endocytosis from the plasma membrane, which appears to be a function of CHC17 in human skeletal muscle. Thus, GLUT4 recapture from the plasma membrane of human skeletal muscle would be mediated by CHC17, as described for mouse and rat models (Gillingham et al., 1999; Huang et al., 2007), while CHC22 is situated to play a role in GSC biogenesis from internal compartments.

CHC22 expression is required for formation of the GLUT4 storage compartment in human myotubes

To investigate the suggested role for CHC22 in formation of the GSC, functional analysis was undertaken using LHCNM2 cells, an immortalized human skeletal muscle myoblast cell line, which differentiates into multinucleated myotubes upon removal of serum (Fig. 3-3, 3-4) (Zhu et al., 2007). Immunofluorescence analysis of multinucleated myotubes revealed GLUT4 partially overlapping with CHC22 and to a lesser extent with CHC17
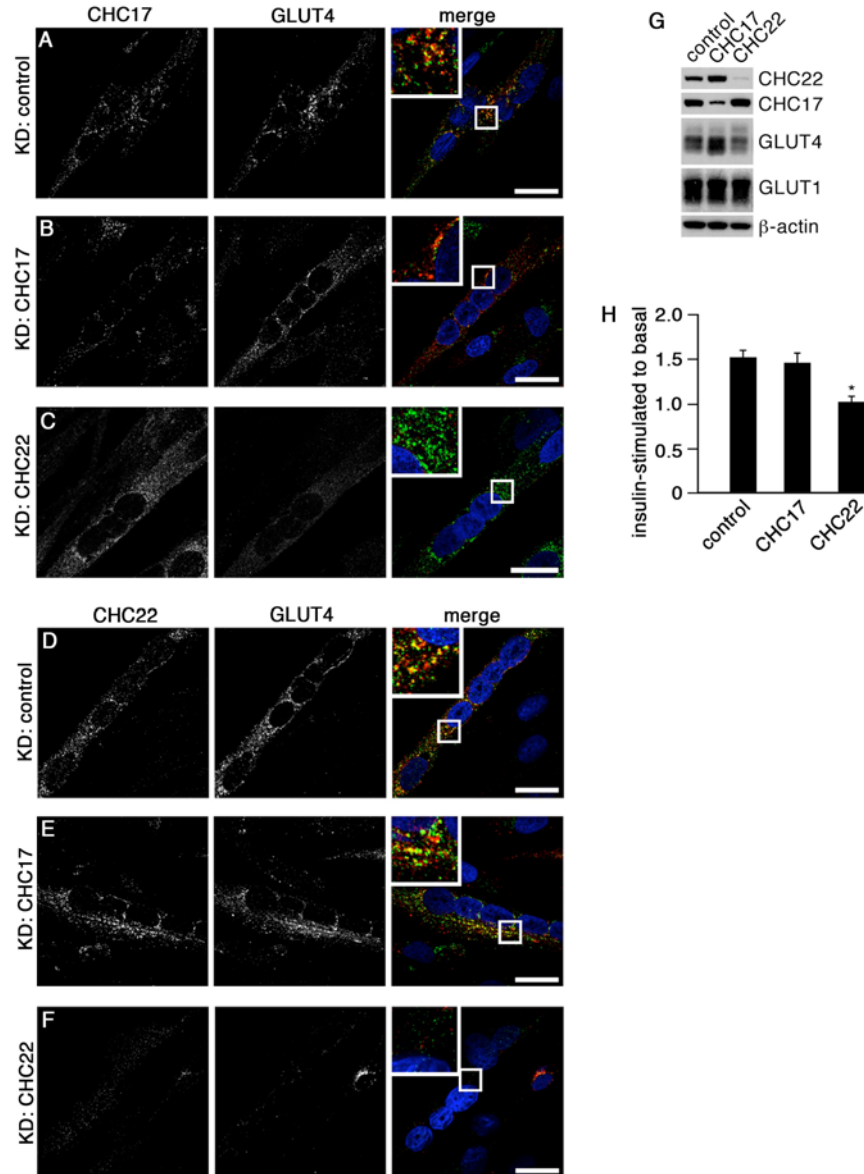
Fig. 3-3. Requirement for CHC22 in GSC formation and insulin-responsiveness in cultured human myotubes. LHCNM2 human myoblasts were differentiated into myotubes, then treated with siRNA targeting CHC17 or CHC22 or with non-specific (control) siRNA (A-F). Samples were analyzed by immunofluorescence and immunoblotting, and for insulin-responsiveness. **(A-F)** Each set of three represents the same sample after treatment with siRNA (knock down (KD) specificity indicated at the left), processed for double immunofluorescence. Black and white images represent labeling by individual antibodies (indicated above the sample) and merge shows both together with an inset showing magnification of the boxed area. Antibodies to CHC17 and CHC22 are detected with Alexa488-conjugated-anti-mouse Ig and Alexa488-conjugated-anti-rabbit Ig (green) respectively and antibody to GLUT4 is detected with Alexa568-conjugated-anti-goat Ig (red). Yellow indicates overlap. Scale bars, 20 μm. **(G)** Whole cell lysates of differentiated LHCNM2 cells treated with siRNA (target specificity indicated above the lanes) were separated by SDS-PAGE and the proteins indicated at the right were detected by immunoblotting. **(H)** Glucose-uptake in response to insulin was assessed in differentiated LHCNM2 cells treated with siRNA (target specificity indicated below each bar). Insulin-stimulated glucose-uptake was normalized to non-stimulated controls (n=5). Asterisk indicates a statistically significant difference.
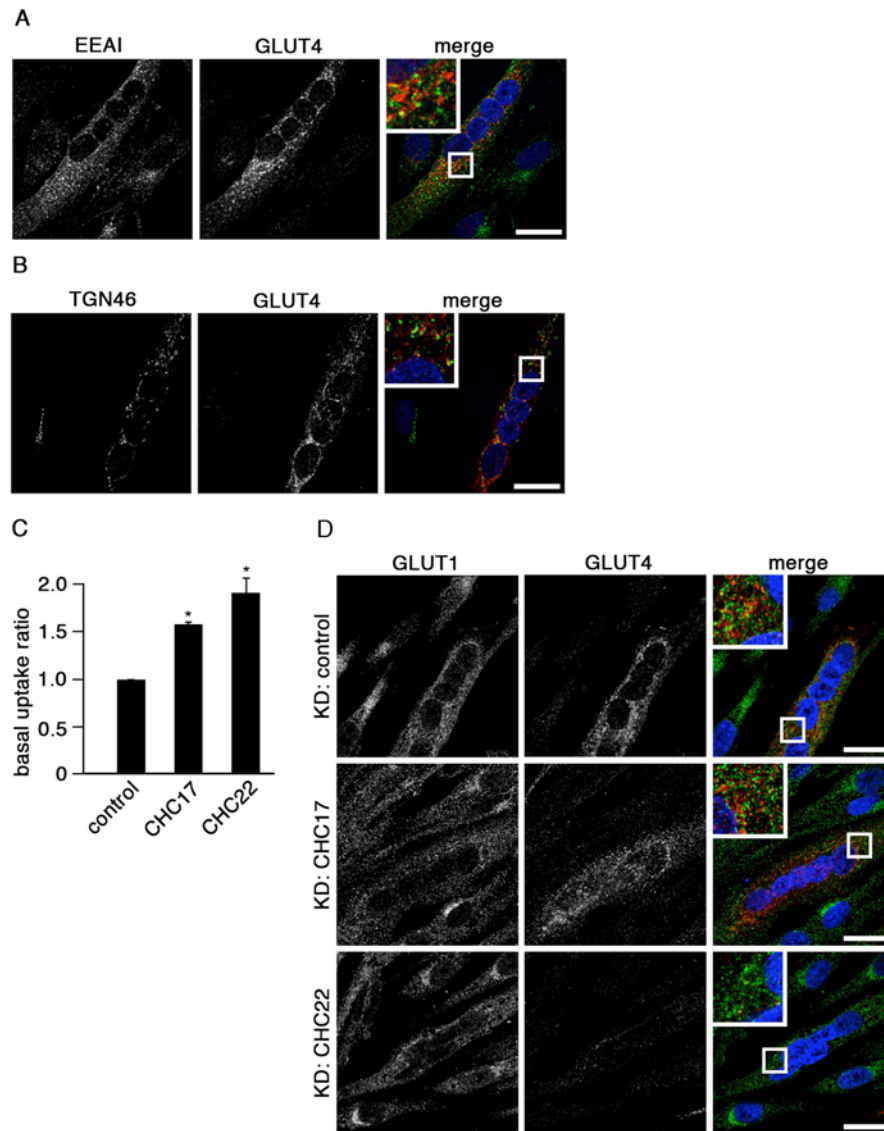
Fig. 3-4. Further analysis of GLUT4 membrane traffic and glucose metabolism in human myotubes. LHCNM2 were grown under differentiation conditions to form myotubes and analyzed as follows. **(A and B)** Myotube cultures were processed for double immunofluorescent labeling with antibodies to GLUT4 detected with Alexa568-conjugated-anti-goat Ig (red) and with antibodies to EEA1 or TGN46 detected with Alexa488-conjugated-secondary antibodies against mouse or rabbit Ig, respectively (green). Scale bars, 20 μm. **(C)** Myotube cultures were treated with siRNA targeting CHC17 or CHC22 or with control siRNA, as indicated below each bar. Basal levels of glucose uptake by each treated culture were measured and normalized to basal levels of glucose-uptake by control siRNA-treated cultures (n=5). Asterisks indicate statistically significant differences. **(D)** Myotube cultures were treated with siRNA targeting CHC17 or CHC22 or with non-specific (control) siRNA. Each set of three micrographs represents the same sample after treatment with siRNA (knock down (KD) specificity indicated at the left), processed for double immunofluorescence. Black and white images represent labeling by individual antibodies (indicated above the micrograph) and merge shows both together with an inset showing magnification of the boxed area. Antibodies to GLUT1 are detected with Alexa488- conjugated-anti-rabbit Ig (green) and antibody to GLUT4 is detected with Alexa568- conjugated-anti-goat Ig (red). Yellow indicates overlap. Scale bars, 20 μm.

(Fig. 3-3, A and D). Hardly any GLUT4 was detectable in mononucleated myoblasts. In myotubes, GLUT4 did not overlap with markers of the early endosome (EEA1) or the TGN (TGN46) (fig. 3-4A, B), suggesting that the GLUT4 detected in myotubes had a distribution typical of the GSC. LHCNM2 cells were transfected with siRNA and high knock-down efficiencies observed (Fig. 3-3G). CHC22 downregulation led to a strong reduction of GLUT4 staining and apparent loss of the GSC (Fig. 3-3, C and F, Fig. 3-4D). In contrast, downregulation of CHC17 slightly reduced the intensity of the intracellular GLUT4 signal in myotubes (Fig. 3-3, B and E), without changing GLUT4 localization. This is consistent with a role for CHC17 in recapture of GLUT4 from the plasma membrane by endocytosis (Huang et al., 2007). The distribution of the constitutively expressed GLUT1 transporter was not affected by downregulation of either CHC (Fig. 3-4D). Cells treated with siRNA against CHC17 regularly showed increased levels of CHC22 protein, while a slight increase in CHC17 upon CHC22 depletion was variable (Fig. 3-3G). These changes likely reflect increased stability from increased membrane association of each clathrin when the other is absent, because they compete for some shared membrane-associated adaptors. It is notable that the level of GLUT4 protein increased upon CHC17 depletion and decreased upon CHC22 depletion, while GLUT1 levels were unchanged (Fig. 3-3G). GLUT4 increase could be explained by greater stability of the GSC when CHC22 levels increase upon CHC17 depletion, and the GLUT4 decrease following CHC22 depletion explained by an alteration in trafficking and diversion to lysosomes in the absence of the GSC. In sum, these siRNA depletion experiments indicate an essential and specific role for CHC22 in biogenesis of the GSC.

Previous studies of GLUT4 membrane traffic in cell cultures have established that the only way to detect endogenous GLUT4 recruitment to the plasma membrane from the

GSC is to measure changes in glucose uptake upon insulin stimulation. This approach is mandated because endogenous GLUT4 that can be detected in internal vesicles becomes diffuse and undetectable once exported to the plasma membrane so insulin-induced recruitment cannot be measured morphologically (Ishiki et al., 2005). Thus, a glucose uptake assay was performed on differentiated LHCNM2 cultures transfected with siRNA targeting the two clathrins (Fig. 3-3H) as a way of assessing integrity and function of the GSC. The assay measures cellular uptake of radioactive glucose following insulin stimulation relative to glucose uptake under basal conditions. The basal uptake is due to the unregulated, constitutive expression of the GLUT1 transporter (9). In cultures that received non-targeting siRNA, insulin treatment induced a 50% increase in glucose uptake compared to non-stimulated cells. This contrasts with similar experiments performed on the mouse C2C12 cell line, which did not show any insulin-response (Tortorella and Pilch, 2002), suggesting human myotubes have a more robust GLUT4 response to insulin compared to murine counterparts. CHC22-depleted LHCNM2 myotubes did not have an insulin-stimulated response. Their glucose uptake showed no difference between insulin-stimulated or basal conditions (ratio of 1.0) (Fig. 3-3H), consistent with loss of the GSC following CHC22 depletion (Fig. 3-3, C and G, Fig. 3--4D). Depletion of CHC17 from the LHCNM2 human myotubes caused a small, but not statistically significant, reduction in insulin sensitivity, with a 40% increase in glucose uptake after insulin treatment (Fig. 3-3H). This effect is explained by decreased recapture of GLUT4 by CHC17 resulting in a decreased intracellular pool. In keeping with this explanation, the basal rate of glucose uptake by cultures depleted for CHC17 was increased (fig. 3-4C), likely reflecting higher basal levels of GLUT4 on the cell surface when endocytosis is inhibited. Interestingly, CHC22 depleted myotubes also exhibited increased basal glucose uptake. This effect is likely due to lack of

sequestration of GLUT4 in the GSC during biosynthesis since CHC22 does not affect endocytosis (Liu et al., 2001).

CHC22-transgenic mice show diabetic symptoms

Analysis of human muscle and myoblasts suggests that the presence of CHC22 and its role in GSC formation might account for some of the documented differences in glucose uptake by mouse and human muscle cells (Sarabia et al., 1992; Tortorella and Pilch, 2002). To investigate the differences in GSC formation and function between mouse and human muscle, we analyzed three strains of mice transgenic for a bacterial artificial chromosome (BAC) comprising the human gene CLTCL1 (formerly CLTD) encoding CHC22, under the control of its own muscle-specific promoter (Fig. 3-5A). The BAC included only one other adjacent gene encoding the citrate transporter SLC25A1 that is already present in the mouse genome. Muscle-specific expression of the CHC22 transgene was verified by immunoblotting tissues from the CHC22-transgenic mice (Fig. 3-5E). The initial expectation was that the CHC22-mice might clear bloodstream glucose more efficiently because they share components of the human GLUT4 trafficking pathway with which CHC22 is able to interact. However, when glucose and insulin tolerance tests were performed, results were opposite to those expected (Fig. 3-6). These were most dramatic in older CHC22-mice (ages 25 to 50 weeks), which showed diabetic symptoms in all three strains of transgenic mice. The older CHC22 mice were hyperglycemic compared to age and weight matched wild-type mice (Fig. 3-6A) and displayed signs of insulin resistance. The insulin-induced glucose clearance of mice older than 20 weeks was decreased relative to insulin-induced clearance in age-matched wild-type mice (Fig. 3-6, B and C). Additionally, for all ages of mice tested, clearance of

injected glucose from the bloodstream (Fig. 3-6, D and E) was slightly less efficient in the

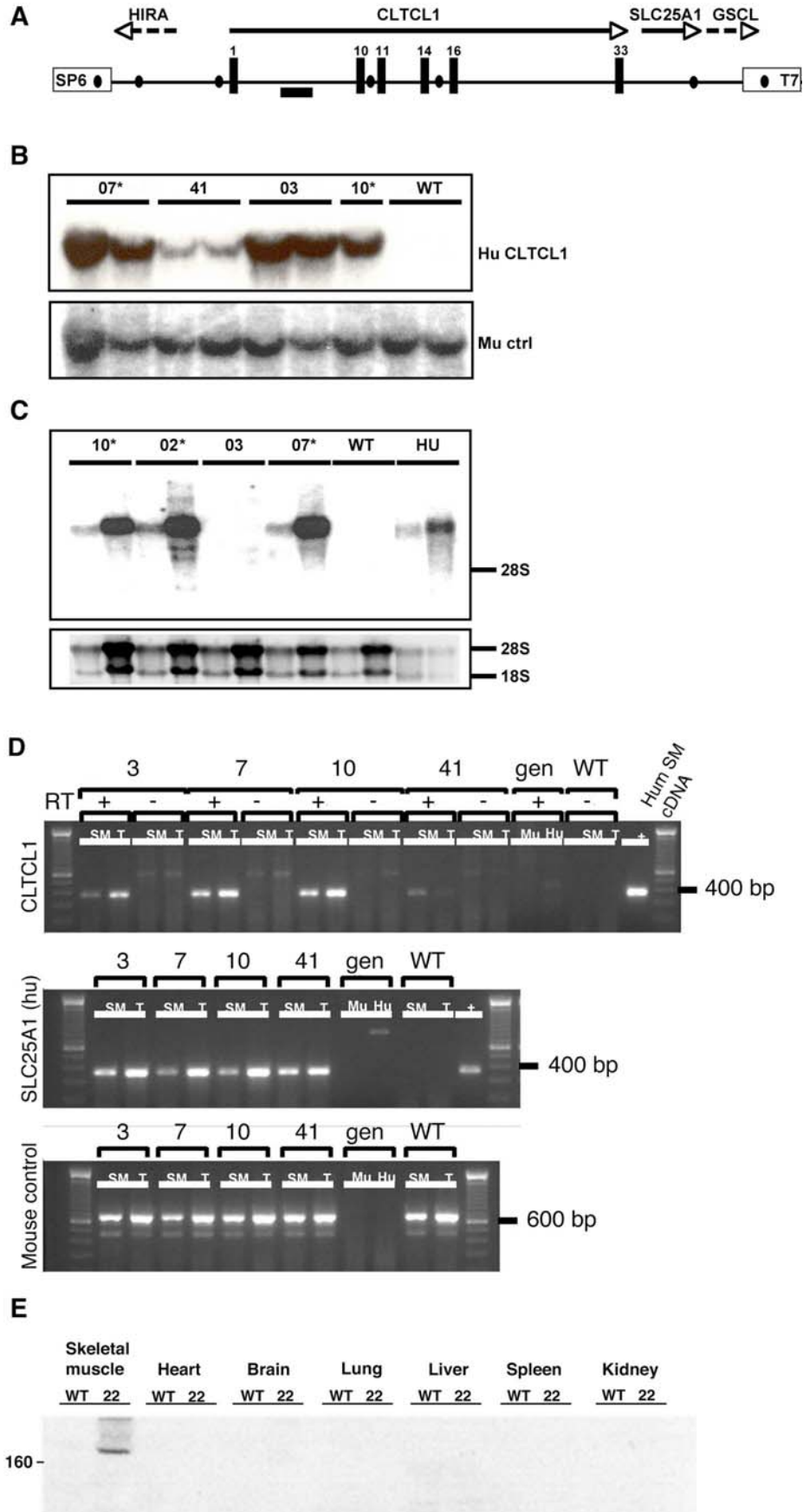CHC22-mice compared to wild-type mice.

Fig. 3-5. Production and characterization of the CHC22 transgenic mice. (A) The genomic interval contained within BAC339F21 is shown. This BAC was used to produce CHC22 transgenic mice. Open boxes represent the SP6 and T7 ends of vector pBACe3.6. Filled boxes symbolize CHC22 exons. Above, solid arrows indicate the transcriptional orientation of genes present on the BAC (CHC22 and SLC25A1). Dashed lines indicate partial genes (HIRA and GSCL). Filled circles represent PCR markers used to genotype the founder animals to assess integrity of the genomic interval and the solid line underneath shows the location of the probe used for Southern hybridization. **(B)** Southern blot analysis of the CHC22 transgenic mice. Genomic DNA from transgenic lines 3, 10, 7 and 41 (two animals from each), as well as from two wild type (WT) animals was analyzed with a probe corresponding to the human CHC22 locus (top blot) as well as a probe corresponding to a single copy locus on mouse chromosome 16 (bottom). The transgenic lines used for experiments described in this manuscript are marked with an asterisk. **(C)** Northern blot analysis of the CHC22 transgenic mice. A probe corresponding to CLTCL1 exons 6-10 was generated by RT PCR and hybridized to 25 mg of RNA from skeletal muscle (left) or testis (right), isolated from each line indicated above the RNA samples. Human RNA (HU) from skeletal muscle or testis (Clontech) served as a positive control and RNA isolated from skeletal muscle and testis of wild type (WT) mice as a negative control. The transgenic lines used for experiments described in this manuscript are marked with an asterisk. **(D)** RT-PCR analysis of human CHC22 (CLTCL1) and SLC25A1 transcripts in skeletal muscle (SM) or testis (T) from lines 3, 10, 7 and 41 or WT mice. RT-PCR was also used to detect transcription of the mouse mitochondrial ribosomal protein L40 (Mrpl40) (mouse control). This control shows that RNA was present in all samples tested, including the WT mouse samples that were negative for amplification human CLTCL1 and SLC25A1. Human skeletal muscle cDNA was used as a positive control for the expression of the human genes (second from right lane of top two gels). Genomic mouse DNA (gen) was used as a negative control for RNA amplification, as well as the absence of reverse transcriptase (RT). Sizing markers are in the far right hand lane for all three gels.

(E) The expression of CHC22 protein was analyzed by immunoblotting tissue lysates from wild-type (WT) or CHC22 transgenic mice (22). Each indicated tissue was harvested, homogenized and solubilized in detergent and 50 mg was loaded in each lane. The migration position of the 160 kDa molecular weight marker protein is indicated at the left of the blot.
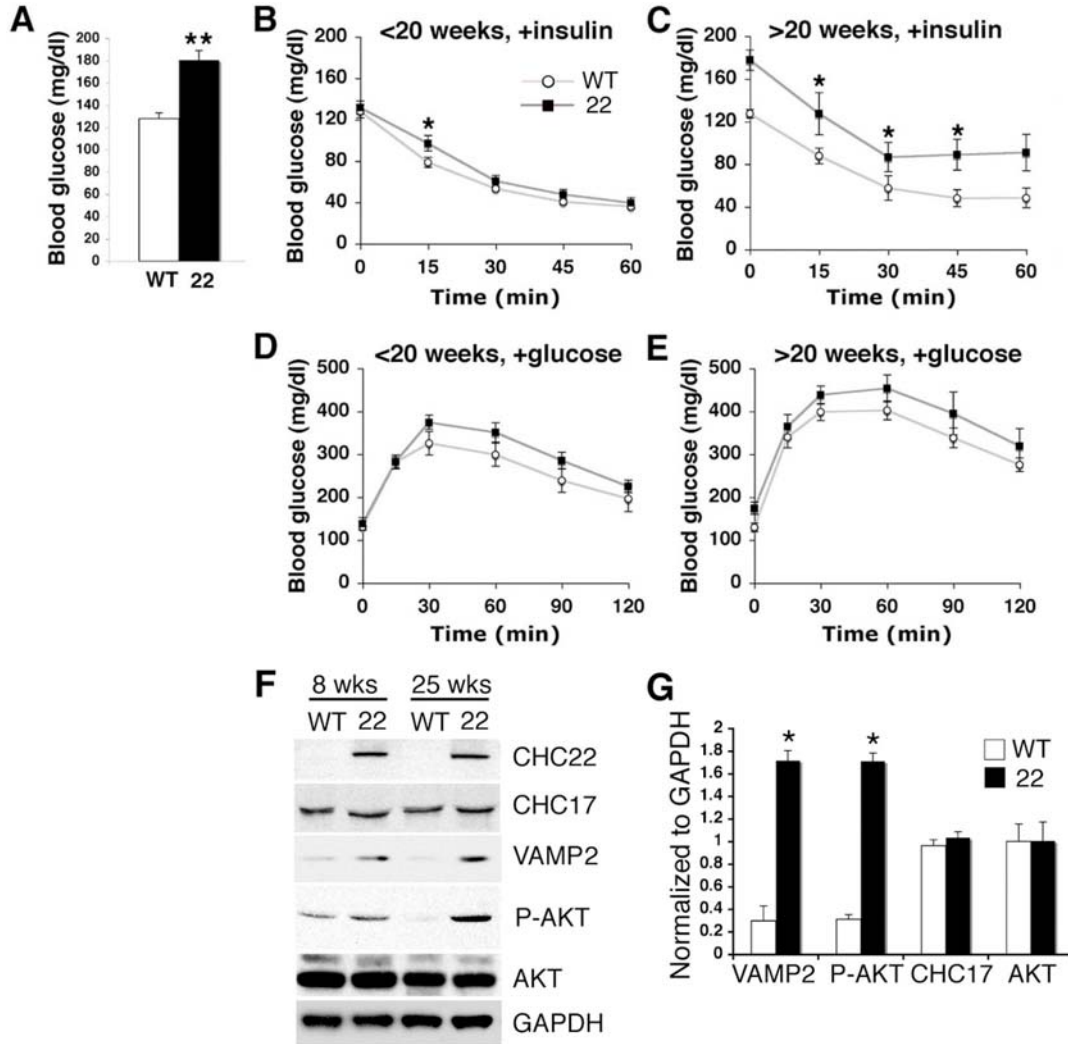
Fig. 3-6. Symptoms of diabetes in CHC22 transgenic mice. CHC22 transgenic mice and age-matched wild-type mice were fasted and their blood glucose levels measured directly (A) or following injection of insulin (B and C) or following injection of glucose (D and E). **(A)** Blood glucose level of wild type (WT, n=10) and CHC22 transgenic mice (22, n=10 representing all three strains) after 6 hours of fasting. **(B and C)** CHC22 transgenic mice of all three strains (ν) or their wild type littermates (ϒ) of age <20 weeks or > 20 weeks were fasted for 6 hours, then injected with insulin. Blood was collected from their tail vein at the indicated time after injection and glucose levels were measured. **(D and E)** CHC22 transgenic mice of all three strains (ν) or their wild type littermates (ϒ) of age <20 weeks or > 20 weeks were fasted for 16 hours, then injected with glucose (2g/kg body weight). Blood was collected from the tail vein at the indicated time after injection and glucose levels measured The curves show average glucose levels of 6 to 10 mice. Statistical analysis was performed using Student's t-test. Asterisks indicate points that are statistically different from each other (P<0.05). Error bars represent ±SEM. **(F)** Skeletal muscle lysate (40 μg) from CHC22 transgenic strain 2 (22) or age-matched wild-type (WT) littermates were analyzed for expression of proteins involved in GLUT4 membrane traffic by immunoblotting with antibodies against proteins indicated at the right, including phosphorylated AKT (p-AKT), total AKT and GAPDH, as a control. The age of the mice analyzed is indicated above the lanes. **(G)** Expression levels of proteins detected in F relative to GAPDH for CHC22 transgenic mice or wild-type littermates, all older than 25 weeks. (n=6 for each mouse strain, error bar represents SD, p<0.05, asterisks indicate statistically significant differences).

The hyperglycemic and insulin resistance phenotypes of the transgenic mice suggest changes in the GLUT4 membrane traffic pathway. To characterize these changes at the protein level, skeletal muscle homogenates were analyzed for expression of proteins involved in GLUT4 transport and glucose metabolism. Increased levels of phosphorylated AKT (pAKT) and of VAMP2 were detected in the skeletal muscle of the CHC22-mice compared to muscle from age-matched wild type mice (Fig. 3-6, F and G). This phenotype was stronger in older CHC22-mice (25 weeks vs 8 weeks) and was observed for all three strains of CHC22-transgenic mice (Fig. 3-8A). Other proteins including total AKT, GLUT4, IRAP, the SNARE Vti1a and CHC17 showed no change in level with age or presence of the transgene in all strains (Fig. 3-6, F and G, and Fig. 3-8A). Thus, the increased level of pAKT (phosphorylation at serine 473 detected by specific antibody) was not due to an increase in total AKT protein. Rather, it is a hallmark of increased signaling in the GLUT4 export pathway, sometimes observed in diabetic conditions (Lizcano and Alessi, 2002; Manning and Cantley, 2007). While insulin levels were not significantly elevated in the transgenic mice (data not shown), their increase in pAKT indicates hyperactivity of the signaling pathway leading to GLUT4 export (Ng et al., 2008) and suggests a compensatory response to disruption of that pathway. The slight increase in GLUT1 levels in the transgenic mice (Fig. 3-8A) could also reflect a compensatory pathway responding to their need for increased glucose clearance. These phenotypes are unlikely to be caused by the only other BAC-encoded transgene, SLC25A1 (formerly CTP), a citrate transporter (Palmieri et al., 1996) that is expressed naturally from the BAC promoter (fig. 3-5D) and has an existing function in mice. The altered glucose metabolism in the transgenic mice is more feasibly explained by a direct effect of the presence of CHC22 clathrin. The elevated level of VAMP2 in the transgenic mice is indicative of altered membrane traffic in the presence of CHC22.

Since VAMP2 participates in GLUT4 release, its altered traffic would impair insulin-stimulated glucose metabolism by disruption of GSC function.

Aberrant sequestration of GLUT4 membrane traffic components in CHC22-transgenic mice

The disruption of GLUT4 membrane traffic by expression of CHC22 in mouse skeletal muscle was confirmed by morphological analysis.   Isolated muscle fibers from the transgenic mice showed that GLUT4, IRAP and VAMP2 were localized to swollen GSC-like structures (Fig. 3-7A). These structures, revealed by serial optical sections of fibers stained for immunofluorescence, were visible as extensive bright patches just underneath the plasma membrane and were not seen in wild-type mouse muscle fibers. Further analysis of muscle fibers showed CHC22 co-localized with GLUT4 and IRAP in these compartments (Fig. 3-83B) and that GLUT1 was excluded (Fig. 3-8C), indicating abnormal expansion of the GSC in the CHC22-transgenic mice relative to wild-type mice. To confirm that the presence of CHC22 could be responsible for excessive sequestration of VAMP2 and GLUT4 in these enlarged compartments, the biochemical interaction between CHC22 and murine components of the GLUT4 trafficking pathway was assessed for mouse muscle (Fig. 3-7B).   VAMP2, GLUT4 and GGA2 co-immunoprecipitated with CHC22 from transgenic mouse muscle, while less GLUT4, no VAMP2 and very little GGA2 were detected in association with CHC17 in either transgenic or wild-type mouse muscle. As seen for human muscle, the endocytic adaptor AP2 segregated with CHC17 and not CHC22. In muscle, the majority of GLUT4 export and subsequent endocytosis occurs at T-tubules (Zhu et al., 2007).
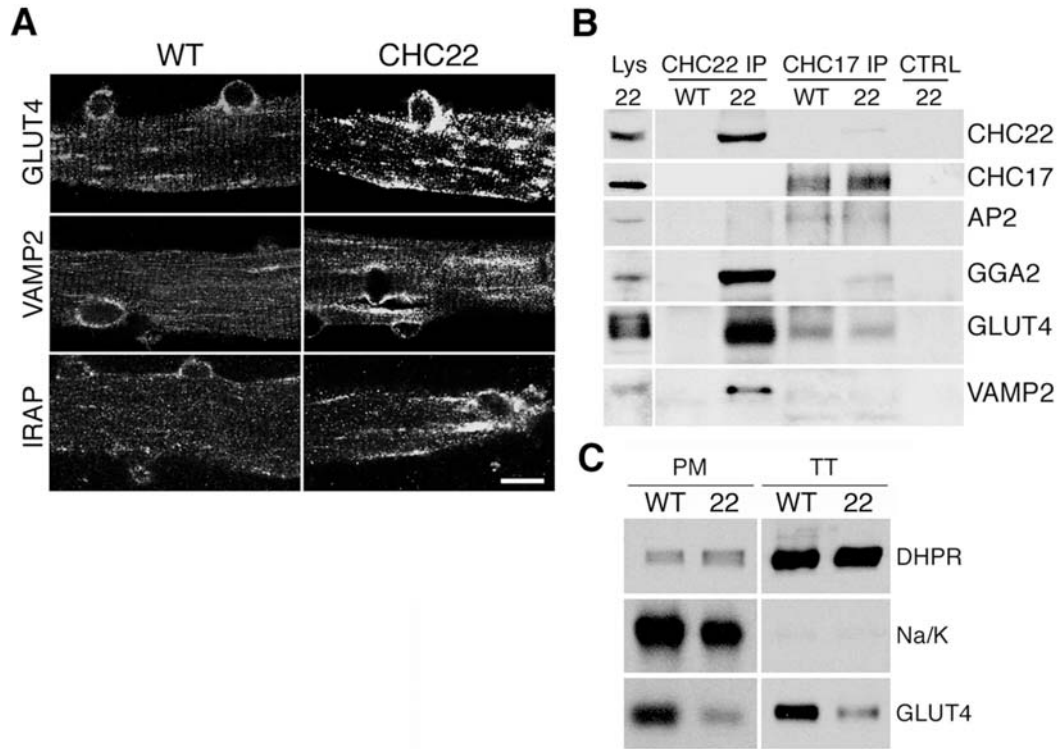
Fig. 3-7. Analysis of GLUT4 membrane traffic in CHC22 transgenic mice. (A) Skeletal muscle fibers were isolated and cultured from (WT) or CHC22 transgenic mice (22) (6 weeks old). These were analyzed by immunofluorescence using antibodies against GLUT4, VAMP2 and IRAP, detected with Alexa488-conjugated secondary antibody. Scale bar represents 20 μm. **(B)** Skeletal muscle lysate (of whole tissue) from wild type (WT) or transgenic CHC22 mice (22) was used for immunoprecipitation (IP) with antibodies against CHC22, CHC17 or an isotype-matched control (CTRL) antibody. Immunoprecipitates were analyzed for the proteins indicated at the right by immunoblotting. Starting lysate (Lys, 1%) of CHC22 mouse muscle is shown. **(C)** Fractionation of plasma membrane and T-tubules from wild-type (WT) or CHC22 transgenic mice (22). Equal amounts of protein from each fraction were analyzed by immunoblotting with antibodies against proteins indicated at the right, including the T-tubule marker dihydropyridine receptor (DHPR) and the plasma membrane marker Na/K-ATPase. These data represent results from all three CHC22-transgenic mouse strains.
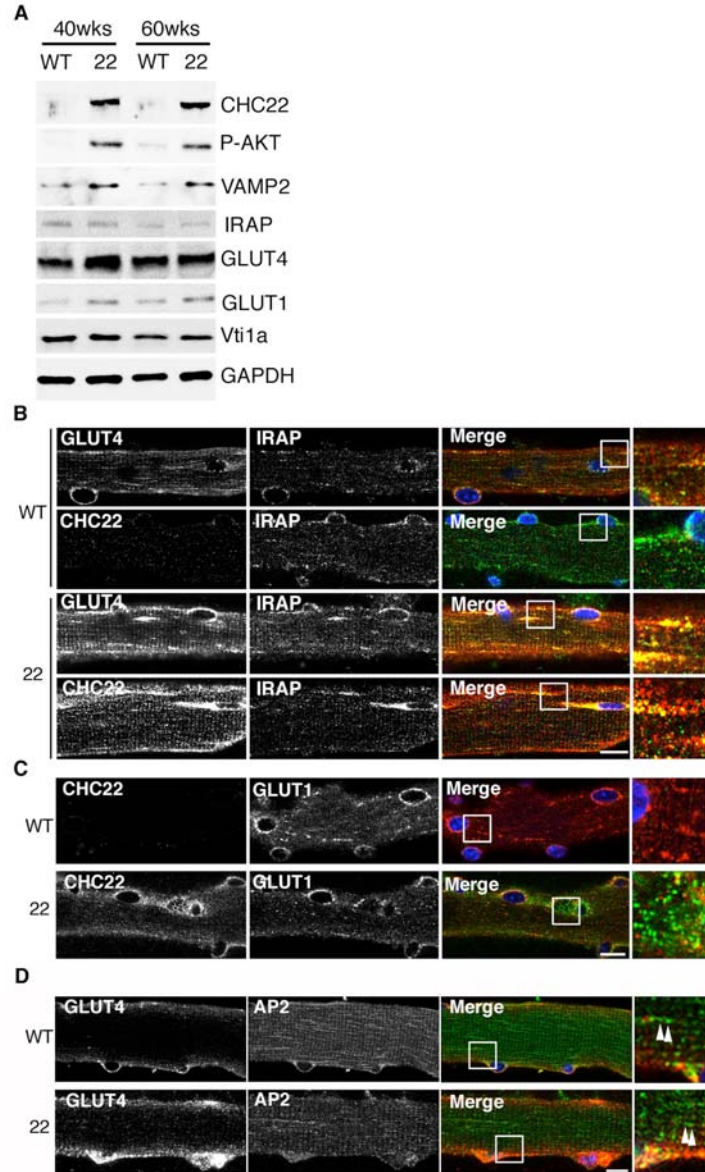
Fig. 3-8. Components of GLUT4 membrane traffic pathway in CHC22 transgenic mice and comparison to GLUT1 expression. (A) Skeletal muscle lysate (of whole tissue) (40 μg) from CHC22 transgenic (22) or age-matched wild-type (WT) littermates was analyzed for expression of proteins involved in GLUT4 membrane traffic by immunoblotting with antibodies against proteins indicated at the right, relative to GAPDH, as a control. The levels of SNARE protein Vti1a and GLUT1 were also measured. The age of the mice analyzed is indicated above the lanes. The CHC22 transgenic mice analyzed in this experiment were derived from strains 7 (40 weeks) and strain 10 (60 weeks), while the samples analyzed in Fig. 5 were from strain 2, demonstrating that VAMP2 and pAKT were elevated in all CHC22-transgenic strains. **(B, C and D)** Muscle fibers from CHC22 transgenic (all strains) (22) or WT mice were processed for double immunofluorescent labeling by antibodies recognizing the indicated proteins and analyzed by confocal microscopy. Polyclonal antibodies against GLUT4, CHC22 and GLUT1 were detected with Cy3-conjugated-anti-rabbit Ig (red) and monoclonal antibodies against IRAP, CHC22 and AP2 were detected with Alexa488-conjugated-anti-mouse Ig (green). Each row of micrographs is the same sample with the black and white images showing staining for the individual proteins and the merge showing these images overlapped in color, with yellow indicating colocalization. Scale bars, 20μm.

The clathrin adaptor at these membranes is AP2 (fig. 3-8D), which shows a distribution pattern typical of the T-tubules. These biochemical and morphological data further dissociate CHC22 function from plasma membrane and T-tubule endocytosis and point to a role in GSC generation from the TGN and endosomes in human skeletal muscle. When this CHC22 function is introduced into mice, which form the GSC without it, their GSC is altered and GLUT4 transport is perturbed.

Recent studies have implicated CHC17 in membrane traffic of several SNARE proteins (Borner et al., 2006; Miller et al., 2007). The strong association of CHC22 with VAMP2 in both human and transgenic mouse skeletal muscle suggests an orthologous role for CHC22 in VAMP2 traffic, which would affect VAMP2 targeting in the CHC22-mice, explaining its increased stability. To investigate the possibility that excessive sequestration of VAMP2 affects GLUT4 recruitment to the plasma membrane, levels of GLUT4 associated with the plasma membrane (PM) and T-tubule (TT) membranes were assessed (Fig. 3-7C). Membranes from transgenic and wild-type mouse muscle were fractionated by differential centrifugation and the identity of the PM and TT fractions confirmed by the respective presence of the Na/K-ATPase and the dihydropyridine receptor. Both membrane fractions from the CHC22 transgenic mice had reduced levels of GLUT4 associated with them relative to levels detected in wild-type mice. Overall, the analysis of GLUT4 distribution in the muscle of CHC22 transgenic mice confirms its inappropriate sequestration in an intracellular compartment with VAMP2 and IRAP resulting in lower expression at the PM and TT. This reduction in steady state levels of surface of GLUT4 indicates that the ongoing insulin response of CHC22-transgenic mouse muscle is defective for GLUT4 release compared to wild-type mice, explaining the hyperglycemia and insulin resistance of the transgenic mice.

Model for species-restricted clathrin function in human glucose metabolism

Here we demonstrate that CHC22 clathrin is required for generation of the GSC in human myoblasts and influences membrane traffic of GLUT4, IRAP and VAMP2, three components of the GSC. The data indicate that CHC22 and its association with the GGA2 adaptor are involved in diversion of these components from the TGN and possibly endosomes to the GSC, but that CHC22 is not involved in GLUT4 endocytosis (Fig. 3-9A, steps 3, 2 and 1, respectively). In spite of this key role for CHC22 in GSC formation in humans, it is absent from mouse skeletal muscle and its artificial presence disrupts the function of the mouse GSC to the extent of inducing some diabetic symptoms. These observations raise the questions of how do mice organize their GSC since they lack CHC22 and how does murine GSC formation relate to what occurs in human skeletal muscle? From the studies of GSC formation in rodent cells, it is clear that GGAs, AP1 and CHC17 play important roles in diverting GLUT4 to the GSC from the constitutive secretory pathway via the TGN, and other adaptors seem to be involved in GLUT4 diversion from endosomes back to the GSC (Li et al., 2007; Watson et al., 2004). These pathways are clearly sufficient to produce a functional GSC in mouse skeletal muscle (Fig. 3-9B). We propose that in the skeletal muscle of the CHC22-transgenic mice (Fig. 3-9C), CHC22 competes for CHC17 binding to GGA2 as it must do in human cells, and excessively sequesters cargo targeted to the GSC such that GLUT4 and VAMP2 cannot be normally released in response to insulin (Fig. 3-8, step 4). Problems with GLUT4 release could be due to CHC22 interfering with the normal equilibrium between exocytosis and endocytosis that allows the GSC to function in mice. GSVs formed in the presence of CHC22 could have an altered composition that affects their ability to be released or mice may lack additional factors needed to regulate CHC22.
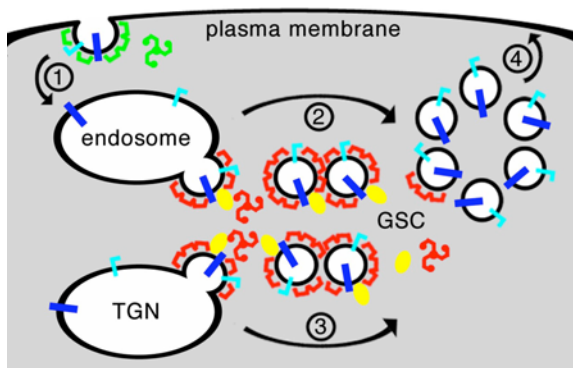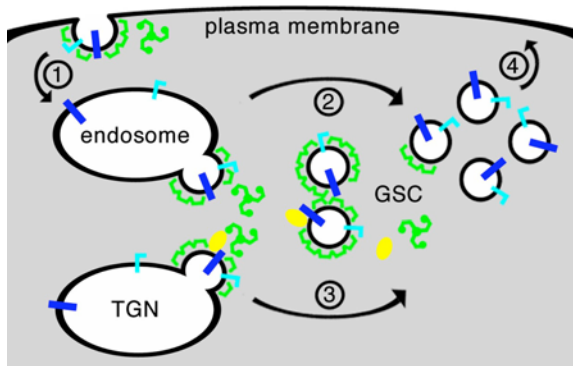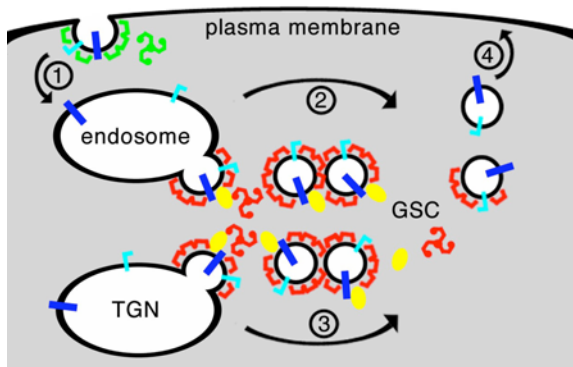
Fig. 3-9. Proposed roles for CHC22 and CHC17 clathrins in GSC formation in human, wild-type mouse and CHC22-transgenic mouse skeletal muscle. Transport steps are indicated by numbers: (1) endocytosis from the plasma membrane, (2) endosome to GSC, (3) TGN to GSC and (4) insulin-induced exocytosis. **(A)** In human muscle, CHC22 is the main clathrin responsible for diversion of GLUT4, VAMP2 and IRAP (not shown) into the GSC from the TGN and possibly endosomes, using the GGA2 adaptor. CHC17 functions in retrieval of GLUT4 from the plasma membrane. **(B)** In wild-type mouse, the GSC can form, but since CHC22 is lacking, the GSC is less stable and more dependent on equilibrium between endocytosis, biogenesis and secretion. In this situation, CHC17 clathrin mediates all the adaptor dependent steps for sorting GLUT4. **(C)** In CHC22-transgenic mouse, CHC22 competes with CHC17 for interactions with GGA2 adaptors and over-stabilizes the GSC, causing its expansion, disruption of the normal equilibrium in mouse and trapping of GSC components, resulting in aberrant GLUT4 function.

Syntaxin 10 and TBC1D3 are other examples of membrane traffic proteins missing from mice but present in humans, setting a precedent for potential species-restricted proteins that could be needed for CHC22 function (Frittoli et al., 2008; Ganley et al., 2008; Wainszelbaum et al., 2008). We note that, in contrast to CHC17, which is about 50%

cytosolic, CHC22 is mainly membrane associated at steady state. In addition, despite its interaction with AP1 and GGA2, CHC22 is not dissociated from intracellular membranes by treatment of cells with Brefeldin A, a drug which disrupts CHC17 binding to the TGN (data not shown). These properties suggest that CHC22 confers greater stability to tubules or vesicles containing GSC components than those formed only in the presence of CHC17, expanding the human GSC compared to that in rodents (Fig. 3-9, A and B). This would correlate with a relatively more robust GLUT4-mediated response to insulin in human myoblasts and muscle compared to the response in mice (Sarabia et al., 1992; Tortorella and Pilch, 2002) and with the excessive sequestration of GSC components in the transgenic mice (Fig. 3-9C).

While much has been learned from mouse models about glucose metabolism that is relevant to human diabetes, the studies reported here highlight some important species-specific differences that will facilitate better understanding of the human disease. By demonstration that GLUT4 membrane traffic differs between human and mouse muscle, our findings could help explain why 70-90% of insulin-stimulated glucose clearance depends on skeletal muscle in humans (Postic et al., 2004; Shepherd and Kahn, 1999), but in mice, the liver is the most influential organ controlling insulin responsive glucose reduction in the bloodstream (Bruning et al., 1998; Michael et al., 2000). Notably however, our findings still verify a role for mouse skeletal muscle in insulin-stimulated glucose clearance since disruption of GLUT4 traffic in mouse skeletal muscle by introduction of CHC22 results in some symptoms of diabetes. Finally, the ability of CHC22 to partially carry out its function in transgenic mice raises the possibility of rescuing the rest of its function and creating a better mouse model in which human glucose metabolism and diabetes can be studied.

Materials and methods

Antibodies

One monoclonal and one polyclonal antibody that specifically recognize CHC22 and not CHC17 have been described (Liu et al., 2001). A second polyclonal antibody against amino acids 1549-1563 from human CHC22 was raised by contract (New England Peptides). The antibody was purified negatively and positively, using recombinantly expressed trimerization domain fragments of human CHC17 and CHC22, respectively, coupled to NHS-Hi-Trap columns (Amersham) and specificity for CHC22 was confirmed by immunoblotting the recombinant fragments. Commercial sources of antibodies were as follows: mouse monoclonal anti-VAMP2 (Synaptic Systems), rabbit polyclonal anti-GLUT4 (Calbiochem), goat polyclonal anti-GLUT4 (Santa Cruz), mouse monoclonal anti-GLUT4 (Sigma), rabbit polyclonal anti-GLUT1 (Abcam) and antibodies to GGA3, TGN46, EEA1, COP1, AP1 and Vti1a (Transduction Laboratories). Anti-CHC17 (mouse monoclonals X22 and TD.1 and rabbit polyclonal against clathrin light chains) and anti-AP2 (AP6) antibodies used in this study were produced by our laboratory and extensively characterized in the literature (references available upon request). Monoclonal anti-GGA1 and GGA2 antibodies were gifts from Juan Bonifacino (NIH, Bethesda) with permission from John Hopwood (Women's and Children's Hospital, Adelaide), and monoclonal anti-IRAP antibody was a gift from Morris Birnbaum (University of Pennsylvania, Philadelphia). Secondary antibodies for immunofluorescence were from Molecular Probes (Alexa488, Alexa568 conjugate) and

Jackson Immunoresearch (Cy3-conjugates). Secondary antibodies coupled to HRP were from Zymed Laboratories.

Muscle tissue lysate and microsome preparation

Membrane microsomes or lysate of whole tissue were prepared from human (fresh autopsy sample) or mouse skeletal muscle (freshly dissected). For muscle lysate, tissue was homogenized with a polytron (3 times 5s, speed 5) in lysis buffer (1gm/7ml 50 mM Tris-HCl pH 7.5, 0.15 M NaCl, 1 mM EDTA, 1% NP40 and 1 protease inhibitor cocktail tablet (1/10ml buffer, Roche, Indianapolis, IN)). Homogenate was centrifuged (10 min, 14,000 x g) and the pellet discarded. Protein concentration of the lysate was determined by Bradford assay (Biorad). For membrane microsomes, tissue was homogenized by dounce (1-2gm/10 ml 200 mM sucrose, 20 mM HEPES pH 7.4, 0.4 mM $CaCl_2$, 2 mM leupeptin, 100 mM phenylmethylsulfonyl fluoride (PMSF) and the low-speed (10 min, x 1,400 g) pellet discarded. Resulting supernatant was centrifuged (50 min, 41,000 x g), yielding microsomes in the pellet and a soluble fraction. The microsome pellet was resupsended in 0.1 M NaCl, 30 mM imidazole pH 6.8, 8% sucrose with protease inhibitors at a final concentration of 8-10 mg/ml and stored at -80°C. Immunoblotting for marker proteins revealed the presence of plasma membrane (AP2 adaptor), endoplasmic reticulum (calnexin) and Golgi (b-COP) membranes in the microsome fraction and by shared sedimentation properties indicated the presence of all cellular membranes (Fig. 2).

Clathrin coated vesicle (CCV) isolation

Human or mouse skeletal muscle microsomes, prepared and stored as above, were diluted (2.5 mg/ml) in ice-cold Buffer A (0.1 M MES pH 6.5, 0.2 mM EGTA, 0.5 mM MgCl2, 0.02% NaN3, 0.2 mM PMSF) and the suspension mixed with an equal volume of 12.5% Ficoll/12.5% sucrose in buffer A, then centrifuged (25 min, 21,000 x g). The supernatant was diluted with four volumes of Buffer A, and CCVs were pelleted (30 min, 136,000 x g), then resuspended in 30–100 μl buffer A using a 0.1-ml hand-held glass homogenizer.

Plasma membrane and T-tubule isolation

Mouse skeletal muscle microsomes were applied to a discontinuous sucrose gradient (25, 32 and 35%, w/w in Buffer A and centrifuged (150,000 x g, 16 h). Membranes at the sample/25% interface (plasma membrane, PM) and the 32/35% interface (transverse tubules, TT) were recovered, diluted with sucrose-free Buffer A and centrifuged (190,000 x g,1 h) (Dombrowski et al., 1996). These membrane fractions were analyzed in Fig. 5C. The PM fraction was further purified by binding to wheat germ agglutinin to eliminate endosomal membranes (Munoz et al., 1995). Analysis of these membranes by immunoblotting confirmed a reduction in PM levels of GLUT4 in the CHC22 transgenic mice compared to wild-type mice (data not shown).

Immunoblot analysis

Protein samples were separated by electrophoresis (4-12% acrylamide gel), then electrophoretically transferred to nitrocellulose (Millipore) and labeled with primary antibodies at 1-5 mg/ml and secondary antibodies coupled to horseradish peroxidase (Jackson ImmunoResearch Laboratories). The presence of CHC22 or other proteins in samples was detected using Western Lightning Chemiluminescence Reagent (Amersham). Quantification was performed using Quantity One software (Biorad).

Immunoprecipitation

Human skeletal muscle microsomes or mouse skeletal muscle tissue lysate were diluted to 500 μg/ml or 3mg/ml respectively in lysis buffer (50 mM Tris-HCl pH 7.5, 0.15 M NaCl, 1 mM EDTA, 1% NP40 and 200 μM PMSF), precleared with 20 μl washed Protein-G-Sepharose (PGS 4 fast flow, Amersham Biosciences) per 400 μl of diluted microsomes or lysate, and incubated with 20 μg of specific antibody overnight (4°C). Then 20 μl washed PGS added and incubated for 1 hr at 4°C, followed by washing (3X with lysis buffer). Pelleted PGS was taken up in sample buffer and subjected to electrophoresis and immunoblotting.

Dissociated fiber cultures

Myofibers were isolated from the dissected *flexor digitorum brevis* muscle of 6-wk old mice by digestion with collagenase 1a (Worthington Biochemical Corp.) and mechanical

dissociation (Kaisto et al., 1999). Isolated fibers were cultured (37°C, 5% CO_2) in Dulbecco's Modified Eagle medium (DMEM) with high glucose, 1% horse serum (GIBCO), and penicillin/streptomycin on coverslips coated with Matrigel (Becton Dickinson Labware, Bedford, MA). Myofibers were used for experiments after overnight culture.

Human myoblast cultures

LHCNM2 human skeletal muscle cells (Zhu et al., 2007) were maintained in tissue culture flasks coated with rat-tail collagen in basal medium (4:1 DMEM:M199, 0.02M HEPES, 0.03 μg/ml $ZnSO_4$, 1.4 μg/ml Vitamin B12) with 10% fetal bovine serum (FBS), 55ng/ml dexamethasone, 2.5ng/ml hepatocyte growth factor (Sigma), 50 U/ml penicillin, 50 mg/ml streptomycin, 0.625 μg/ml fungizone (growth medium). Differentiation was induced by culturing in fusion medium (basal medium with 0.5% FBS, 10 μg/ml insulin, 50 μg/ml apo-transferrin and 5.5 ng/ml dexamethasone) followed by differentiation medium (basal medium with 0.5% FBS, 55 ng/ml dexamethasone). Differentiation medium was applied as soon as multinucleated myotubes appeared in the culture, normally after about 7 days and cells were differentiated for an additional 7 days. After this procedure, approximately 30% of the myoblasts were fused into multinucleated myotubes. For siRNA treatment, cells were transfected twice 72h apart using 10nM siRNA and HiPerfect transfection reagent (Qiagen) according to manufacturer's instructions. Targeting and non-specific control siRNAs were synthesized by Qiagen. DNA sequences targeted were AAGCAATGAGCTGTTTGAAGA for CHC17 and TCGGGCAAATGTGCCAAGCAA and AACTGGGAGGATCTAGTTAAA for CHC22 (1:1

mixture of siRNAs were used). Experiments were performed 72h after the final transfection.

Immunofluorescence microscopy

Adult human or mouse skeletal muscle was embedded in Tissue-Tek OCT compound (Miles Inc.), frozen, and stored at -80°C. Cryosections (10 μm thick) collected on microscope slides were fixed (15 min, 4% paraformaldehyde in PBS, RT), washed (2X, 10 min, PBS, 4°C), permeabilized (5 min, 0.5% Triton X-100 in PBS, RT) and blocked (30 min, PBS with 0.1% Triton X-100, 0.5% bovine serum albumin (BSA)). Sections were incubated with primary antibodies (overnight, 4°C, 2-5 mg/ml in PBS with 0.1% Triton X-100, 0.5% BSA) and washed (3X, 10 min, 4°C, PBS with 0.1% Triton X-100). Sections were then incubated with secondary antibodies (manufacturers' dilutions, 30 min, RT), washed (3X, 10 min, PBS with 0.1% Triton X-100, RT), and mounted with anti-fading solution (DABCO) containing DAPI (300 nM). For double labeling, the two primary antibodies (from different species) or the two secondary antibodies were added simultaneously at the appropriate step. Secondary antibodies were labeled with either Alexa-488, Alexa-546 (Molecular Probes), or Cy3 (Jackson ImmunoResearch Laboratories). For myofibers isolated from mouse muscle, immunolabeling was performed directly in the 24-well culture plate. Cells were fixed (15 min, 4% paraformaldehyde in PBS, RT) washed (2X, 5 min, PBS), permeabilized (10 min. PBS with 0.5% Triton X-100), and immunolabeled using the same procedure described for human and mouse muscle sections. For LHCNM2 cells grown on coverslips, cells were washed in warm PBS, fixed in warm PFA (3.7% in PBS, 10min), then washed (2X, 5 min, PBS), permeabilized (4 min. 3% BSA, 0.5% Triton X-100 in PBS) and blocked in

blocking solution (3% BSA in PBS, 30 min). Antibody labeling was by inversion of coverslips on 20μl blocking solution with primary or secondary antibodies (1-5μg/ml) or DAPI (300nM) on parafilm and washing with PBS. Samples were mounted in Prolong Antifade Kit (Invitrogen). Muscle sections, LHCNM2 cells and myofibers from mouse muscle were analyzed by confocal laser scanning microscopy using a Nikon EZ-C1Si operating system an ApoPlan 100x, 1.40NA oil lens. DAPI, Alexa-488, Alexa-568, or Cy3 fluorescence was sequentially excited using lasers with wavelengths of 405 (DAPI), 488 (Alexa 488) and 561 nm (Alexa 568, Cy3). Z-series from the top to the bottom of fibers were sequentially collected for each channel with a step of 0.9-1μm between each frame. Data for this study were acquired at the Nikon Imaging Centers at UCSF.

Glucose uptake assay

Glucose uptake assays were based on published procedures (Li and Kandror, 2005). Fully differentiated LHCNM2 cells were stimulated with 100nM insulin in differentiation medium for 10 min, washed twice with warm Krebs-Ringer-Henseleit (KRH) solution (121mM NaCl, 4.9mM KCl, 1.2mM $MgSo_4$, 0.33mM $CaCl_2$, 12mM HEPES), followed by addition of warm 0.1mM 2-Desoxyglucose in KRH with 1mCi/ml ^{3}[H]-2-Desoxy-Glucose for 5 min and reactions stopped by addition of ice-cold 25mM 2-Desoxyglucose in KRH. Cells were then washed twice with KRH, 4°C and lysed in 0.1% SDS in KRH. To determine non-specific glucose uptake, 5mM Cytochalasin B (CytB) was included when ^{3}[H]-2-Desoxy-Glucose was added in parallel samples. Protein concentration of lysates were determined using Bradford reagent (Biorad) and radioactivity measured by scintillation counting. The ratio of insulin-stimulated glucose uptake to basal glucose

uptake was calculated using the following equation, where A is activity measured in cpm:

$$(A_{insulin} - A_{insulin + CytB}) / A_{basal} - A_{basal + CytB}).$$

Generation of BAC transgenic mice

BAC339F21 containing the CLTCL1 gene was isolated from the RPCI11 BAC library (www.chori.org/bacpac). The ends were sequenced to determine the exact boundaries. DNA for pronuclear injections was isolated using the Endo-free Plasmid Maxi Kit (Qiagen) and transferred into injection buffer (10mM Tris HCl ph 7.5, 0.1 mM EDTA, 100mM NaCl) using a pre-equilibrated sepharose CL4b column. Circular BAC DNA was injected into the pronucleus of fertilized FVB zygotes at a concentration of 3 ng/ml. Injections were performed by the Transgenic Core at the Dana Farber Cancer Institute. Founders were identified by PCR using vector-specific primers for pBACe3.6 (BACT7-F AATGCTCATCCGGAGTTCC and BACT7-R ACTGGTGAAACTCACCCAGG).   Five founders were generated (#2, 3, 7, 10, 41) and further analyzed by PCR using human specific PCR primers across the region (fig. S2). All five founders contained all markers (data not shown).

Genetic analysis of transgenic lines

Approximate transgene copy numbers were determined by Southern blot hybridization using a human intragenic CLTCL1 probe (intron 6-7) and a mouse probe corresponding to a single copy locus from mouse chromosome 16 (BAC72mu2-F: TAGCCACTCCACAAGGCAG and BAC72mu2-R: CCCTGAGCTACGTCTTCTGG). After transfer of the genomic DNA to a nylon membrane, the membrane was cut and the

probes detecting human or mouse genes were hybridized separately to the resulting membrane pieces each of which comprised the target fragments. For Northern analysis, a probe corresponding to CLTCL1 exons 6-10 was generated by RT PCR and hybridized to 25 mg of total RNA. Human RNA from skeletal muscle and testis (Clontech) served as a positive control (fig. S2). Line 41 generated an aberrant transcript (data not shown) and was therefore excluded from further analyses.

Glucose and insulin tolerance tests

Mice were fasted (14 to 16 hrs), then injected intraperitoneally with D-glucose (1 mg/gm body weight). Blood was collected from the tail vein prior to injection (time 0) and 15, 30, 60, 90 and 120 min post-injection. Glucose levels were measured using a Freestyle Flash Glucometer (Abbott). For insulin tolerance tests, fasted mice were administered recombinant insulin (bovine, Sigma) intraperitoneally (1 U/kg of body weight in 0.9% NaCl solution), and glucose levels were measured at 15, 30, 45 and 60 min post-injection.

Chapter 4 - Discussion and further directions

In this study I explored the functions of a novel clathrin heavy chain isoform, CHC22. Although it displays 85% sequence identity to CHC17, its well-characterized homologue, both clathrin heavy chains do not function together, nor can they substitute for one another. Instead, both act independently in different sorting pathways in the cell for specific cargo.

Studies in HeLa

HeLa cells were used to compare CHC17 and CHC22-function side by side. Hela cells are advantageous for these studies, since they represent a non-specialized cell model. Furthermore, Hela are readily maintained in culture and protocols for performing a variety of assays is readily available. Indeed, HeLa is the cell model of choice for numerous membrane traffic studies.

I could demonstrate that CHC22 neither acts together with, nor substitutes for CHC17 function. This is consistent with previous data generated in the Brodsky laboratory (Liu et al., 2001; Towler et al., 2004a). CHC22 involvement in various functions mediated by CHC17 was tested for including clathrin-mediated endocytosis and mitotic spindle recruitment. Further studies of functions of CHC17 in membrane traffic at the TGN and early endosomes, as defined by the early endosome antigen EEAI, indicated that CHC22 is not directly involved in these either, despite possible interactions with the relevant clathrin adaptors AP1 and AP3. However, I revealed a function for CHC22 in sorting of cargo in an endosomal compartment. Both M6PR- and Shiga-Toxin-trafficking

were inhibited in a post early endosomal compartment as defined by the absence of EEAI on M6PR- and STxB-containing vesicles in CHC22-depleted cells. This contrasts with TGN46 trafficking, which was influenced by CHC17- but not CHC22-depletion. This places CHC22 function downstream of CHC17 function in endosomal sorting.

STxB has been crucial in defining endosomal sorting pathways, since it tafficks in a unidirectional manner from the plasma membrane via early endosomes to the TGN (Mallard et al., 1998). Subsequent studies defined a role for CHC17 in STxB sorting in EEAI-positive early endosomes (Saint-Pol et al., 2004) which was reproduced in this study. Recently, it was proposed that CHC17 and retromer act synergistically in STxB export from EEAI-positive endosomes as depletion of retromer results in accumulation of STxB in EEAI-negative tubules emanating from EEAI-positive structures. Formation of these tubules also required CHC17 (Popoff et al., 2007). Depletion of CHC22 led to accumulation of STxB in EEAI-negative vesicles. Notably, STxB was found on EEAI-positive structures after 15 min. of internalization even in CHC22-depleted cells, stongly suggesting that a block in its trafficking occurred in a compartment downstream of EEAI-positive early endosomes.

M6PR accumulated in the same compartment in CHC22-depleted cells, suggesting that is shares these vesicles with STxB. In contrast to STxB, M6PR is blocked in the TGN in CHC17-depleted cells, due to its export from the TGN being CHC17-mediated, an effect previously described in the literature (Hinrichsen et al., 2003; Meyer et al., 2000). Also, SNX1-depletion impairing retromer function on M6PR-trafficking resulted in accumulation

of the receptor in EEAI-positive early endosomes, again mirroring published data (Arighi et al., 2004; Seaman, 2004).

The third trafficking molecule that I assessed was TGN46. Its retrograde trafficking from endosomes to TGN required CHC17 but not CHC22, the depletion of which did not result in any change on TGN46 localization or protein stability. In addition, I did not detect any effect of SNX1-depletion on TGN46, in agreement with current literature (Arighi et al., 2004; Bujny et al., 2007; Franch-Marro et al., 2008) contrasting with one report describing fragmented Golgi staining of TGN46 in retromer depleted cells (Seaman, 2004). This suggests that retrograde trafficking of TGN46 is CHC17-mediated but independent of retromer and CHC22 function. This places TGN46 endosome exit upstream of the latter two activities.

Studies in LHCNM2

CHC22 expression is highest in skeletal muscle and upregulated in skeletal muscle differentiation. Therefore, skeletal muscle specific functions for CHC22 were hypothesized, as muscle displays several tissue-specific membrane trafficking pathways utilizing muscle-specific isoforms of ubiquitous trafficking molecules (Towler et al., 2004b). To test for muscle-specific functions of CHC22, LHCNM2 cells were cultivated. This cell line is an immortalized cell line derived from primary human myoblasts (Zhu et al., 2007). LHCNM2 myoblasts displayed the ability to differentiate into multinucleated myotubes upon the removal of serum. In addition, the fusion process was highly dependent on the concentration of dexamethasone in the media. These cells are not as

versatile as HeLa cells and grow very slowly. In comparison to the commonly used skeletal muscle cell lines C2C12 (derived from mouse) or L6 (derived from rat), LHCNM2 grow more slowly and fusion is less effective at about 30 - 40 % fused nuclei to 70 - 80 % in C2C12 (Fulco et al., 2008). Nonetheless, some key experiments could be performed in LHCNM2 cells, as they allowed for effective depletion of proteins using siRNA and displayed robust insulin-induced glucose-uptake. Notably, depletion of either clathrin heavy chain did not result in altered differentiation properties when compared to control cells.

One muscle-specific trafficking pathway is the formation of the GLUT4-storage compartment (GSC). This specialized compartment accumulates GLUT4 glucose transporter under basal conditions, to release it in the presence of insulin, rapidly increasing the concentration of glucose transporter on the cell surface. GLUT4 is trafficked to the GSC from both TGN for newly synthesized protein and endosomes for protein recycled from the plasma membrane.

When comparing LHCNM2 cells depleted of either clathrin heavy chain with control cells, I found that CHC22 but not CHC17 is required for formation of the GSC. This was observed both by immunofluorescence, and in a glucose-uptake assay testing function of the GSC. GLUT4-staining, found throughout the cytoplasm in control and CHC17-depleted cells indicative of the vesicular nature of the GSC, was abolished in CHC22-depleted cells. This strongly suggests that a GSC is not formed in these cells. Total GLUT4-levels were also decreased in CHC22-depleted cells, presumably due to increased lysosomal degradation caused by missorting resulting from to the lack of CHC22. Translocation of GLUT4 measured by increased glucose uptake in control cells

stimulated with insulin when compared to basal conditions, was not observed in CHC22-depleted cells further demonstrating the lack of a functional GSC. CHC17 depletion did not affect either GSC-formation or function.

CHC17 has been shown to at least partly mediate GLUT4 endocytosis (Antonescu et al., 2008; Huang et al., 2007). CHC17 involvement in sorting of GLUT4 at the TGN and endosomes has not been directly demonstrated. However, a role for monomeric CHC17 adaptors, the GGAs, has been described in TGN export of GLUT4 (Watson et al., 2004; Watson and Pessin, 2008). A comparable function for GGAs in endosome export of GLUT4 is currently discussed in the literature, with conflicting data being available so far (Li and Kandror, 2005; Watson and Pessin, 2008). Notably all of this data was gathered in rodent cell lines, which do not express CHC22. Data from our laboratory indicates that GGA2 associates more strongly with CHC22 than with CHC17 in human tissue samples. Taken together, the available data defines roles for both clathrin heavy chains in distinct trafficking steps of GLUT4 in humans.

Model of endosomal sorting of various cargos by clathrin heavy chains

Trying to fit all the data available into one model for endosomal trafficking has been challenging, starting with the nature of the compartment itself. Extreme ideas range from segregated vesicular membranes to one large network termed the "tubular endosomal network" (Bonifacino and Rojas, 2006; Maxfield and McGraw, 2004). Notably, temporal distinction between CHC17-, retromer- and CHC22-function could be possible in both models proposed. Also, in all of these considerations one has to take into account the

possibility, that different cargoes are not necessarily sorted together and sorting one cargo out of a compartment leaves this compartment behind with a different protein composition and potentially different reactivity. For example, EEAI-positive endosomes that were described earlier as carrying M6PR, STxB and GLUT4 also carry Tfr-R and EGF-R at some point in their trafficking to the plasma membrane and lysosomes respectively. Other protein determinants have been defined as being required for their transport such as SNX4 for Tfr-R-recycling (Traer et al., 2007) or the ESCRT protein complexes for EGF-R (Williams and Urbe, 2007). Nonetheless, the use of different model cargoes defining specific trafficking routes seems to be a good approach to try to understand endosomal trafficking. Here I try to summarize our current understanding of these processes (Fig. 4-1) and to highlight potential alternative pathways and open questions.
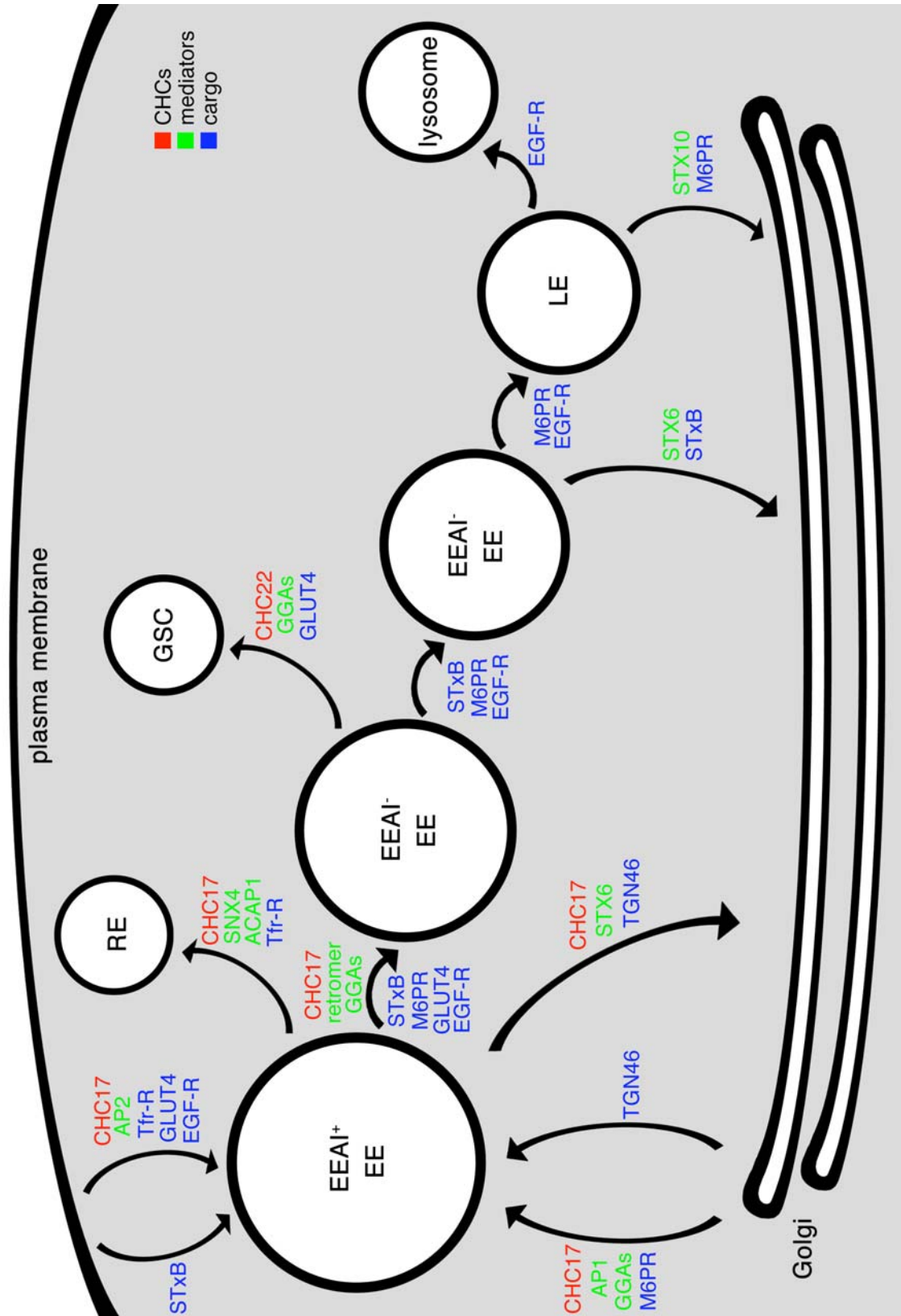
Fig. 4-1: Model of endosomal trafficking. Model depicting endosomal sorting and maturation from early to late endosomes in humans from left to right, with cargo arriving from the plasma membrane and the TGN.

The model assumes that cargo arrives in EEAI-positive early endosomes and is subsequently sorted to their respective target membranes. Immediately upon arrival at this endosomal stage, Tfr-R is recycled back to the plasma membrane via recycling endosomes. Mediators of this sorting step include SNX4 (Traer et al., 2007), and ACAP1 (Li et al., 2007). Recycling of Tfr-R was initially described as being clathrin-independent (Mayor et al., 1993), although this view has recently been challenged (Li et al., 2007). In contrast, recycling of TGN46 to the TGN seems to be CHC17-dependent but retromer- and CHC22-independent (shown in this study), suggesting its rapid export from early endosomes. Notably, STX6 has been demonstrated to be required for retrograde sorting of TGN46 (Ganley et al., 2008).

The role of CHC17 and retromer in M6PR and STxB exit from the EEAI-positive early endosome has been discussed above. Subsequently a role for CHC22 has been demonstrated in this study. Details of further trafficking of M6PR and STxB remain unclear, however these two cargoes have to separate in a downstream step. STxB is thought to traffic from an early endosomal compartment directly to the TGN (Mallard et al., 1998), while M6PR traffic via late endosomes (Lombardi et al., 1993). STX6 and STX10 have recently been used to distinguish between these two pathways (Ganley et al., 2008).

Based on the blocking effect of CHC22-depletion on M6PR and STxB-trafficking occurring in an EEAI-negative compartment, I hypothesize that GLUT4 sequestration to the GSC occurs in the same compartment. While CHC22-depletion results in GSCs not being formed, it prevents or at least slows down further maturation of the M6PR and STxB-containing compartment. This places the CHC22-dependent step downstream of

sorting from the EEAI-positive compartment and upstream of sorting M6PR and STxB from one another. Since CHC22-depletion does not affect TGN46 trafficking, the EEAI-positive early endosome seems largely unaffected. This begs the question, how is GLUT4 exported from this compartment? On one hand, comparisons to M6PR and STxB suggest, that GLUT4 is also retrieved from EEAI-positive endosomes by means of CHC17 and retromer. On the other hand, it has been demonstrated that GLUT4 is ubiquitinated and GGAs are potentially involved in its exit from EEAI-positive endosomes. In case of the EGF-R, GGAs have been demonstrated to bind the ubiquitinated receptor which is subsequently exported from early endosomes (Piper and Luzio, 2007; Puertollano and Bonifacino, 2004; Scott et al., 2004). However, ubiquitinated EGF-R is degraded in lysosomes, while GLUT4 is sequestered into the GSC. This would require the deubiquitination of GLUT4 to save it from lysosomal degradation. Given such a deubiquitination activity exists, it remains unclear if this activity is present in GSCs or endosomes and if CHC22 sorts ubiquitinated or deubiquitinated GLUT4. Further experimentation into the exit of GLUT4 from EEAI-positive early endosomes is therefore required. GLUT4 has also been shown to be sumoylated, which also affects the insulin-response in these cells (Giorgino et al., 2000) but the physiological relevance of this event is unknown.

Another way to look at the problem of GLUT4 exiting the EEAI-positive endosome is to ask, how CHC22 is recruited onto GLUT4-containing vesicles. CHC22 associates with GGA2 in adult skeletal muscle suggesting that GGA2 could recruit CHC22 onto membranes. Also, CHC22 has been demonstrated to bind SNX5 (Towler et al., 2004a), which has been suggested to be part of the retromer complex (Wassmer et al., 2007). I gathered some preliminary data suggests CHC22 could also bind SNX1. One possible

mode of action for CHC22 could be to stabilize vesicles derived from early endosomes en route to late endosomes and the TGN. Structural analyses of retromer revealed it forming tubules (Hierro et al., 2007). However, tubules have not yet been observed to connect endosomes and TGN. Possibly, retromer derived tubules fall apart and are subsequently stabilized by CHC22. One could imagine a hand-off model in which retromer components SNX1 and SNX5 recruit CHC22, which subsequently binds GGAs, that are still bound on the emerging tube. Consistent with this idea is SNX5 binding the proximal leg of CHC22 and GGAs potentially binding the terminal domain of CHC22. Upon recruitment, CHC22 could act in sorting GLUT4 out of the newly formed vesicles.

A stabilizing effect as outlined above would shift the balance in dynamics of this pathway towards the newly formed vesicle but not fundamentally change the actual pathway. This fits well with CHC22-depletion only having a moderate effect in overall efficiency of M6PR trafficking when compared to CHC17-depletion. Also, this is consistent with mice having a functional, although less robust GSC. Furthermore, in mice adipocytes about 40 % of GLUT4 is found in a Tfr-R containing compartment, defined as early endosomes (Karylowski et al., 2004). In contrast, virtually no colocalization was found between EEAI and GLUT4 in LHCNM2 cells and human tissue samples, strongly arguing for a more complete diversion of GLUT4 from early endosomes.

Future directions

As outlined above there are still very many questions concerning CHC22-function. The exact characterization of CHC22 behaviour in cells regarding binding and regulation is

largely elusive at this point. Ideally, electron microscopy would be performed on cells immunolabelled for CHC22. Also, other cargo molecules should be tested for their dependence on CHC22. That way it should be possible to further pinpoint CHC22 function regarding the exact temporal order in endosomal sorting as well as its exact localization.

Largely ignored in this study is the biochemistry of CHC22. A great deal of information has been gathered about CHC17 by *in vitro* studies using the purified protein or fragments thereof (Fotin et al., 2004; Liu et al., 1995; Ungewickell and Branton, 1981; Ungewickell and Ungewickell, 1991; Ybe et al., 1999). Recently, a protocol has been published for purification of recombinant full-length CHC17 in insect cells (Rapoport et al., 2008). Similar approaches could be used to purify CHC22 or fragments of CHC22. In contrast to CHC17, which is highly expressed in brain, CHC22 is predominantly expressed in skeletal muscle, which is readily available from bovine and chicken. However, while antibodies against CHC17 recognize the bovine isoform, antibodies raised against human CHC22 failed to recognize bovine or chicken CHC22. A new antibody raised against a peptide of human CHC22 has not been tested against chicken CHC22 yet. Comparing the human and corresponding chicken sequences (amino acids 1549-1563), there are two amino acid changes (position 1551: Q to E; position 1563: R to Q) making it unlikely but possible, that this antibody recognizes chicken CHC22. In this case a protocol could be established that purifies CHC22-coated vesicles, possibly involving an immunoisolating step using CHC22-specific antibody to exclude CHC17-coated vesicles. CHC22-coated vesicles could subsequently be analyzed in mass spectrometry to determine their protein content. Also, CHC22 could be purified from

coated vesicles by dissociating the vesicles and performing size exclusion chromatography.

In case of expression of recombinant protein fragments, a 6xHis-sequence could be used to trace the protein. With purified protein in hand, various tests could be performed regarding assembly characteristics and membrane association. Protocols for such experiments are already exemplified by comparable experiments on CHC17.

Probably the most interesting question is why mice have lost CHC22 and how they compensate for this loss. Answering this would give us a better understanding of current mouse models for diabetes, and help us create better models with respect to the human situation. Also, it would shed light on CHC22 function in humans. Since mice transgenic for human CHC22 display an extended but non-functional GSC, it is conceivable that mice lack additional factors required for GSC function compared to humans. One such candidate is human STX10, which is not present in the mouse genome. mRNA expression of STX10, while found in all tissues, is increased in pancreas, heart and skeletal muscle (Tang et al., 1998). STX10 is a SNARE-protein of the syntaxin family, and like STX6 is involved in fusion of retrograde endosomal transport vesicles to the TGN. Interestingly, there are a number of reports from various labs implicating STX6 in endosomal sorting of GLUT4 (Perera et al., 2003; Shewan et al., 2003; Watson and Pessin, 2008). This data was collected in rodent models. As noted previously, STX6 and STX10 have been used to distinguish retrograde pathways of STxB and M6PR (Ganley et al., 2008). While this study demonstrated functions for STX6 and STX10 at the TGN, it also suggested that both syntaxins could play a role in inner-endosomal fusion events. Therefore one approach will be to express STX10 alongside CHC22 in mouse skeletal muscle. The mouse skeletal muscle cell line C2C12 can be used in these experiments.

Native C2C12 do not show any response to insulin with respect to glucose uptake (Tortorella and Pilch, 2002) - a notable contrast to LHCNM2 human skeletal muscle and one of the main arguments for a more robust GSC in humans. Potentially, an insulin-response could be triggered by expression of CHC22 and STX10 in these cells. Another cell system to use would be primary muscle cells from mice transgenic for CHC22. CHC22-transgenic mice already show an expanded GSC, which is non-functional. Adding STX10 could potentially reinstate function of the enlarged GSC. Ideally, a stable cell line from CHC22-transgenic mice would be established, which can then be used for screening several candidates for reinstating a functional GSC. Since primary cells can be difficult to transfect, a stable cell line expressing CHC22 would also guarantee a consistent background for subsequent transfection studies.

Another candidate for reinstating correct GSC function in mice expressing CHC22 is TBC1D3, a regulator of EGF-R signaling through ERK and Akt-kinases Like STX10 TBC1D3 is non-existent in mice (Hodzic et al., 2006; Wainszelbaum et al., 2008). Interestingly, the TBC1D3 gene is located close to the CHC17 gene in the human genome (17.12 and 17q11-qter, respectively). Since GSC-activation is mediated in an Akt-dependent mechanism, one could imagine a requirement for TBC1D3 in this process. Also, TBC1D3 has been demonstrated to interact with GGA3 and to be involved in macropinocytosis (Frittoli et al., 2008). However, TBC1D3 is only present in hominoid species, therefore lacking from several vertebrates that express CHC22.

Finally, it could be possible that CHC22 is involved in cellular processes other than endosomal traffic. One potentially relevant related membrane pathway is macropinocytosis. As mentioned above TBC1D3 is involved in EGF-stimulated

macropinocytosis via an interaction with GGA3. Notably, the unique interaction partner of CHC22, SNX5, as well as SNX1 have also been shown to be involved in macropinocytosis (Bryant et al., 2007; Kerr et al., 2006). These studies have been carried out in the human cell lines MCF-7 and HEK, which contain readily detectable CHC22-levels. Besides SNX1 and SNX5, newly formed macropinocytic compartments contain the early endosomal marker EEAI (Kerr et al., 2006). Macropinosomes mature rapidly as the late endosomal marker Rab7 can be detected on them within 2-4 minutes after establishment (Racoosin and Swanson, 1993), before they eventually fuse with lysosomes. Potentially, CHC22 may play an analogous role in macropinosome maturation as it does in endosome maturation. The field of macropinocytosis will likely become even more prominent with the recent high profile discovery of vaccinia virus and potentially other pox viruses inducing membrane ruffling and macropinocytosis as a means to gain cell entry (Mercer and Helenius, 2008).

In conclusion, I demonstrated CHC22 to be required for endosomal sorting of various cargoes in epithelial and skeletal muscle cells and for generation of the specialized glucose storage compartment in skeletal muscle. Thereby a novel sorting pathway independent of CHC17 has been defined. This pathway is critical for insulin activity and glucose homeostasis in humans and therefore of clinical relevance for type 2 diabetes. Further investigations will aim at better understanding of the molecular mechanism involved in CHC22 function and deepen our understanding of human type 2 diabetes.

References

Acton, S., and Brodsky, F. M. (1990). Predominance of clathrin light chain LCb correlates with the presence of a regulated secretory pathway. J Cell Biol *111*, 1419-1426.

Antonescu, C. N., Diaz, M., Femia, G., Planas, J. V., and Klip, A. (2008). Clathrin and Non-Clathrin Mediated Glut4 Endocytosis in Myocytes: Effect of Mitochondrial Uncoupling. Traffic.

Appenzeller-Herzog, C., and Hauri, H. P. (2006). The ER-Golgi intermediate compartment (ERGIC): in search of its identity and function. J Cell Sci *119*, 2173-2183.

Arighi, C. N., Hartnell, L. M., Aguilar, R. C., Haft, C. R., and Bonifacino, J. S. (2004). Role of the mammalian retromer in sorting of the cation-independent mannose 6-phosphate receptor. J Cell Biol *165*, 123-133.

Bai, H., Doray, B., and Kornfeld, S. (2004). GGA1 interacts with the adaptor protein AP-1 through a WNSF sequence in its hinge region. J Biol Chem *279*, 17411-17417.

Banting, G., Maile, R., and Roquemore, E. P. (1998). The steady state distribution of humTGN46 is not significantly altered in cells defective in clathrin-mediated endocytosis. J Cell Sci *111 (Pt 23),* 3451-3458.

Benmerah, A., and Lamaze, C. (2007). Clathrin-coated pits: vive la difference? Traffic *8*, 970-982.

Bennett, E. M., Lin, S. X., Towler, M. C., Maxfield, F. R., and Brodsky, F. M. (2001). Clathrin hub expression affects early endosome distribution with minimal impact on receptor sorting and recycling. Mol Biol Cell *12*, 2790-2799.

Bonifacino, J. S. (2004). The GGA proteins: adaptors on the move. Nat Rev Mol Cell Biol *5*, 23-32.

Bonifacino, J. S., and Rojas, R. (2006). Retrograde transport from endosomes to the trans-Golgi network. Nat Rev Mol Cell Biol *7*, 568-579.

Borner, G. H., Harbour, M., Hester, S., Lilley, K. S., and Robinson, M. S. (2006). Comparative proteomics of clathrin-coated vesicles. J Cell Biol *175*, 571-578.

Brodsky, F. M., Chen, C. Y., Knuehl, C., Towler, M. C., and Wakeham, D. E. (2001). Biological basket weaving: Formation and function of clathrin-coated vesicles. Annu Rev Cell Dev Biol *17*, 517-568.

Bruning, J. C., Michael, M. D., Winnay, J. N., Hayashi, T., Horsch, D., Accili, D., Goodyear, L. J., and Kahn, C. R. (1998). A muscle-specific insulin receptor knockout exhibits features of the metabolic syndrome of NIDDM without altering glucose tolerance. Mol Cell *2*, 559-569.

Bryant, D. M., Kerr, M. C., Hammond, L. A., Joseph, S. R., Mostov, K. E., Teasdale, R. D., and Stow, J. L. (2007). EGF induces macropinocytosis and SNX1-modulated recycling of E-cadherin. J Cell Sci *120*, 1818-1828.

Bryant, N. J., Govers, R., and James, D. E. (2002). Regulated transport of the glucose transporter GLUT4. Nat Rev Mol Cell Biol *3*, 267-277.

Bugnard, E., Zaal, K. J., and Ralston, E. (2005). Reorganization of microtubule nucleation during muscle differentiation. Cell Motil Cytoskeleton *60*, 1-13.

Bujny, M. V., Popoff, V., Johannes, L., and Cullen, P. J. (2007). The retromer component sorting nexin-1 is required for efficient retrograde transport of Shiga toxin from early endosome to the trans Golgi network. J Cell Sci *120*, 2010-2021.

Carlton, J., Bujny, M., Peter, B. J., Oorschot, V. M., Rutherford, A., Mellor, H., Klumperman, J., McMahon, H. T., and Cullen, P. J. (2004). Sorting nexin-1 mediates tubular endosome-to-TGN transport through coincidence sensing of high- curvature membranes and 3-phosphoinositides. Curr Biol *14*, 1791-1800.

Chen, C. Y., and Brodsky, F. M. (2005). Huntingtin-interacting protein 1 (Hip1) and Hip1-related protein (Hip1R) bind the conserved sequence of clathrin light chains and thereby influence clathrin assembly in vitro and actin distribution in vivo. J Biol Chem *280*, 6109-6117.

Colanzi, A., and Corda, D. (2007). Mitosis controls the Golgi and the Golgi controls mitosis. Curr Opin Cell Biol *19*, 386-393.

Conner, S. D., and Schmid, S. L. (2003). Regulated portals of entry into the cell. Nature *422*, 37-44.

Dombrowski, L., Roy, D., Marcotte, B., and Marette, A. (1996). A new procedure for the isolation of plasma membranes, T tubules, and internal membranes from skeletal muscle. Am J Physiol *270*, E667-676.

Fotin, A., Cheng, Y., Sliz, P., Grigorieff, N., Harrison, S. C., Kirchhausen, T., and Walz, T. (2004). Molecular model for a complete clathrin lattice from electron cryomicroscopy. Nature *432*, 573-579.

Franch-Marro, X., Wendler, F., Guidato, S., Griffith, J., Baena-Lopez, A., Itasaki, N., Maurice, M. M., and Vincent, J. P. (2008). Wingless secretion requires endosome-to-Golgi retrieval of Wntless/Evi/Sprinter by the retromer complex. Nat Cell Biol *10*, 170-177.

Frittoli, E., Palamidessi, A., Pizzigoni, A., Lanzetti, L., Garre, M., Troglio, F., Troilo, A., Fukuda, M., Di Fiore, P. P., Scita, G., and Confalonieri, S. (2008). The Primate-specific Protein TBC1D3 Is Required for Optimal Macropinocytosis in a Novel ARF6-dependent Pathway. Mol Biol Cell *19*, 1304-1316.

Fulco, M., Cen, Y., Zhao, P., Hoffman, E. P., McBurney, M. W., Sauve, A. A., and Sartorelli, V. (2008). Glucose restriction inhibits skeletal myoblast differentiation by activating SIRT1 through AMPK-mediated regulation of Nampt. Dev Cell *14*, 661-673.

Gaietta, G. M., Giepmans, B. N., Deerinck, T. J., Smith, W. B., Ngan, L., Llopis, J., Adams, S. R., Tsien, R. Y., and Ellisman, M. H. (2006). Golgi twins in late mitosis revealed by genetically encoded tags for live cell imaging and correlated electron microscopy. Proc Natl Acad Sci USA *103*, 17777-17782.

Ganley, I. G., Carroll, K., Bittova, L., and Pfeffer, S. (2004). Rab9 GTPase regulates late endosome size and requires effector interaction for its stability. Mol Biol Cell *15*, 5420-5430.

Ganley, I. G., Espinosa, E., and Pfeffer, S. R. (2008). A syntaxin 10-SNARE complex distinguishes two distinct transport routes from endosomes to the trans-Golgi in human cells. J Cell Biol *180*, 159-172.

Garvey, W. T., Maianu, L., Zhu, J. H., Brechtel-Hook, G., Wallace, P., and Baron, A. D. (1998). Evidence for defects in the trafficking and translocation of GLUT4 glucose transporters in skeletal muscle as a cause of human insulin resistance. J Clin Invest *101*, 2377-2386.

Geuze, H. J., Slot, J. W., Strous, G. J. A. M., Haslik, A., and von Figura, K. (1985). Possible pathways for lysosomal enzyme delivery. J Cell Biol *101*, 2253-2262.

Ghosh, P., Dahms, N. M., and Kornfeld, S. (2003a). Mannose 6-phosphate receptors: new twists in the tale. Nat Rev Mol Cell Biol *4*, 202-212.

Ghosh, P., Griffith, J., Geuze, H. J., and Kornfeld, S. (2003b). Mammalian GGAs act together to sort mannose 6-phosphate receptors. J Cell Biol *163*, 755-766.

Gillingham, A. K., Koumanov, F., Pryor, P. R., Reaves, B. J., and Holman, G. D. (1999). Association of AP1 adaptor complexes with GLUT4 vesicles. J Cell Sci *112 (Pt 24)*, 4793-4800.

Giorgino, F., de Robertis, O., Laviola, L., Montrone, C., Perrini, S., McCowen, K. C., and Smith, R. J. (2000). The sentrin-conjugating enzyme mUbc9 interacts with GLUT4 and GLUT1 glucose transporters and regulates transporter levels in skeletal muscle cells. Proc Natl Acad Sci U S A *97*, 1125-1130.

Hanover, J. A., Willingham, M. C., and Pastan, I. (1984). Kinetics of transit of transferrin and epidermal growth factor through clathrin-coated membranes. Cell *39*, 283-293.

Harding, C., Heuser, J., and Stahl, P. (1983). Receptor-mediated endocytosis of transferrin and recycling of the transferrin receptor in rat reticulocytes. J Cell Biol *97*, 329-339.

Hierro, A., Rojas, A. L., Rojas, R., Murthy, N., Effantin, G., Kajava, A. V., Steven, A. C., Bonifacino, J. S., and Hurley, J. H. (2007). Functional architecture of the retromer cargo-recognition complex. Nature *449*, 1063-1067.

Hinrichsen, L., Harborth, J., Andrees, L., Weber, K., and Ungewickell, E. J. (2003). Effect of clathrin heavy chain- and alpha -adaptin specific small interfering RNAs on endocytic accessory proteins and receptor trafficking in HeLa cells. J Biol Chem.

Hinrichsen, L., Meyerholz, A., Groos, S., and Ungewickell, E. J. (2006). Bending a membrane: how clathrin affects budding. Proc Natl Acad Sci USA *103*, 8715-8720.

Hodzic, D., Kong, C., Wainszelbaum, M. J., Charron, A. J., Su, X., and Stahl, P. D. (2006). TBC1D3, a hominoid oncoprotein, is encoded by a cluster of paralogues located on chromosome 17q12. Genomics *88*, 731-736.

Huang, S., and Czech, M. P. (2007). The GLUT4 glucose transporter. Cell Metab *5*, 237-252.

Huang, S., Lifshitz, L. M., Jones, C., Bellve, K. D., Standley, C., Fonseca, S., Corvera, S., Fogarty, K. E., and Czech, M. P. (2007). Insulin stimulates membrane fusion and GLUT4 accumulation in clathrin coats on adipocyte plasma membranes. Mol Cell Biol *27*, 3456-3469.

Ishiki, M., Randhawa, V. K., Poon, V., Jebailey, L., and Klip, A. (2005). Insulin regulates the membrane arrival, fusion, and C-terminal unmasking of glucose transporter-4 via distinct phosphoinositides. J Biol Chem *280*, 28792-28802.

Kaisto, T., Rahkila, P., Marjomaki, V., Parton, R. G., and Metsikko, K. (1999). Endocytosis in skeletal muscle fibers. Exp Cell Res *253*, 551-560.

Kandror, K. V., and Pilch, P. F. (1994). gp160, a tissue-specific marker for insulin-activated glucose transport. Proc Natl Acad Sci USA *91*, 8017-8021.

Karylowski, O., Zeigerer, A., Cohen, A., and McGraw, T. E. (2004). GLUT4 is retained by an intracellular cycle of vesicle formation and fusion with endosomes. Mol Biol Cell *15*, 870-882.

Kedra, D., Peyrard, M., Fransson, I., Collins, J. E., Dunham, I., Roe, B. A., and Dumanski, J. P. (1996). Characterization of a second human clathrin heavy chain polypeptide gene (*CHL-22*) from chromosome 22q11. Hum Mol Gen *5*, 625-631.

Kerr, M. C., Lindsay, M. R., Luetterforst, R., Hamilton, N., Simpson, F., Parton, R. G., Gleeson, P. A., and Teasdale, R. D. (2006). Visualisation of macropinosome maturation by the recruitment of sorting nexins. J Cell Sci *119*, 3967-3980.

Kirchhausen, T. (2000). Clathrin. Annu Rev Biochem *69*, 699-727.

Le Grand, F., and Rudnicki, M. A. (2007). Skeletal muscle satellite cells and adult myogenesis. Curr Opin Cell Biol *19*, 628-633.

Li, J., Peters, P. J., Bai, M., Dai, J., Bos, E., Kirchhausen, T., Kandror, K. V., and Hsu, V. W. (2007). An ACAP1-containing clathrin coat complex for endocytic recycling. J Cell Biol *178*, 453-464.

Li, L. V., and Kandror, K. V. (2005). Golgi-localized, gamma-ear-containing, Arf-binding protein adaptors mediate insulin-responsive trafficking of glucose transporter 4 in 3T3-L1 adipocytes. Mol Endocrinol *19*, 2145-2153.

Lippincott-Schwartz, J., Yuan, L. C., Bonifacino, J. S., and Klausner, R. D. (1989). Rapid redistribution of Golgi proteins into the ER in cells treated with Brefeldin A: Evidence for membrane cycling from Golgi to ER. Cell *56*, 801-813.

Liu, S.-H., Towler, M. C., Chen, E., Chen, C.-Y., Song, W., Apodaca, G., and Brodsky, F. M. (2001). A novel clathrin homolog that co-distributes with cytoskeletal components functions in the trans-Golgi network. EMBO J *20*, 272-284.

Liu, S.-H., Wong, M. L., Craik, C. S., and Brodsky, F. M. (1995). Regulation of clathrin assembly and trimerization defined using recombinant triskelion hubs. Cell *83*, 257-267.

Liu, S. H., Marks, M. S., and Brodsky, F. M. (1998). A dominant-negative clathrin mutant differentially affects trafficking of molecules with distinct sorting motifs in the class II major histocompatibility complex (MHC) pathway. J Cell Biol *140*, 1023-1037.

Lizcano, J. M., and Alessi, D. R. (2002). The insulin signalling pathway. Curr Biol *12*, R236-238.

Lombardi, D., Soldati, T., Riederer, M. A., Goda, Y., Zerial, M., and Pfeffer, S. R. (1993). Rab9 functions in transport between late endosomes and the trans Golgi network. EMBO J *12*, 677-682.

Long, K. R., Trofatter, J. A., Ramesh, V., McCormick, M. K., and Buckler, A. J. (1996).
Cloning and characterization of a novel human clathrin heavy chain gene (CLTCL).
Genomics *35*, 466-472.

Mallard, F., Antony, C., Tenza, D., Salamero, J., Goud, B., and Johannes, L. (1998).
Direct pathway from early/recycling endosomes to the Golgi apparatus revealed through
the study of shiga toxin B-fragment transport. J Cell Biol *143*, 973-990.

Manning, B. D., and Cantley, L. C. (2007). AKT/PKB signaling: navigating downstream.
Cell *129*, 1261-1274.

Mardones, G. A., Burgos, P. V., Brooks, D. A., Parkinson-Lawrence, E., Mattera, R., and
Bonifacino, J. S. (2007). The trans-Golgi network accessory protein p56 promotes long-
range movement of GGA/clathrin-containing transport carriers and lysosomal enzyme
sorting. Mol Biol Cell *18*, 3486-3501.

Maxfield, F. R., and McGraw, T. E. (2004). Endocytic recycling. Nat Rev Mol Cell Biol *5*,
121-132.

Mayor, S., Presley, J. F., and Maxfield, F. R. (1993). Sorting of membrane components
from endosomes and subsequent recycling to the cell surface occurs by a bulk flow
process. J Cell Biol *121*, 1257-1269.

Mercer, J., and Helenius, A. (2008). Vaccinia virus uses macropinocytosis and apoptotic
mimicry to enter host cells. Science *320*, 531-535.

Meyer, C., Zizioli, D., Lausmann, S., Eskelinen, E. L., Hamann, J., Saftig, P., von Figura, K., and Schu, P. (2000). mu1A-adaptin-deficient mice: lethality, loss of AP-1 binding and rerouting of mannose 6-phosphate receptors. EMBO J *19*, 2193-2203.

Michael, M. D., Kulkarni, R. N., Postic, C., Previs, S. F., Shulman, G. I., Magnuson, M. A., and Kahn, C. R. (2000). Loss of insulin signaling in hepatocytes leads to severe insulin resistance and progressive hepatic dysfunction. Mol Cell *6*, 87-97.

Miller, S. E., Collins, B. M., McCoy, A. J., Robinson, M. S., and Owen, D. J. (2007). A SNARE-adaptor interaction is a new mode of cargo recognition in clathrin-coated vesicles. Nature *450*, 570-574.

Motley, A., Bright, N. A., Seaman, M. N., and Robinson, M. S. (2003). Clathrin-mediated endocytosis in AP-2-depleted cells. J Cell Biol *162*, 909-918.

Munoz, P., Rosemblatt, M., Testar, X., Palacin, M., and Zorzano, A. (1995). Isolation and characterization of distinct domains of sarcolemma and T- tubules from rat skeletal muscle. Biochem J *307*, 273-280.

Ng, Y., Ramm, G., Lopez, J. A., and James, D. E. (2008). Rapid Activation of Akt2 Is Sufficient to Stimulate GLUT4 Translocation in 3T3-L1 Adipocytes. Cell Metab *7*, 348-356.

Owen, D. J., Collins, B. M., and Evans, P. R. (2004). ADAPTORS FOR CLATHRIN COATS: Structure and Function. Annu Rev Cell Dev Biol *20*, 153-191.

Palmieri, F., Bisaccia, F., Capobianco, L., Dolce, V., Fiermonte, G., Iacobazzi, V., Indiveri, C., and Palmieri, L. (1996). Mitochondrial metabolite transporters. Biochim Biophys Acta *1275*, 127-132.

Pearse, B. M. F. (1976). Clathrin: A unique protein associated with intracellular transfer of membrane by coated vesicles. Proc Natl Acad Sci USA *73*, 1255-1259.

Perera, H. K., Clarke, M., Morris, N. J., Hong, W., Chamberlain, L. H., and Gould, G. W. (2003). Syntaxin 6 regulates Glut4 trafficking in 3T3-L1 adipocytes. Mol Biol Cell *14*, 2946-2958.

Pfeffer, S. R. (2007). Unsolved mysteries in membrane traffic. Annu Rev Biochem *76*, 629-645.

Piper, R. C., and Luzio, J. P. (2007). Ubiquitin-dependent sorting of integral membrane proteins for degradation in lysosomes. Curr Opin Cell Biol *19*, 459-465.

Ploug, T., van Deurs, B., Ai, H., Cushman, S. W., and Ralston, E. (1998). Analysis of GLUT4 distribution in whole skeletal muscle fibers: identification of distinct storage compartments that are recruited by insulin and muscle contractions. J Cell Biol *142*, 1429-1446.

Popoff, V., Mardones, G. A., Tenza, D., Rojas, R., Lamaze, C., Bonifacino, J. S., Raposo, G., and Johannes, L. (2007). The retromer complex and clathrin define an early endosomal retrograde exit site. J Cell Sci *120*, 2022-2031.

Postic, C., Dentin, R., and Girard, J. (2004). Role of the liver in the control of carbohydrate and lipid homeostasis. Diabetes Metab *30*, 398-408.

Poupon, V., Girard, M., Legendre-Guillemin, V., Thomas, S., Bourbonniere, L., Philie, J., Bright, N. A., and McPherson, P. S. (2008). Clathrin light chains function in mannose phosphate receptor trafficking via regulation of actin assembly. Proc Natl Acad Sci USA *105*, 168-173.

Puertollano, R., and Bonifacino, J. S. (2004). Interactions of GGA3 with the ubiquitin sorting machinery. Nat Cell Biol *6*, 244-251.

Puthenveedu, M. A., Bachert, C., Puri, S., Lanni, F., and Linstedt, A. D. (2006). GM130 and GRASP65-dependent lateral cisternal fusion allows uniform Golgi-enzyme distribution. Nat Cell Biol *8*, 238-248.

Racoosin, E. L., and Swanson, J. A. (1993). Macropinosome maturation and fusion with tubular lysosomes in macrophages. J Cell Biol *121*, 1011-1020.

Radulescu, A. E., Siddhanta, A., and Shields, D. (2007). A role for clathrin in reassembly of the Golgi apparatus. Mol Biol Cell *18*, 94-105.

Randhawa, V. K., Bilan, P. J., Khayat, Z. A., Daneman, N., Liu, Z., Ramlal, T., Volchuk, A., Peng, X. R., Coppola, T., Regazzi, R.*, et al.* (2000). VAMP2, but not VAMP3/cellubrevin, mediates insulin-dependent incorporation of GLUT4 into the plasma membrane of L6 myoblasts. Mol Biol Cell *11*, 2403-2417.

Rapoport, I., Boll, W., Yu, A., Bocking, T., and Kirchhausen, T. (2008). A motif in the clathrin heavy chain required for the hsc70/auxilin uncoating reaction. Mol Biol Cell *19*, 405-413.

Riederer, M. A., Soldati, T., Shapiro, A. D., Lin, J., and Pfeffer, S. R. (1994). Lysosome biogenesis requires Rab9 function and receptor recycling from endosomes to the trans-Golgi network. J Cell Biol *125*, 573-582.

Rojas, R., Kametaka, S., Haft, C. R., and Bonifacino, J. S. (2007). Interchangeable but essential functions of SNX1 and SNX2 in the association of retromer with endosomes and the trafficking of mannose 6-phosphate receptors. Mol Cell Biol *27*, 1112-1124.

Royle, S. J., Bright, N. A., and Lagnado, L. (2005). Clathrin is required for the function of the mitotic spindle. Nature *434*, 1152-1157.

Saint-Pol, A., Yelamos, B., Amessou, M., Mills, I. G., Dugast, M., Tenza, D., Schu, P., Antony, C., McMahon, H. T., Lamaze, C., and Johannes, L. (2004). Clathrin adaptor epsinR is required for retrograde sorting on early endosomal membranes. Dev Cell *6*, 525-538.

Sarabia, V., Lam, L., Burdett, E., Leiter, L. A., and Klip, A. (1992). Glucose transport in human skeletal muscle cells in culture. Stimulation by insulin and metformin. J Clin Invest *90*, 1386-1395.

Scott, P. M., Bilodeau, P. S., Zhdankina, O., Winistorfer, S. C., Hauglund, M. J., Allaman, M. M., Kearney, W. R., Robertson, A. D., Boman, A. L., and Piper, R. C. (2004). GGA proteins bind ubiquitin to facilitate sorting at the trans-Golgi network. Nat Cell Biol *6*, 252-259.

Seaman, M. N. (2004). Cargo-selective endosomal sorting for retrieval to the Golgi requires retromer. J Cell Biol *165*, 111-122.

Seaman, M. N. (2005). Recycle your receptors with retromer. Trends Cell Biol *15*, 68-75.

Shepherd, P. R., and Kahn, B. B. (1999). Glucose transporters and insulin action--implications for insulin resistance and diabetes mellitus. N Engl J Med *341*, 248-257.

Shewan, A. M., van Dam, E. M., Martin, S., Luen, T. B., Hong, W., Bryant, N. J., and James, D. E. (2003). GLUT4 recycles via a trans-Golgi network (TGN) subdomain enriched in Syntaxins 6 and 16 but not TGN38: involvement of an acidic targeting motif. Mol Biol Cell *14*, 973-986.

Sirotkin, H., Morrow, B., DasGupta, R., Goldberg, R., Patanjali, S. R., Shi, G., Cannizzaro, L., Shprintzen, R., Weissman, S. M., and Kucherlapati, R. (1996). Isolation of a new clathrin heavy chain gene with muscle-specific expression from the region commonly deleted in velo-cardio-facial syndrome. Hum Mol Genet *5*, 617-624.

Smith, C. J., Grigorieff, N., and Pearse, B. M. F. (1998). Clathrin coats at 21 Å resolution: A cellular assembly designed to recycle multiple membrane receptors. EMBO J *17*, 4943-4953.

Tang, B. L., Low, D. Y., Tan, A. E., and Hong, W. (1998). Syntaxin 10: a member of the syntaxin family localized to the trans-Golgi network. Biochem Biophys Res Commun *242*, 345-350.

ter Haar, E., Musacchio, A., Harrison, S. C., and Kirchhausen, T. (1998). Atomic structure of clathrin: A β propeller terminal domain joins an α zigzag linker. Cell *95*, 563-573.

Tortorella, L. L., and Pilch, P. F. (2002). C2C12 myocytes lack an insulin-responsive vesicular compartment despite dexamethasone-induced GLUT4 expression. Am J Physiol Endocrinol Metab *283*, E514-524.

Towler, M. C., Gleeson, P. A., Hoshino, S., Rahkila, P., Manalo, V., Ohkoshi, N., Ordahl, C., Parton, R. G., and Brodsky, F. M. (2004a). Clathrin Isoform CHC22, a Component of Neuromuscular and Myotendinous Junctions, Binds Sorting Nexin 5 and Has Increased Expression during Myogenesis and Muscle Regeneration. Mol Biol Cell *15,* 3181-3195.

Towler, M. C., Kaufman, S. J., and Brodsky, F. M. (2004b). Membrane traffic in skeletal muscle. Traffic *5,* 129-139.

Traer, C. J., Rutherford, A. C., Palmer, K. J., Wassmer, T., Oakley, J., Attar, N., Carlton, J. G., Kremerskothen, J., Stephens, D. J., and Cullen, P. J. (2007). SNX4 coordinates endosomal sorting of TfnR with dynein-mediated transport into the endocytic recycling compartment. Nat Cell Biol *9*, 1370-1380.

Ungewickell, E., and Branton, D. (1981). Assembly units of clathrin coats. Nature *289*, 420-422.

Ungewickell, E., and Ungewickell, H. (1991). Bovine brain clathrin light chains impede heavy chain assembly *in vitro*. J Biol Chem *266*, 12710-12714.

Ungewickell, E. J., and Hinrichsen, L. (2007). Endocytosis: clathrin-mediated membrane budding. Curr Opin Cell Biol *19*, 417-425.

Wainszelbaum, M. J., Charron, A. J., Kong, C., Kirkpatrick, D. S., Srikanth, P., Barbieri, M. A., Gygi, S. P., and Stahl, P. D. (2008). The Hominoid-specific Oncogene TBC1D3 Activates Ras and Modulates Epidermal Growth Factor Receptor Signaling and Trafficking. J Biol Chem *283*, 13233-13242.

Wakeham, D. E., Abi-Rached, L., Towler, M. C., Wilbur, J., Parham, P., and Brodsky, F. M. (2005). Clathrin heavy and light chain isoforms originated by independent mechanisms of gene duplication during chordate evolution. Proc Natl Acad Sci USA *102*, 7209-7214.

Wassmer, T., Attar, N., Bujny, M. V., Oakley, J., Traer, C. J., and Cullen, P. J. (2007). A loss-of-function screen reveals SNX5 and SNX6 as potential components of the mammalian retromer. J Cell Sci *120*, 45-54.

Watson, R. T., Khan, A. H., Furukawa, M., Hou, J. C., Li, L., Kanzaki, M., Okada, S., Kandror, K. V., and Pessin, J. E. (2004). Entry of newly synthesized GLUT4 into the insulin-responsive storage compartment is GGA dependent. EMBO J *23*, 2059-2070.

Watson, R. T., and Pessin, J. E. (2008). Recycling of IRAP from the plasma membrane back to the insulin-responsive compartment requires the Q-SNARE syntaxin 6 but not the GGA clathrin adaptors. J Cell Sci *121*, 1243-1251.

Wilbur, J. D., Hwang, P. K., and Brodsky, F. M. (2005). New faces of the familiar clathrin lattice. Traffic *6*, 346-350.

Williams, D., and Pessin, J. E. (2008). Mapping of R-SNARE function at distinct intracellular GLUT4 trafficking steps in adipocytes. J Cell Biol *180*, 375-387.

Williams, R. L., and Urbe, S. (2007). The emerging shape of the ESCRT machinery. Nat Rev Mol Cell Biol *8*, 355-368.

Ybe, J. A., Brodsky, F. M., Hofmann, K., Lin, K., Liu, S. H., Chen, L., Earnest, T. N., Fletterick, R. J., and Hwang, P. K. (1999). Clathrin self-assembly is mediated by a tandemly repeated superhelix. Nature *399*, 371-375.

Zhu, C. H., Mouly, V., Cooper, R. N., Mamchaoui, K., Bigot, A., Shay, J. W., Di Santo, J. P., Butler-Browne, G. S., and Wright, W. E. (2007). Cellular senescence in human myoblasts is overcome by human telomerase reverse transcriptase and cyclin-dependent kinase 4: consequences in aging muscle and therapeutic strategies for muscular dystrophies. Aging Cell *6*, 515-523.

Appendix

Curriculum Vitae

Persönliche Daten

Name: Peter-Christopher Esk

Geburtsdatum: 28. Januar 1978

Geburtsort: Hannover

Wissenschaftlicher Werdegang

Abitur: 03. Juli 1998, Gymnasium Ganderkesee.

Studium: 01. Oktober 1999 – 28. März 2005, Studium der Biochemie an der Gottfried Wilhelm Leibniz Universität Hannover, Abschluss: Diplom, Diplomarbeit: "Charakterisierung des endocytotischen Proteins CALM" angefertigt im Labor von Prof. Dr. Ernst Ungewickell im Institut für Zellbiologie im Zentrum Anatomie der MH Hannover.

Promotion: seit 01. Juni 2005: Promotion im Fach Zell- und Entwicklungsbiologie an der Gottfried Wilhelm Leibniz Universität Hannover, Durchführung der Doktorarbeit im Labor von Prof. Frances M. Brodsky, DPhil. in der GW Hooper Foundation, University of California, San Francisco.

Publications

Peer-reviewed articles

Meyerholz A, Hinrichsen L, Groos S, Esk PC, Brandes G, Ungewickell EJ. Effect of clathrin assembly lymphoid myeloid leukemia protein depletion on clathrin coat formation. *Traffic*. 2005 Dec;6(12):1225-34 (not related to this dissertation)

Abstracts

Hoshino S, Ishii A, Ohkoshi, N, Esk C, Brodsky FM. Expression of clathrin heavy chain isoform CHC22 in the inflammatory myopathies. New Directions in Biology and Disease of Skeletal Muscle. April 23-26. Dallas, Texas

Christopher Esk, Sachiko Hoshino, Stephane Vassilopoulos, Frances M. Brodsky. Clathrin isoform CHC22 is implicated in membrane traffic at the Golgi during myogenesis. Gordon Research Conference, Molecular Membrane Biology. July 8-13 2007. Andover, New Hampshire

Manuscripts in revision and preparation:

A role for the CHC22 clathrin heavy chain isoform in glucose metabolism by human skeletal muscle. Stéphane Vassilopoulos*, Christopher Esk*, Sachiko Hoshino*, Birgit H. Funke, Chih-Ying Chen, Alex M. Plocik, Woodring E. Wright, Raju Kucherlapati, Frances M. Brodsky (*: equal contribution). manuscript in review

Distinct functions for clathrin heavy chain isoforms in endosomal sorting. Christopher Esk, Chih-Ying Chen, Frances M. Brodsky. manuscript in preparation

Running title: Skeletal muscle generation is characterized by increased levels of membrane traffic components that regulate glucose metabolism and is inhibited by pertubation of their function. Sachiko Hoshino, Stephane Vassilopoulos, Christopher Esk, Frances M Brodsky. manuscript in preparation

Running title: Clathrin heavy chain and clathrin light chain behaviour. Chih-Ying Chen, Jennifer S Bennetts, Christopher Esk and Frances M Brodsky. manuscript in preparation

Acknowledgments

First off I would like to thank Prof. Frances Brodsky and Prof. Ernst Ungewickell for making this thesis possible. It was their good will and support that allowed me to perform my research in the way I did.

To Frances I am greatly indebted for a tremendous amount of guidance, mentorship, insight into being a scientist, a great deal of freedom and last but not least trust in my work. Prof. Ernst Ungewickell allowed me to go through with this project and offered great advice. In time, I might actually purify the protein.

A very big "Thank you!" to past and present members of the Brodsky lab. Sachiko Hoshino and Stephane Vassilopoulos worked hard from opposite ends of the CHC22 story, allowing me to look at the bigger picture. They, together with Amy Foraker, Jean Chen, Sabrina Taner, Michael Lane, Jeremy Wilbur and Tim Evans, make this a great lab to do science in. I enjoyed everyone's support, ideas, insights, earthquake watch, paranoia, wit, jokes and cakes. Also, thank you to Jen Bennetts, Venus Manalo, Sherri Newmyer, Tina Tran, Marcelo Pando and Michael Reese for the above. Thanks also to Mandy Gomez for doing a great job organizing the paperwork.

I would also like to thank the Hooper staff and members for making this a great place to work in. Whether it is technical and administrative support or new insights into seemingly unrelated science, it was always helpful. Also, it forced me to think about the great "Where is the tumor?"-question, hopefully making me a better scientist.